Translational Methods for Quantitative Prediction of Metabolic Herbal Product-Drug Interactions: Case Study with Milk Thistle

Scott Joseph Brantley

A dissertation submitted to the faculty of the University of North Carolina at Chapel Hill in partial fulfillment of the requirements for the degree of Doctor of Philosophy in the UNC Eshelman School of Pharmacy (Pharmaceutical Sciences).

Chapel Hill
2013

Approved By:

Mary F. Paine, R.Ph, Ph.D.

Kim L.R. Brouwer, PharmD, Ph.D.

Christine M. Walko, PharmD

Nicholas H. Oberlies, Ph.D.

E. Claire Dees, MD.

Abstract

SCOTT BRANTLEY: Translational Methods for Quantitative Prediction of Metabolic Herbal Product-Drug Interactions: Case Study with Milk Thistle
(Under the direction of Mary F. Paine, R.Ph., Ph. D.)

The misperception that herbal products are safe has perpetuated multibillion dollar sales of these products, exposing the public to potentially harmful herb-drug interactions when constituents in the herbal supplement inhibit drug metabolizing enzymes. Regulation of herbal products is not as rigorous as drug products. Consequently, evaluation of inhibitory properties of an herbal product typically is not requested before marketing. Traditional drug-drug interaction evaluation methods often are inadequate to evaluate herbal product interaction liability due to the mixture of bioactive constituents, high inherent variability between batches and manufacturers, and limited pharmacokinetic knowledge of constituents. Milk thistle was selected as an exemplar herbal product due to high usage rates in patient populations, particularly the hepatically-impaired; availability of isolated, purified constituents; and disparate effects between previous clinical interaction studies. Initial screens of inhibitory activity against the clinically relevant drug metabolizing enzymes, cytochrome P450 (CYP) 2C9 and CYP3A4, prioritized milk thistle constituents for further evaluation. The main constituents, silybin A and silybin B, inhibited CYP2C9 in a reversible manner (K_i, 10 and 4.8 μM, respectively) and CYP3A4 in an irreversible manner (K_I, 110 and 89 μM, respectively). Incorporation of these *in vitro* kinetic parameters into a physiologically based pharmacokinetic (PBPK) model facilitated predictions of the interaction liability of milk thistle administration with FDA-recommended probe substrates of CYP2C9

(warfarin) and CYP3A4 (midazolam). Administration of large doses of the milk thistle product silibinin (1440 mg/day) was predicted to increase the peak concentration and systemic exposure of both warfarin and midazolam by roughly 5%. Proof-of-concept clinical evaluation of these silibinin-drug interactions confirmed the low interaction potential of the selected milk thistle product, as midazolam and warfarin exposure was increased modestly (9 and 13%, respectively). This mechanistic modeling and simulation approach facilitated prospective evaluation of interactions between a well-characterized herbal product and two widely used and clinically relevant probe substrates. This framework could be applied to other herbal products to predict the magnitude and likelihood of interactions with conventional drugs, guide pharmacotherapeutic decisions, and improve patient care.

To my family, for their steadfast support and dedication during my scholastic journey.

Table of Contents

List of Tables

List of Figures

List of Abbreviations

ANOVA analysis of variance

$AUC_{0\text{-}inf}$ area under the concentration-time curve from zero to infinite time

$AUC_{0\text{-}last}$ area under the concentration-time curve from zero to the last measured concentration

B/P blood to plasma partition ratio

BCRP breast cancer resistance protein

bid two times daily

BLQ below the limit of quantification

CI confidence interval

Cl/F apparent oral clearance

C_{last} last measured concentration

Cl_{int} intrinsic clearance

C_{max} maximum concentration

CTRC Clinical and Translational Research Center

CV coefficient of variation

CYP cytochrome P450

DDIs drug-drug interactions

DMSO dimethyl sulfoxide

f_a fraction absorbed

FDA US Food and Drug Administration

f_u fraction unbound in plasma

$f_{u,ent}$ fraction unbound in enterocytes

$f_{u,liver}$ fraction unbound in hepatocytes

HPLC high pressure liquid chromatography

IC_{50} half-maximal inhibitory concentration

k_a first-order absorption rate constant

KCl potassium chloride

kg kilogram

K_i inhibitory potency

K_I concentration of a mechanism-based inhibitor associated with half maximal inactivation rate

k_{inact} maximal inactivation rate constant

K_m substrate concentration associated with half maximal metabolic rate

MDCK Madin-Darby canine kidney

MDR1 gene encoding P-glycoprotein

mg milligram

min minute

mL milliliter

mM millimolar

mol mole

MRP multi-drug resistance-associated protein

NaCl sodium chloride

NC not calculated

ND not detected

OATP organic anion transporting polypeptide

PBPK physiologically-based pharmacokinetic

PD pharmacodynamics

P-gp P-glycoprotein

PK pharmacokinetics

rCYP recombinant CYP

SD standard deviation

SE standard error

SULTs sulfotransferases

$t_{1/2}$ terminal elimination half-life

tid three times daily

t_{max} time to reach maximal concentration

UPLC ultra-high pressure liquid chromatography

V_{max} maximal metabolic rate

λz terminal elimination rate constant

µg microgram

µg/mL microgram per milliliter

µM micromolar

µmol/L micromoles/liter

Chapter 1

Herb-Drug Interactions: Challenges and Opportunities for Improved Predictions

Introduction

Brief History of Natural Product Use for Medicinal Purposes. Healing plants gracing Neanderthal tombs and in the personal belongings of Ötzi the Iceman indicate that knowledge of the pharmacologic activity of herbs and other natural products predates written records (Tyler, 2000; Goldman, 2001). Exploitation of natural products for both therapeutic and nefarious purposes during the Greek and Roman empires was well-documented by Hippocrates and Galen (Forte and Raman, 2000). Perhaps the most famous early use of an herbal product for pharmacologic activity was the execution of Socrates by poison hemlock. By the early 19th century, scientific methods had advanced such that promotion of botanical products for healing was considered quackery (Winslow and Kroll, 1998). During the 1950s in the United States (US), herbal products began to regain popularity due to pharmaceutical tragedies such as thalidomide (Brownie, 2005). The herbal product market continued to grow in the 1960s, as consumers focused on the perceived lack of side effects and advances in scientific knowledge about natural products (Winslow and Kroll, 1998; Tyler, 2000). In 1974, the World Health Organization (WHO) began encouraging developing countries to supplement modern pharmacotherapy with traditional herbal medicines to fulfill needs unmet by conventional drugs (Winslow and Kroll, 1998). Herbal product sales in the US have continued to increase, reaching an estimated 5.1 billion dollars in 2010 (Blumenthal et al., 2011).

Prevalence of Co-administration of Herbal Products with Conventional Medications. An accurate estimate of the prevalence of herbal product usage and co-administration with conventional medications is difficult, as consumers of herbal products seldom inform their health care providers (Gardiner et al., 2006). Since these products usually are self-administered as a means to treat or prevent the onset of a medical condition (Winslow and Kroll, 1998), concomitant intake with conventional medications can be expected (Gardiner et al., 2006; Kennedy et al., 2008). The National Health Interview Survey provides the most comprehensive evaluation of herbal product usage rates in the US, the most recent of which reported that approximately 20% of the US population acknowledges taking herbal products (Bent, 2008). This percentage may be even greater in patients with medical conditions such as chronic gastrointestinal disorders, insomnia, liver disease, chronic pain, depression, asthma, and women undergoing menopause (Gardiner et al., 2006). Of the survey responders who took an herbal product with conventional therapy, nearly 70% neglected to inform their health care providers (Gardiner et al., 2006; Kennedy et al., 2008). These practices raise concerns for adverse herb-drug interactions.

Biochemical Mechanisms of Herb-Drug Interactions

Inhibition of Drug Metabolizing Enzymes. Drug-mediated inhibition of drug metabolizing enzymes is the most common and most well-studied mechanism underlying drug-drug interactions (DDIs) (Wienkers and Heath, 2005). Enzyme inhibition can manifest as reversible or irreversible loss of activity. *Reversible Inhibition.* Competitive inhibition occurs when the 'perpetrator' drug or other xenobiotic binds to the active site of the enzyme and prevents the 'victim' drug from binding (Lin and Lu, 1998; Hollenberg, 2002) (Figure 1.1). The simplest case occurs when two substrates for the same enzyme are administered concomitantly, although the perpetrator drug need not be a substrate for the enzyme to demonstrate competitive inhibition (Kunze et al., 1991).

The functional consequence of competitive inhibition is that higher concentrations of the victim drug are needed to compete for the binding site, thereby increasing the concentration needed for half-maximal rate of metabolism (K_m) while having no change in the maximal rate of metabolism (V_{max}) (Lin and Lu, 1998; Hollenberg, 2002). Noncompetitive inhibition occurs when the perpetrator drug binds to a region of the enzyme that alters the ability to metabolize the victim drug (Figure 1.1). Since the perpetrator drug does not bind to the same site in the enzyme as the victim drug, increasing victim drug concentrations cannot compensate for the decrease in enzyme activity, leaving K_m unchanged while lowering V_{max} (Lin and Lu, 1998; Hollenberg, 2002). Uncompetitive inhibition occurs when the perpetrator drug binds to the enzyme-victim drug complex. Binding to the enzyme-substrate complex modulates both V_{max} and K_m (Lin and Lu, 1998; Hollenberg, 2002). For all of these situations, the return to basal enzyme activity relies purely on removal of the perpetrator drug from the system. Clinically, reversible inhibition manifests as an increase in the systemic exposure of the victim drug due to changes in clearance and/or bioavailability. *Irreversible Inhibition.* Inhibition perpetrated by compounds that do not associate and dissociate rapidly from the enzyme is termed time-dependent inhibition (TDI). Mechanism-based inhibition (MBI), often observed as TDI, is characterized by irreversible or quasi-irreversible noncovalent binding of a reactive metabolite to the enzyme (Grimm et al., 2009). The resultant binding can impede access to the active site, target the protein for proteasomal degradation, or alkylate the heme (Silverman and Daniel, 1995; Kalgutkar et al., 2007) (Figure 1.1). Comprehensive reviews detailing the mechanisms and clinical implications of irreversible inhibition have been published (Venkatakrishnan et al., 2007; Grimm et al., 2009). Due to the time-dependent nature, onset of irreversible inhibition in vivo can appear delayed from initial exposure to the perpetrator drug (Grimm et al., 2009). As with reversible inhibition, irreversible inhibition will lead to increased systemic exposure

of the victim drug. Unlike reversible inhibition, the interaction can persist following removal of the perpetrator drug because recovery of enzyme activity depends on *de novo* protein synthesis (Grimm et al., 2009).

Inhibition of Protein-Mediated Flux. Compared to metabolism-based interactions, information about transporter-based interactions is limited, although the knowledge gap is narrowing (Han, 2011). Similar to drug metabolizing enzymes, transporters are susceptible to competitive and noncompetitive reversible inhibition due to perpetrator compounds blocking the drug binding site or causing a conformational change that decreases transport activity, respectively (Arnaud et al., 2010; Harper and Wright, 2013). Inhibitors of transporter activity can bind to regions of the transporter on either side of the lipid bilayer, creating scenarios in which inhibition may be either *cis* or *trans* in nature (Jutabha et al., 2010). In addition to these traditional modes of inhibition, the in vitro activity of drug transporters can be modulated by the composition of the cell membrane albeit clinical implications remain unknown (Annaba et al., 2008; Molina et al., 2008; Kis et al., 2009; Clay and Sharom, 2013). Inhibition of transporter activity in vivo can manifest as increased or decreased systemic exposure, and possibly altered organ exposure, of the victim drug depending on site of transporter expression and direction of flux.

Induction of Drug Metabolizing Enzymes and Transporters. In addition to inhibition, DDIs can reflect increased enzyme or transporter expression. Common mechanisms of induction include increased gene transcription and stabilization of mRNA or active protein (Okey, 1990). The predominant mechanism for enzyme and transporter induction is a receptor-mediated increase in gene transcription due to perpetrator compounds activating one or more nuclear receptors (Hewitt et al., 2007). Binding of the perpetrator compound to the ligand binding domain of a nuclear receptor causes the activated receptor to bind to the xenobiotic response element located in the promoter

region of the gene (Figure 1.1). This process leads to increased transcription and subsequent translation of mRNA into enzyme protein (Lin and Lu, 1998). Induction of protein function also can reflect stabilization of mRNA or protein (Novak and Woodcroft, 2000; Raucy et al., 2004; Kato et al., 2005; Menez et al., 2012). Enzyme induction manifests clinically as increased clearance or decreased bioavailability of the victim drug, whereas induction of transporter expression manifests as increased or decreased circulating concentrations of the victim drug depending upon the site of transporter expression.

Challenges with Evaluating Herb-Drug Interactions

Variability in Composition of Herbal Products. Unlike most drug products, herbal products frequently consist of multiple constituents that vary in composition, both between manufacturers and between batches from the same manufacturer. The putative bioactive agents in herbal products often are plant-derived secondary metabolites produced as part of normal plant metabolism or as a reaction to environmental stress (Rousseaux and Schachter, 2003). The relative concentration of each pharmacologically active compound may vary widely depending on growing conditions such as temperature and rainfall (Rousseaux and Schachter, 2003). A simple comparison to illustrate this variability is the extreme differences in wine quality and price between vineyards and vintages, even when produced from the same type of grapes (Paine and Oberlies, 2007). Additional attention should be paid to the composition of herbal products to ensure reproducibility within studies and to permit comparisons between studies.

Identification of Causative Agents. Modulation of drug metabolizing enzymes and transporters by herbal products can reflect interactions with one or more herbal product constituents. The net effect can result from additive, synergistic, or antagonistic interactions between multiple constituents (Efferth and Koch, 2011). Consequently, identification of the interacting agent(s) is needed to make accurate predictions of herb-

drug interactions. Some herbal products, including St. John's wort and milk thistle, are well-characterized, and individual constituents have been isolated in quantities sufficient for interaction screening (Obach, 2000; Weber et al., 2004; Lee et al., 2006b; Graf et al., 2007; Tatsis et al., 2007; Brantley et al., 2010). Other techniques, such as bioactivity-guided fractionation (Kim et al., 2011; Roth et al., 2011), can be used to elucidate the causative agents from herbal products.

Pharmacokinetic Disposition of Causative Constituents. As with conventional DDI predictions, knowledge of the pharmacokinetic disposition of the perpetrator herbal product is needed to make accurate predictions of herb-drug interactions. Herbal products with extensive clearance in the liver and small intestine are still marketed (*e.g.*, resveratrol) whereas traditional pharmaceutical compounds with these characteristics typically are excluded from further development. This extensive elimination or low bioavailability results in low circulating levels of the 'parent' herbal product. Another consequence of a high pre-systemic clearance is that the systemic concentration of the natural product perpetrator, if measurable, may be a less-than-ideal surrogate for the concentration at the site of interaction. However, upon oral dosing, high exposure of the perpetrator (parent and/or metabolite) during first-pass can inhibit intestinal extraction or first-pass hepatic extraction of victim drugs. With respect to induction, concentrations of the parent and metabolite should be monitored with chronic exposure.

Regulatory Perspectives on Herbal Products

While regulatory agencies often require full characterization of the drug interaction liability of conventional pharmaceutical agents prior to market approval, perspectives vary regarding evaluation of herbal products. Herbal product usage is woven into cultural traditions, rendering establishment of regulatory precedent difficult (Rousseaux and Schachter, 2003). Although the primary responsibility of regulatory

agencies is the safety of the general public, cultural and traditional use of herbal products limits the ability of regulatory agencies to restrict herbal pharmacotherapy. Regulatory agencies have developed different methods for addressing the delicate balance between availability and safety. Cultural and economic factors often dictate the final course of action. Regulatory views on herbal products in the US, the European Union, and Canada are summarized below.

Regulation in the United States. The Food and Drug Administration (FDA) received jurisdiction to regulate herbal products under the Dietary Supplement Health and Education Act (DSHEA) of 1994 (Table 1.1). This Act provides the legal definition of dietary supplements, including herbal products, and dictates that such supplements be regulated as foods rather than drugs. Under this classification, dietary supplements are presumed to be safe “within a broad range of intake”. Herbal products marketed after passage of the DSHEA are subject to a pre-market review of safety data, whereas products sold prior to passage of the DSHEA are exempt (de Lima Toccafondo Vieira and Huang, 2012). Contrary to conventional drugs, the burden of proof is on the FDA to demonstrate that these products pose “significant or unreasonable risk” before removal from the market (Brownie, 2005). Supplement manufacturers are prohibited from making claims about the ability of herbal products to diagnose, mitigate, treat, cure, or prevent a specific disease or class of diseases without undergoing evaluation as conventional drugs (DSHEA). For herbal products with established drug interaction liability, the FDA requires mention of potential herb-drug interactions in the prescribing information of victim drugs but not in the label, of the perpetrator herbal product.

Regulation in the European Union. Herbal product usage varies widely among countries of the European Union (EU), leading to differences in regulatory classifications in individual countries. Germany and France have a long history of herbal product use and report a combined sales of 3.2 billion dollars in 2003 (De Smet, 2005). In contrast,

Portugal, Hungary, Ireland, Slovakia, Finland, and Norway have less developed histories of herbal product use, with less than 0.15 billion dollars in combined sales in 2003 (De Smet, 2005). Initial attempts in 2002 to harmonize these disparate views generated safe lists of vitamins and minerals, but national rules for other nutrients and dietary supplements remained intact (Directive 2002/46/EC). With regulation of herbal products left to the agencies in each member country, there were 27 different national perspectives regarding regulation of herbal products (Table 1.1). The second attempt in 2004 in market harmonization created a category termed 'traditional herbal medicinal products' (THMP) and has provided some harmonization at the national level for medicinal products with traditional or historical uses (Silano et al., 2011). Market authorization of a product as a THMP requires that the product be on the market for at least 30 years, 15 of which must be in an EU member country (Silano et al., 2011). Registration under this directive requires more information than the US FDA requires for herbal products but less information than the US FDA or European Medicines Agency (EMA) require for conventional drugs. Herbal product manufactures were given until April 2011 to register a product for consideration as an herbal medicine (Silano et al., 2011). Although market harmonization has begun, decisions as to market authorization are still left to individual member countries. This incomplete harmonization creates an environment where an herbal product can be marketed as a food supplement in one country, a THMP in another country, and prohibited in a third country (Silano et al., 2011).

Regulation in Canada. Herbal products are regulated by the Natural Health Product Directorate (NHPD) branch of Health Canada (Table 1.1). The role of the NHPD is to "ensure that Canadians have ready access to natural health products that are safe, effective and of high quality while respecting freedom of choice and philosophical and cultural diversity" (Health Canada, 2006). Unlike in the US and the EU, herbal product

manufacturers must provide evidence to support both the safety and efficacy of a product before market approval. As part of the safety information required for approval, manufacturers must provide a safety summary report containing information regarding the interaction potential with other medicinal products, foods, or standardized laboratory tests (Health Canada, 2006). Upon approval, herbal products receive a product license and identification number. All approved herbal products are required to meet strict labeling requirements. Moreover, removal of an herbal product from the market is less cumbersome than in the US. The Health Minister can suspend sales of natural health products if a manufacturer does not provide requested safety information or if the Minister has reasonable grounds to believe that the product is not complying with other provisions of NHPD regulations.

Herb-Drug Interaction Predictions

Current Prediction Strategies. Compared to qualitative descriptions of herb-drug interactions, prospective quantitative predictions of these interactions are at best in embryonic stages. Since herbal products are not regulated in the same manner as drugs, assessment of herb-drug interaction liability often is not requested prior to marketing. As such, herb-drug interaction studies typically are initiated only upon receipt of case reports documenting a putative interaction or in vitro experiments highlighting a potential interaction. Shifting the evaluation paradigm to prospective predictions would allow consumers and healthcare providers to make informed decisions regarding the addition of herbal products to conventional drug regimens.

Limitations of Current Prediction Strategies. Current herb-drug interaction predictions are limited due to the aforementioned challenges in evaluating drug interaction liability of herbal products. Natural products typically are complex mixtures of potentially bioactive compounds, any of which may interact with drug metabolizing enzymes or transporters. Static prediction equations are not amenable to complex

interactions due to multiple constituents; consequently, more sophisticated prediction strategies, such as physiologically-based pharmacokinetic modeling (PBPK), are preferable (US FDA, 2012; Huang, 2012). Summarized below are current approaches for evaluating the DDI potential of conventional pharmaceutical compounds that can be applied to natural products. Information from in vitro experiments, pre-clinical and clinical studies, and in silico simulations can be used to assess herb-drug interaction potential. The herb-drug interaction of milk thistle was evaluated using these techniques and is presented as a case study. Systematic generation of herb-drug interaction information would help predict, mitigate, and ideally prevent, adverse herb-drug interactions in the general population.

Evaluation of HDI using in vitro systems. In vitro systems are foundational tools used to estimate the contribution of drug metabolizing enzymes and transporters to the disposition of an herbal product. Moreover, results derived from in vitro experiments can be used to predict quantitatively the potential for a DDI. Common in vitro systems to assess drug metabolism include microsomal fractions, recombinant enzymes, and hepatocytes. Transport activity typically is determined using cell lines such as Caco-2 or Madin-Darby canine kidney (MDCK) cells, where bi-directional transport can be measured, or cells overexpressing particular transporters (Cvetkovic et al., 1999; Cui et al., 2001; Troutman and Thakker, 2003; Kindla et al., 2011; Kimoto et al., 2013; Kock et al., 2013). To estimate biliary transport, sandwich-cultured hepatocytes can be used to mimic 3-dimensional hepatic architecture (Liu et al., 1999; Annaert et al., 2001). Refinement of these systems continues to provide improved estimates of drug disposition.

Human-derived microsomes or recombinant enzymes are used to determine both the potency and mechanism of enzyme inhibition. Details about the appropriate conduct of these studies are described elsewhere (Bjornsson et al., 2003; Grimm et al., 2009).

Cell lines are used to determine whether the drug can inhibit transport of probe substrates such as digoxin (P-glycoprotein) or statins (breast cancer resistance protein [BCRP] and organic anion transporting polypeptide [OATP]). The likelihood of observing inhibition in vivo can be estimated by using the in vitro-determined kinetic parameters, as well as observed systemic concentrations (if available). A caveat is that circulating concentrations may not represent the DDI liability during first-pass metabolism.

Unlike inhibition experiments that can rely on human liver microsomes, induction experiments must rely on intact cells. Determination of induction is dependent upon the measurement of mRNA or protein expression for both metabolic enzymes and transporters. The induction response of immortalized cells (e.g., Caco-2 or HepG2) may not be as robust as in human hepatocytes because the immortalization process may have decreased or altered expression of particular transcription factors or nuclear receptors.

Evalution of HDI in Pre-Clinical Animal Models. The use of animal models is a critical step in the drug development process. Although predictions can be made using in vitro data, several key characteristics of drug disposition can only be determined in vivo, namely the relative contribution of metabolic and excretory routes to total drug clearance. Moreover, mass-balance and the percent contribution of an enzymatic pathway to overall elimination can only be estimated using in vivo data. Without in vivo data, the appropriateness of PBPK models cannot be assessed. Information derived from properly designed pharmacokinetic studies can be used to develop or refine PBPK models. Thus, in addition to helping determine bioavailability and tissue localization of a drug, animals can provide an estimate of exposure to metabolites following administration of the parent drug. In general, in vitro data are scaled to determine DDI liability and whether human in vivo DDI studies should be conducted. In some instances, animals can provide mechanistic insight into the DDI that is not amenable to with a

human study. A major disadvantage of the use of animal models is the possibility of discordant metabolic and transport pathways compared to humans. Not surprisingly, animals have enzyme or transporter orthologs that differ in tissue expression or substrate specificity (Martignoni et al., 2006; Chu et al., 2013).

Clinical Studies. Best practices for appropriate conduct of clinical herb-drug interaction studies closely resemble those for food-drug interaction studies as reviewed previously (Won et al., 2012). As with food-drug interaction studies, the critical step in herb-drug interaction studies is quantification of the putative perpetrator compound(s) in the herbal product. Recently, the Consolidated Standards of Reporting Trials (CONSORT) checklist was updated to include herbal medicinal products (Gagnier et al., 2006). The interventions section of this checklist was extended to highlight the importance of the name, characteristics, dosage regimen, quantitative description, and qualitative testing of the herbal product. Although this checklist is meant to allow quality reporting of trials involving herbal medicines, the major emphasis of this update also is applicable to interaction studies. Ideally, with increased awareness, herb-drug interaction studies will more resemble those for DDIs, guidances for which have been discussed extensively elsewhere (EMA, 2012; US FDA, 2012).

In Silico Simulation Software Packages. Modeling and simulation-based strategies have become useful tools in DDI predictions. PBPK models in particular are emphasized in regulatory recommendations for (1) predicting the likelihood and magnitude of drug interactions and (2) providing greater insight into causes of uncertainty and variability in evaluation of DDIs (EMA, 2012; US FDA, 2012). Several commercial software packages that facilitate model development are available. PBPK models can be developed using differential equation solving software packages such as MATLAB® Simulink®, Berkeley Madonna™, and acslX. These programs do not contain pre-defined model structures or differential equations, thus leaving the model complexity

and flexibility dependent upon the ambition and coding experience of the modeler. PBPK modeling software such as Simcyp®, PK-Sim®, GastroPlus®, and MATLAB® SimBiology provide template model structures at the expense of full customization. Regardless of the software package chosen, PBPK models require more parameters than other modeling strategies. Compound-independent physiologic parameters such as organ weights and blood flows can be obtained from the literature (Brown et al., 1997; Boecker, 2003). Compound-dependent parameters such as tissue partition coefficients, absorption rates, and metabolic clearances can be determined from in vitro and animal experiments or estimated from physicochemical parameters of the natural product (Poulin and Theil, 2000; Rodgers and Rowland, 2007). PBPK models of victim and perpetrator compounds can be linked through relevant interaction mechanisms, such as reversible or time-dependent inhibition, to simulate herb-drug interactions (US FDA, 2012). Comprehensive reviews of PBPK model software and applications have been published (Khalil and Laer, 2011; Rowland et al., 2011; Zhao et al., 2012).

Case Study: Milk Thistle

Herbal Product Identification and Usage. Milk thistle (*Silybum marianum* (L.) Gaertn.) is a member of the Asteraceae plant family whose use in treating hepatic disorders was documented by Pliny the Elder (AD 23-79) (Kroll et al., 2007; Post-White et al., 2007). More recently, extracts from the plant have shown promise in pre-clinical studies for treatment of hepatic disorders such as acute hepatitis, chronic hepatitis B, and hepatitis C infections (Wei et al., 2012). However, the clinical efficacy in treating these disorders has been limited (Gordon et al., 2006; Rambaldi et al., 2007; Seeff et al., 2008; El-Kamary et al., 2009; Payer et al., 2010; Fried et al., 2012). In addition to treatment for liver disease, milk thistle extracts may mitigate drug-induced hepatotoxicity from chemotherapeutic agents used for childhood acute lymphoblastic leukemia (Ladas et al., 2010) and acute myelogenous leukemia (McBride et al., 2012). Milk thistle

extracts and chemical derivatives are used in the treatment of fulminant liver failure caused by death cap (*Amanita phalloides*) mushroom poisoning (Mengs et al., 2012). Although milk thistle research remains focused on liver ailments, recent research has highlighted potential uses for treatment of obsessive compulsive disorder (Sayyah et al., 2010; Camfield et al., 2011), type II diabetes (Huseini et al., 2006), beta-thalassemia major (Gharagozloo et al., 2009), influenza A (Song and Choi, 2011), and prostate cancer chemoprevention (Agarwal et al., 2006; Flaig et al., 2007; Vidlar et al., 2010). Continuous use of milk thistle products for nearly 2000 years in treating various ailments suggests putative efficacy; however, clinical evidence remains limited.

Extracts from milk thistle are commercially available with varying degrees of purification and chemical modification. Crude milk thistle extract is available and often is standardized to contain 65-80% silymarin and 20-35% fatty acids (Kroll et al., 2007). Silymarin is a mixture of at least seven flavonolignans and the flavonoid taxifolin (Figure 1.2). Flavonolignans are formed by conjugation of taxifolin with coniferyl alcohol to create structural isomers with the same molecular weight, permitting rudimentary calculations of silymarin concentrations in molar units (Kim et al., 2003a; Davis-Searles et al., 2005; Graf et al., 2007). Although the abundance of flavonolignans varies among different preparations, the most prevalent flavonolignans usually are the diastereoisomer pair silybin A and silybin B (Davis-Searles et al., 2005; Wen et al., 2008). Silychristin and silidianin also are relatively abundant in most silymarin preparations (Davis-Searles et al., 2005; Wen et al., 2008). The diastereoisomeric pair isosilybin A and isosilybin B, as well as isosilychristin, are relatively scarce in most preparations (Davis-Searles et al., 2005; Wen et al., 2008). Semi-purification of the crude extract yields a roughly 1:1 mixture of silybin A and silybin B, which is termed silibinin. The semi-purified mixture of isosilybin A and isosilybin B (isosilibinin) has been used in pre-clinical research but is not yet available as a commercial preparation (Kroll et al., 2007). Chemical modification of

silybin A and silybin B to increase water solubility for administration as an intravenous formulation led to generation of the dihemisuccinate ester derivative, Legalon SIL (Mengs et al., 2012). Since milk thistle products are purified from natural sources, large differences exist in the relative composition of the various constituents. With the exception of the prescription preparations available in some countries, there is no regulatory requirement for consistency between products. Consequently, high batch-to-batch and manufacturer-to-manufacturer variability in the relative abundance of milk thistle constituents is commonplace (Davis-Searles et al., 2005; Lee et al., 2006a; Wen et al., 2008).

Metabolism of Milk Thistle Constituents. Investigations into the metabolic clearance of milk thistle flavonolignans have focused on the oxidative and conjugative metabolism of silibinin. The major oxidative metabolite of silibinin is an *O*-demethyl product generated by cytochrome P450 (CYP) 2C8 in human liver microsomes (Gunaratna and Zhang, 2003; Jancova et al., 2007). All milk thistle flavonolignans share the methoxy moiety, part of the coniferyl alcohol, which does not participate in the conjugation to taxifolin. Thus, oxidation of this moiety could be similar among all flavonolignans. Formation of the mono- and di-methylated products was much lower than *O*-demethyl product upon oxidation of silibinin (Gunaratna and Zhang, 2003). Milk thistle flavonolignans are conjugated extensively by uridine 5'-diphospho-glucuronosyltransferases (UGTs). In human liver microsomes and hepatocytes, conjugation of silybin A and silybin B demonstrated preferential formation of the 7-*O*-glucuronide (Jancova et al., 2011). Among recombinant UGTs, UGT1A1, -1A3, -1A8, and -1A10 contributed to silybin A and silybin B metabolism (Jancova et al., 2011).

Pharmacokinetics of Milk Thistle Constituents. Following oral administration, milk thistle flavonolignans are absorbed rapidly, with maximal systemic concentrations achieved in less than two hours (Weyhenmeyer et al., 1992; Kim et al., 2003b; Wen et

al., 2008). As with many natural products based on a flavonoid scaffold, milk thistle bioavailability is low due to extensive pre-systemic conjugation by UGTs and sulfotransferases (SULTs) (Wen et al., 2008). Upon reaching the systemic circulation, parent flavonolignan clearance is rapid, with a terminal elimination half-life of less than 4 hours (Kim et al., 2003b; Wen et al., 2008). Systemic exposure to conjugated flavonolignans is consistently higher than parent flavonolignans. For example, exposure to conjugated isosilybin B was nearly 24-fold higher than that of the unconjugated parent in healthy volunteers following a 600 mg milk thistle dose (Wen et al., 2008). Subsequent to conjugation, flavonolignans are transported into the bile (Schandalik et al., 1992), and deconjugation in the intestine permits reabsorption and enterohepatic recirculation of flavonolignans. Renal clearance of total (unconjugated plus conjugated) silybin A and silybin B is roughly 30 mL/min, with approximately 5% of the dose eliminated in the urine as conjugates (Weyhenmeyer et al., 1992). Compared to healthy volunteers, Hepatitis C and nonalcoholic fatty liver disease patients have increased exposure to milk thistle flavonolignans and conjugated flavonolignans (Schrieber et al., 2008). Patients with extrahepatic biliary obstruction show increased systemic exposure to total, but not parent silibinin. This observation suggests that biliary excretion is rate-limiting for the clearance of conjugated metabolites but not the parent flavonolignans (Schandalik and Perucca, 1994).

Inhibition of Drug Metabolizing Enzymes. The inhibitory effects of milk thistle extracts and constituents depend on the preparation as well as the enzyme system and substrate tested. Silibinin has been shown to be a mechanism-based inhibitor of CYP2C9 and CYP3A4 in expressed enzymes (Sridar et al., 2004) or a reversible inhibitor of CYP2C9 (Jancova et al., 2007; Brantley et al., 2010) and CYP3A4 (Zuber et al., 2002; Jancova et al., 2007) in human liver microsomes (Table 1.2). The inhibitory potency of silibinin towards CYP3A4 appears to be substrate-dependent, with higher

potency towards oxidation of nifedipine (Beckmann-Knopp et al., 2000; Zuber et al., 2002) and testosterone (Jancova et al., 2007) than erythromycin (Beckmann-Knopp et al., 2000). Although silibinin constitutes nearly 50% of silymarin, silymarin extract is a more potent inhibitor of CYP2C19-mediated (*S*)-mephenytoin 4'-hydroxylation than silibinin (K_i = 2.2 μM vs. IC_{50} > 200 μM) (Beckmann-Knopp et al., 2000). Compared to the cytochromes P450, inhibition of UGT activity by milk thistle constituents is less studied. Silibinin demonstrated potent inhibition of recombinant UGT1A1-mediated 7-hydroxy-4-trifluoromethylcoumarin metabolism (IC_{50} = 1.4 μM) (Sridar et al., 2004), whereas milk thistle extract inhibited UGT1A-mediated estradiol metabolism in human liver microsomes, with an IC_{50} of nearly 40 μM (Mohamed et al., 2010).

Modulation of Drug Metabolizing Enzymes and Transporters in Cell Systems. The effect of milk thistle extracts on enzyme expression and activity in intact cell systems differs depending on the extract, cell system, and probe substrate examined. Silymarin was shown to decrease CYP3A4-mediated testosterone metabolism by 50% relative to vehicle control in human hepatocytes (Venkataramanan et al., 2000). Silibinin had no effect on cortisol metabolism in CYP3A4-expressing Caco-2 cells (Patel et al., 2004) (Table 1.3). The effect of milk thistle on P-glycoprotein (P-gp) was even more variable than on drug metabolizing enzymes. Silibinin decreased P-gp expression by nearly 70% in Caco-2 cells (Budzinski et al., 2007) but had no effect on ritonavir transport in either Caco-2 or MDCK cells (Patel et al., 2004). In contrast, silymarin inhibited the P-gp-mediated transport of digoxin and vinblastine in Caco-2 cells (Zhang and Morris, 2003a) and of daunomycin in MDA435/LCC6 cells (Zhang and Morris, 2003b). In addition to inhibition of efflux transporters, silymarin inhibited uptake of estradiol-17B-glucuronide and estrone-3-sulfate mediated by organic anion-transporting polypeptides (OATPs) 1B1, 1B3, and 2B1 in *xenopus* oocytes and HEK cells (Deng et al., 2008; Köck et al., 2013).

Milk Thistle-Drug Interaction Predictions. To date, no studies have investigated the drug interaction liability of milk thistle using *in silico* modeling and simulation. Of the reported in vitro studies that mention herb-drug interaction with milk thistle products, the majority urge caution when milk thistle products are co-administered with sensitive victim drugs due to unknown interaction liability (Beckmann-Knopp et al., 2000; Venkataramanan et al., 2000; Nguyen et al., 2003; Sridar et al., 2004; Etheridge et al., 2007; Deng et al., 2008; Brantley et al., 2010; Mohamed et al., 2010; Doehmer et al., 2011; Mohamed and Frye, 2011). The remaining studies dismiss interaction liability due to the low plasma concentrations of milk thistle constituents or low inhibitory potency (Zuber et al., 2002; Jancova et al., 2007; Doehmer et al., 2008). Taken together, accurate predictions of herb-drug interaction liability remain elusive.

Pre-Clinical Milk Thistle-Drug Interaction Studies. Silymarin increased resperidone exposure and maximal plasma concentration in rats following repeated oral doses, consistent with inhibition of P-gp (Lee et al., 2013) (Table 1.4). Silibinin also increased systemic exposure to tamoxifen in rats in a dose-dependent manner (Kim et al., 2010). Unlike for humans, tamoxifen disposition in the rat has not been defined. Although the exact mechanism for this increased exposure could not be identified, the net effect could reflect inhibition of one or more rodent orthologs of the relevant human enzymes and transporters.

Clinical Milk Thistle-Drug Interaction Studies. The clinical interaction liability of milk thistle products has been examined over the past decade (Table 1.5). Apart from increased exposure to losartan and talinolol (Han et al., 2009b), the majority of studies reported no clinically significant interactions. Limitations in study design and lack of information about the composition of the milk thistle preparations may have hampered detection of a clinically significant interaction.

Relatively low doses of silymarin (140 mg TID) inhibited the CYP2C9- and CYP3A4-mediated hepatic clearance of losartan, leading to a doubling in losartan exposure in *CYP2C9*1/*1* subjects. Individuals carrying the *CYP2C9*3* allele (reduced activity allele of CYP2C9) experienced an increase in maximal losartan concentrations without a significant increase in systemic exposure (Han et al., 2009b). Losartan is a prodrug that is converted to the active metabolite E-3174 by CYP2C9. Consistent with a decrease in formation clearance by CYP2C9, exposure to the active metabolite was decreased following milk thistle administration. The decrease was relatively modest (~15%), indicating limited clinical importance of this interaction (Han et al., 2009b). However, clinically important interactions with larger doses of milk thistle or a more sensitive CYP2C9 substrate cannot be dismissed.

Studies of the interaction between milk thistle and HIV-protease inhibitors demonstrated no interaction; however, extrapolations of the results are limited due to study design considerations. Long-term administration of milk thistle products (2-4 weeks) at various doses (160-450 mg TID) did not lead to significant changes in indinavir exposure or maximal concentration (Piscitelli et al., 2002; DiCenzo et al., 2003; Mills et al., 2005). Plasma exposure and maximal concentration of indinavir decreased following milk thistle administration (by 8.8 and 9.2%, respectively), which is inconsistent with inhibition of CYP3A4 (Piscitelli et al., 2002). Interaction studies with indinavir are not amenable to fixed sequence design because indinavir alone exhibits significant decreases in systemic exposure following long-term treatment. Compared to baseline conditions, healthy volunteers showed a 40% decrease in exposure 7 days after a 28-day cycle of indinavir (Mills et al., 2005). Indinavir also is a potent CYP3A inhibitor, which would decrease study sensitivity to detect mild or moderate inhibition of CYP3A. As with indinavir, milk thistle administration with ritonavir or darunavir was not associated with a significant change in drug exposure in HIV-infected patients (Molto et al., 2012).

Ritonavir also is a potent CYP3A inhibitor, which would decrease greatly the sensitivity to detect further enzyme inhibition.

Summary and Perspectives

Herbal product usage likely will continue to increase, in part due to attempts by consumers to decrease medical costs through self-diagnosis and treatment. In parallel, the prevalence of concomitant administration of herbal products with conventional medications will increase. Despite the mounting likelihood of herb-drug interactions, there remains no standard system for evaluating herb-drug interaction liability. The complex nature and high compositional variability of herbal products make evaluation of herb-drug interactions more challenging than DDIs. Moreover, regulatory agencies request varying degrees of pre-market safety information regarding herbal products. Taken together, there is an unprecedented opportunity to develop a framework for improving predictions of herb-drug interactions. The strategies to evaluate conventional DDIs, such as integrating in vitro parameters and the pharmacokinetics of individual herbal product constituents into PBPK interaction models, should be applied to herbal products in a prospective manner. Adoption of these strategies may streamline safety assessment of natural products, assist in the management of herb-drug interactions, and ultimately promote the safe use of herbal products.

Project Overview

The risk of untoward interactions between herbal products and conventional drugs is increasing as a function of the increasing usage of herbal products. Despite the increased risk, there remains no standard system for evaluating herb-drug interaction potential. Complicating this evaluation is the large compositional variability and unidentified constituents in herbal products. Advances in isolation and purification techniques allow testing of the interaction potential of individual constituents using standard in vitro methods. Incorporation of the recovered kinetic parameters into a physiologically based pharmacokinetic (PBPK) model will allow improved herb-drug interaction predictions. Extrapolation of this methodology will facilitate improved decisions regarding the addition of herbal products to conventional pharmacology.

The goal of this dissertation project was to evaluate the potential of an herbal product-drug interaction using a PBPK modeling approach and milk thistle as an exemplar herbal product. The central hypothesis was that integrating the in vitro inhibition kinetics of individual milk thistle constituents into a PBPK interaction model will enable accurate predictions of herb-drug interactions. The central hypothesis was tested with the subsequent specific aims:

Specific Aim 1: Determine the interaction potential of milk thistle constituents and commercial preparations using in vitro screens of CYP inhibition.

Hypothesis: Human liver- and intestine-derived systems can be used to determine the inhibitory potency of individual milk thistle constituents, as well as commercial preparations, on key drug metabolizing enzymes.

1A. Determine the reversible and/or mechanism-based inhibition kinetics of milk thistle commercial preparations and individual constituents on CYP2C9 activity using human-derived microsomes and recombinant enzymes.

1B. Determine the reversible and/or mechanism-based inhibition kinetics of commercially available milk thistle preparations and individual constituents on CYP3A4/5 using human-derived microsomes and recombinant enzymes.

Specific Aim 2: Predict the clinical impact of co-administration of a milk thistle product with prototypic cytochrome P450 probe substrates.

Hypothesis: PBPK interaction models can accurately predict the likelihood and magnitude of an herbal product-drug interaction.

2A. Develop a PBPK model for the cytochrome P450 probe substrates (*S*)-warfarin (CYP2C9) and midazolam (CYP3A4/5).

2B. Develop a PBPK model for selected milk thistle constituents using parameters obtained from Aim 1.

2C. Develop a PBPK interaction model using parameters obtained from Aim 1 and integrating the models created in Aim 2A and 2B.

Specific Aim 3: Evaluate model predictions *via* a proof-of-concept clinical study.

Hypothesis: Predictions of herbal product-drug interactions can be validated using a proof-of-concept clinical study.

3A. Determine the relative composition of a selected milk thistle product with regard to the inhibitory constituents identified in Aim 1.

3B. Evaluate the accuracy of the PBPK model predictions *via* a clinical study.

The purpose of this dissertation was to determine if PBPK interaction models can facilitate predictions of the likelihood and magnitude of herb -drug interactions through identification of drug interaction perpetrators contained in the exemplar herbal product milk thistle and simulating the interaction potential of those constituents on the metabolism of victim drugs. This novel framework will provide a streamlined approach to study herbal product-drug interactions, and has the potential to predict drug interactions from current and future combinations of herbal products and victim drugs.

Legends to Figures

Figure 1.1. Biochemical mechanisms of metabolic herb-drug interactions. In the absence of herbal constituents, drug molecules are metabolized by enzymes. Competitive inhibition by an herbal constituent prevents the drug molecule from binding to the active site of the enzyme. Noncompetitive inhibition by an herbal constituent decreases the catalytic activity of the drug metabolizing enzyme without interfering with the binding of drug molecule to the enzyme active site. Uncompetitive inhibition by an herbal constituent modulates apparent affinity and activity by binding to the enzyme-drug molecule complex. Irreversible inhibition occurs when the herbal constituent mediates enzymatic degradation. Enzyme induction occurs when herbal constituents bind to nuclear receptors and activate mRNA expression and protein synthesis.

Figure 1.2. Chemical structures of milk thistle constituents.

Table 1.1 Key regulatory guidance points

Guidance Points	**Country / Union**		
	United States	European Union	Canada
Regulatory Authorization	Dietary Supplement Health and Education Act of 1994	Directive 2002/46/EC Directive 2004/24/EC	Natural Health Products Regulations
Regulatory Agency	US Food and Drug Administration	European Medicines Agency (EMA) Committee on Herbal Medicinal Products	Health Canada (Natural Health Product Directorate branch)
Classifications	Dietary Supplements	Traditional Plant Food Supplement Traditional Herbal Medicinal Products	Natural Health Product
Safety data required pre-marketing	Yes for ingredients introduced after 1994	Extent of required data dependent on classification and member country competent authority	Yes for all products
Adverse Event Reporting	Manufacturers are required to inform FDA of any adverse events reported directly to the manufacturer	Pharmacovigilance maintained by EMA, manufacturers, and health care practitioners	Manufacturers required to monitor adverse events and report serious adverse events to Health Canada
Requirement of Good Manufacturing Practices	Modeled after food GMP Required for all manufacturers in 2010	Required for all products	Required for all products
Label Requirements	• Name of each ingredient • Quantity of each ingredient • Contact information for the manufacturer • The statement “Not evaluated by the FDA. Not intended to diagnose, treat, cure, or prevent any disease”	• Exact centesimal product formula • Exact nature of plants/extracts present • Conditions of use • Possible interactions with drugs and/or foods	• Common and proper name of each medicinal ingredient • Quantity of each medicinal ingredient • Recommended use, dose, route of administration, duration of use • Risk information • Lot number and expiry date • Description of source material for each medicinal ingredient
Permissible Health Claims	Characterize the means by which the dietary supplement acts to maintain the normal structure or function in humans Not required to be pre-approved	Health claims must be consistent with recognized physiological effect and the degree to which the claimed effect is demonstrated. Evaluated before marketing	Health claims regarding preventing Schedule A diseases are allowed provided that they are supported by sufficient evidence

Table 1.2 Milk thistle interaction kinetics in enzyme preparations.

Enzyme Source	Milk Thistle Preparation	Enzyme	Substrate	Outcome	Reference
Pooled HLM	Silybin A	CYP2C9	(*S*)-Warfarin	K_i, 10 μM	(Brantley et al., 2010)
	Silybin B			K_i, 4.8 μM	
E. coli expressed	Silibinin	CYP2C9	7-EFC[a]	K_I 5 μM	(Sridar et al., 2004)
		CYP3A4	7-BFC[b]	K_I 32 μM	
			Testosterone	K_I 166 μM	
HLM (2 preparations)	Silibinin	CYP1A2	Caffeine	IC_{50}, >200, >200 μM	(Beckmann-Knopp et al., 2000)
		CYP2A6	Coumarin	IC_{50}, >200, >200 μM	
		CYP2C9	*(S)*-Warfarin	IC_{50}, 43, 45 μM	
		CYP2C19	*(S)*-Mephenytoin	IC_{50}, >200, >200 μM	
		CYP2D6	Dextromethorphan	IC_{50}, 173, >200 μM	
		CYP2E1	Chlorozoxazone	IC_{50}, >200, >200 μM	
		CYP3A4	Denitronifedipine	IC_{50}, 29,46 μM	
			Erythromycin	IC_{50}, >200, >200 μM	
HLM (2 preparations)	Silibinin	CYP2D6	Bufuralol	K_i, nd, 8.2 μM	(Zuber et al., 2002)
		CYP2E1	ρ-Nitrophenol	K_i, nd, 28.7 μM	
		CYP3A4	Nifedipine	K_i 4.9, 9.0 μM	
Pooled HLM	Silibinin	CYP1A2	Ethoxyresorufin	K_i, 165 μM	(Jancova et al., 2007)
		CYP2C9	Diclofenac	K_i, 75 μM	
		CYP3A4	Testosterone	K_i, 21 μM	
Pooled HLM	Silymarin[c]	CYP2C19	*(S)*-Mephenytoin	K_i, 2.2 μM	(Doehmer et al., 2008)
		CYP2D6	Bufarolol	K_i, 11.6 μM	
		CYP3A4	Testosterone	K_i, 12.0 μM	
Pooled HLM	Milk Thistle Extract	CYP2C8	Paclitaxel	K_i, 8.35 μg/mL	(Doehmer et al., 2011)
		CYP2C9	Diclofenac	K_i, 9.42 μg/mL	
		CYP2C19	Mephenytoin	K_i, 33.0 μg/mL	
		CYP2D6	Bufarolol	K_i, 68.9 μg/mL	
		CYP3A4	Testosterone	K_i, 12.5 μg/mL	
Pooled (n=3) HLM	Milk Thistle Extract[d]	CYP1A2	Acetanilide	<20% ↓ in activity at 10 μM	(Etheridge et al., 2007)
		CYP2C8	Paclitaxel	66% ↓ in activity at 10 μM	
		CYP2C9	Tolbutamide	No inhibition at 1 μM[e]	
		CYP2C19	*(S)*-Mephenytoin	<30% ↓ in activity at 10 μM	
		CYP2D6	Dextromethorphan	<20% ↓ in activity at 10 μM	
		CYP2E1	ρ-Nitrophenol	<20% ↓ in activity at 10 μM	
		CYP3A4	Midazolam	43% ↓ in activity at 10 μM	
			Testosterone	43% ↓ in activity at 10 μM	
Recombinant	Silibinin	UGT1A1	7-HFC[f]	IC_{50}, 1.4 μM	(Sridar et al., 2004)
		UGT1A6		IC_{50}, 28 μM	
		UGT1A9		IC_{50}, 20 μM	
		UGT2B7		IC_{50}, 92 μM	
		UGT2B15		IC_{50}, 75 μM	
Pooled HLM	Milk Thistle Extract	UGT1A1	Estradiol	IC_{50}, 18 μg/mL	(Mohamed et al., 2010)
Pooled HLM	Milk Thistle Extract	UGT1A4	Trifluoperazine	Interference	(Mohamed and Frye, 2011)
		UGT1A6	Seratonin	IC_{50}, 59.5 μg/mL	
		UGT1A9	Mycophenolic acid	IC_{50}, 33.6 μg/mL	

HLM, human liver microsomes; nd, not determined
[a]7-EFC, 7-ethoxy-4-(trifluoromethyl)coumarin
[b]7-BFC, 7-benzyloxy-4-(trifluoromethyl)coumarin
[c]Concentrations reported as silibinin equivalents
[d] Standardized to silybin B (21.1% of extract) content
[e]Activity not reported at 10 μM
[f]7-HFC, 7-hydroxy-4-(trifluoromethyl)coumarin

Table 1.3 Milk thistle interaction kinetics in cell systems.

Cell System	Milk Thistle Preparation	Enzyme or Transporter	Substrate	Incubation Conditions	Outcome	Reference
Human Hepatocytes	Silymarin	CYP3A4	Testosterone	48 hours at 100 µM	50% ↓ in activity	(Venkataramanan et al., 2000)
		UGT1A6/9	4MU		65% ↓ in activity	
Human hepatocytes	Silibinin	CYP1A2	NA	72 hours at 100 µM	No change in mRNA or protein expression	(Kosina et al., 2005)
		CYP3A4				
Human Hepatocytes	Silymarin	CYP2C9	Diclofenac	72 hours at 100 µM	No induction	(Doehmer et al., 2008)
		CYP3A4	Testosterone			
Human Hepatocytes (3 donors per enzyme)	Milk Thistle Extract	CYP1A2	7-Ethoxyresorufin	72 hours at 50 µg/mL	1.1-8.5 fold induction	(Doehmer et al., 2011)
		CYP2B6	(*S*)-Mephenytoin		0.3-2.7 fold induction	
		CYP2C9	Diclofenac		0.7-1.6 fold induction	
		CYP2E1	Chlorzoxazone		2.0-3.0 fold induction	
		CYP3A4	Testosterone		0.4-1.3 fold induction	
Caco-2 cells	Silibinin	CYP3A4	NA	48 hours at 10 µM	9% ↓ in protein	(Budzinski et al., 2007)
		P-gp			69% ↑ in protein	
Caco-2 cells	Silymarin	P-gp	Digoxin	1 hour at 150 µM	23% ↑ in accumulation	(Zhang and Morris, 2003a)
			Vinblastine		80% ↑ in accumulation	
Caco-2 cells	Silibinin	CYP3A4	Cortisol	30 minutes	No inhibition	(Patel et al., 2004)
		P-gp	Ritonavir		No change in transport	
MDR1 transfected MDCK cells		P-gp	Ritonavir			
MDA435/LCC6 cells	Silymarin	P-gp	Daunomycin	2 hours at 50 µM	4.5 fold ↑ in accumulation	(Zhang and Morris, 2003b)
Panc-1 cells	Silymarin	MRP1	Daunomycin	2 hours at 100 µM	3.1 fold ↑ in accumulation	(Nguyen et al., 2003)
			Vinblastine		3.3 fold ↑ in accumulation	
BCRP-overexpressing membrane vesicles	Milk Thistle Extract	BCRP	Methotrexate	2 minutes at 1,000 µg/mL	45.4% ↓ in transport	(Tamaki et al., 2010)
MCF-7 MX100 cells	Silymarin	BCRP	Mitoxantrone	15 min preincubation, 30 min coincubation	EC_{50}, 33.7 µM	(Zhang et al., 2004)
BCRP transfected MDCK cells	Silymarin	BCRP	Rosuvastatin	1 h incubation	Ki, 97.9 uM	(Deng et al., 2008)
OATP1B1 transfected *xenopus* oocytes		OATP1B1		30 min incubation	Ki, 0.93 uM	
HEK293-OATP1B1	Silymarin	OATP1B1	Estradiol-17-β-glucuronide	3 min incubation	IC_{50}, 1.3 µM	(Köck et al., 2013)
HEK293-OATP1B3		OATP1B3			IC_{50}, 2.2 µM	
MDCKII-OATP2B1		OATP2B1	Estrone-3-sulfate		IC_{50}, 0.3 µM	

4MU, 4-methylumbelliferone; NA, not applicable

Table 1.4 Milk thistle interaction kinetics in pre-clinical animal models.

Milk Thistle Preparation	Animal Species (n)	Test Substrate Administration Regimen	Enzyme[a] or Transporter	Outcome	Reference
Silibinin 0.5 mg/kg PO[b]	Rats (6/arm)	Tamoxifen 10 mg/kg PO	CYP3A4 CYP2D6 P-gp	1.2 fold ↑ in C_{max} 1.2 fold ↑ in AUC_{inf}	(Kim et al., 2010)
Silibinin 2.5 mg/kg PO				1.5 fold ↑ in C_{max} 1.4 fold ↑ in AUC_{inf}	
Silibinin 10 mg/kg PO				1.8 fold ↑ in C_{max} 1.7 fold ↑ in AUC_{inf}	
Silibinin 175 mg/kg 7 days prior to test substrate	Male Sprague-Dawley Rats (6/arm)	Trazodone 5 mg/kg IV[c]	CYP3A4	12% ↓ in C_{max} No change in AUC	(Chang et al., 2009)
Silibinin 350 mg/kg 7 days prior to test substrate				30% ↓ in C_{max} 8% ↓ in AUC	
Silymarin 500 mg/kg 7 days prior to test substrate				No change in C_{max} 20% ↓ in AUC	
Silymarin 1,000 mg/kg 7 days prior to test substrate				No change in C_{max} 43% ↓ in AUC	
Silymarin 1,000 mg/kg 4 hours prior to test substrate				238% ↑ in C_{max} 3% ↑ in AUC	
Silymarin 40 mg/kg PO coadministered with test substrate	Rats	Resperidone 6 mg/kg PO	P-gp	1.3 fold ↑ in C_{max} No change in AUC_{inf}	(Lee et al., 2013)
Silymarin 40 mg/kg PO 5 days prior to test substrate				2.4 fold ↑ in C_{max} 1.7 fold ↑ in AUC_{inf}	
Silibinin 30 mg/kg IV	Rats (6/arm)	Pyrazinamide 50 mg/kg IV	Xanthine oxidase	21% ↑ in C_{max} 5% ↑ in AUC	(Wu and Tsai, 2007)
		Pyrazinoic acid 30 mg/kg IV		320% ↑ in C_{max} 420% ↑ in AUC	
Silibinin 100 mg/kg PO for 4 days		Pyrazinamide 50 mg/kg IV		22% ↑ in C_{max} 6% ↓ in AUC	
		Pyrazinoic acid 30 mg/kg IV		260% ↑ in C_{max} 350% ↑ in AUC	

[a]Human ortholog responsible for metabolism/transport of test substrate
[b]Orally administered
[c]Intravenously administered

Table 1.5 Clinical evaluation of milk thistle drug interaction liability

Milk Thistle Preparation Administration Regimen	Subjects (n)	Probe Substrate Administration Regimen	Enzyme or Transporter	Clinical Outcome	Reference
Milk Thistle 175 mg BID for 4 weeks	12 healthy volunteers (6 women)	Caffeine 100 mg	CYP1A2	4.8% ↓ in Phenotypic Ratio	(Gurley et al., 2004)
		Debrisoquine 5 mg	CYP2D6	1.0% ↓ in Phenotypic Ratio	
		Clorzoxazone 250 mg	CYP2E1	1.1% ↑ in Phenotypic Ratio	
		Midazolam 8 mg	CYP3A4	7.8% ↓ in Phenotypic Ratio	
Milk Thistle 175 mg TID for 2 weeks	6 healthy Chinese men (CYP2C9*1/*1)	Losartan 50 mg	CYP2C9	90% ↑ in C_{max} 110% ↑ in AUC_{0-inf}	(Han et al., 2009b)
	6 healthy Chinese men (CYP2C9*1/*3)			41% ↑ in C_{max} 1.0% ↑ in AUC_{0-inf}	
Milk Thistle 300 mg TID for 2 weeks	16 healthy volunteers (8 women)	Debrisoquine 5 mg	CYP2D6	3.2% ↓ in urinary recovery ratio	(Gurley et al., 2008)
Milk Thistle 200 mg TID for 4 days	6 cancer patients (4 women)	Irinotecan 125 mg/m2 90 min IV infusion	CYP3A4 and UGT1A1	7.7% ↑ in C_{max} 16% ↑ in AUC	(van Erp et al., 2005)
200 mg TID for 12 days				3.2% ↑ in C_{max} 14% ↑ in AUC	
Milk Thistle 175 TID for 3 weeks	10 healthy volunteers (4 women)	Indinavir 800 mg 4 doses 8 hours apart	CYP3A4	9.2% ↓ in C_{max} 8.8% ↓ in AUC_{0-8}	(Piscitelli et al., 2002)
Milk Thistle 160 mg TID for 2 weeks	10 healthy volunteers (3 women)	Indinavir 800 mg 4 doses 8 hours apart	CYP3A4	11% ↓ in C_{max} 6.3% ↓ in AUC_{0-8}	(DiCenzo et al., 2003)
Milk Thistle 450 mg TID for 30 days	16 healthy male volunteers	800 mg indinavir 3 doses 8 hours apart	CYP3A4	4.9% ↓ in C_{max} 4.4% ↓ in AUC_{0-8}	(Mills et al., 2005)
Milk Thistle 150 mg TID for 2 weeks	15 male HIV patients (4 co-infected with HCV)	Darunavir 600 mg	CYP3A4	17% ↓ in C_{max} 14% ↓ in AUC_{0-12}	(Molto et al., 2012)
		Ritonavir 100 mg		10% ↓ in C_{max} 11% ↓ in AUC_{0-12}	
Milk thistle extract 300 mg TID for 14 days	19 healthy volunteers (9 women)	Midazolam 8 mg	CYP3A4	6.5% ↑ in C_{max} 2.8% ↑ in AUC	(Gurley et al., 2006a)
Milk Thistle 280 mg 10 and 1.5 hours before nifedipine	16 healthy male volunteers	Nifedipine 10 mg	CYP3A4	30% ↓ in C_{max} 13% ↑ in AUC_{0-inf}	(Fuhr et al., 2007)
Silymarin 140 mg TID for 14 days	12 healthy male volunteers	Ranitidine 150 mg	CYP3A4 and P-gp	7.6% ↑ in C_{max} 4.2% ↓ in AUC_{0-12}	(Rao et al., 2007)
Silymarin 140 mg TID for 3 days before and 2 days after rosuvastatin	8 Healthy Korean men	Rosuvastatin 10 mg 1 hour after AM silymarin	OATP1B1 & BCRP	7.5% ↓ in C_{max} 6.5% ↓ in AUC	(Deng et al., 2008)
Milk Thistle 175 mg TID for 2 weeks	6 healthy Chinese men MDR1 3435CC	Talinolol 100 mg	P-gp	43% ↑ in C_{max} 22% ↑ in AUC_{0-inf}	(Han et al., 2009a)
	6 healthy Chinese men MDR1 3435CT			40% ↑ in C_{max} 37% ↑ in AUC_{0-inf}	
	6 healthy Chinese men MDR1 3435TT			1% ↑ in C_{max} 21% ↑ in AUC_{0-inf}	
Milk thistle 300 mg TID for 14 days	16 healthy volunteers (8 women)	Digoxin 0.4 mg	P-gp	13% ↓ in C_{max} 9.4% ↓ in AUC_{0-24}	(Gurley et al., 2006b)

Figure 1.1. Biochemical mechanisms of metabolic drug herb-drug interactions

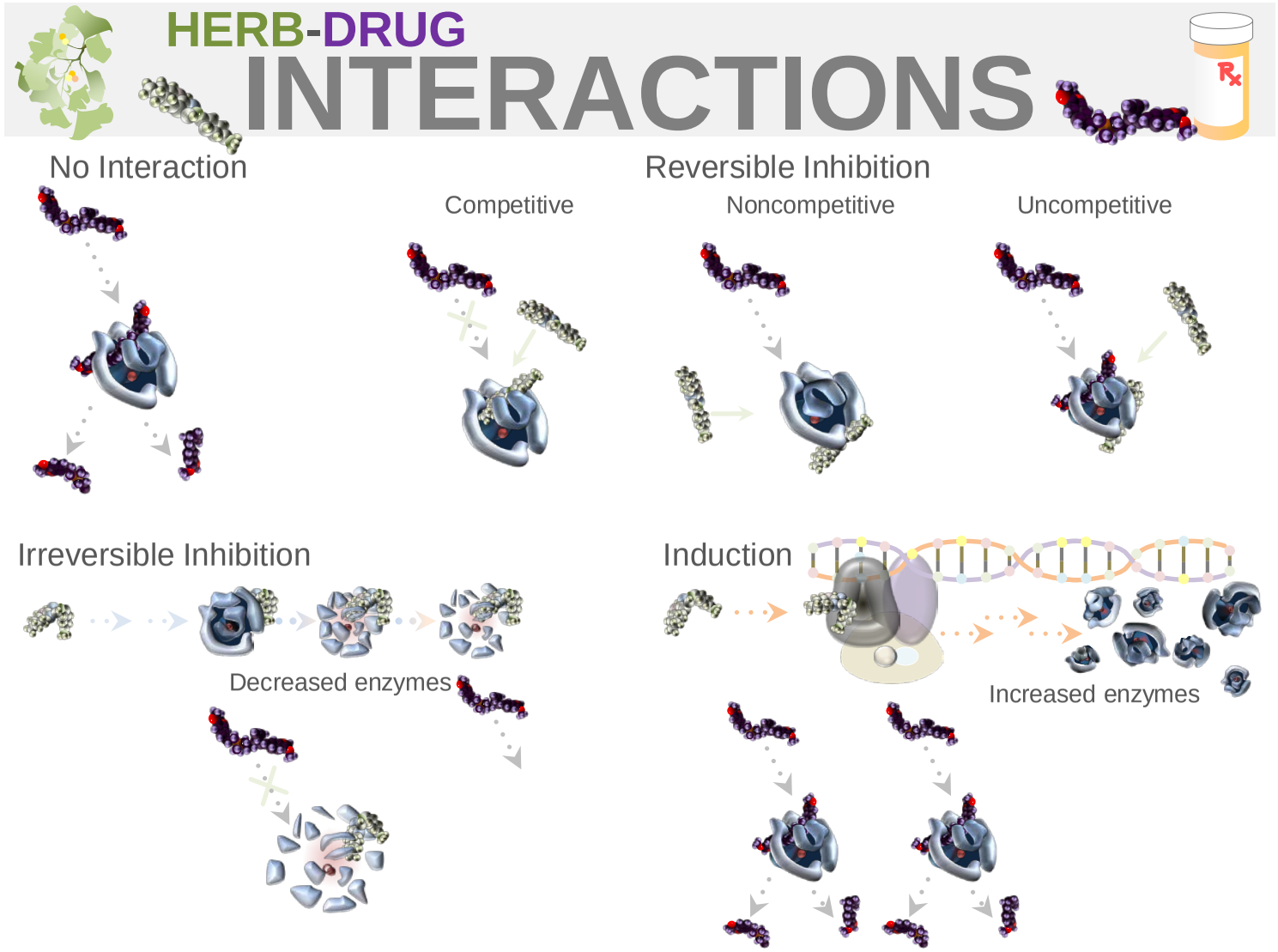

Figure 1.2. Chemical structures of milk thistle constituents

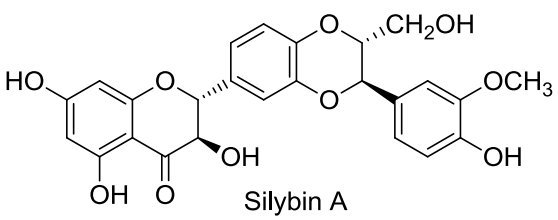

Silybin A

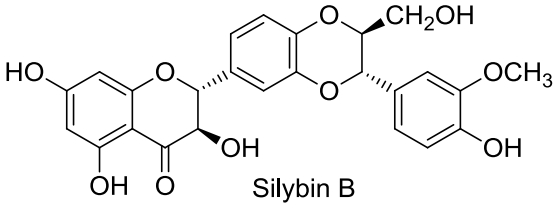

Silybin B

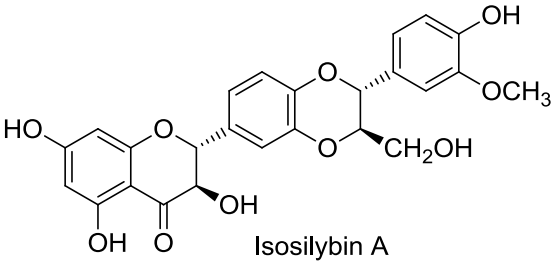

Isosilybin A

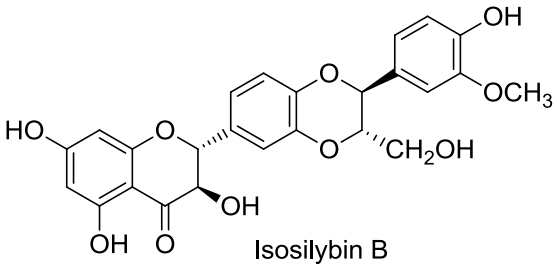

Isosilybin B

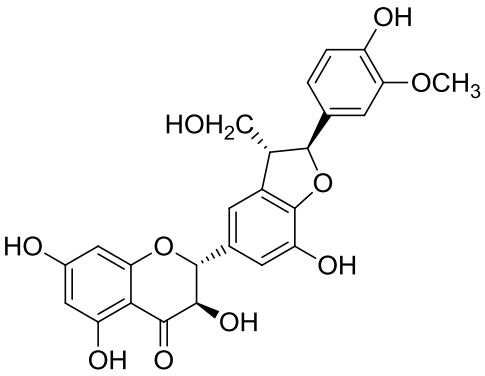

Silychristin

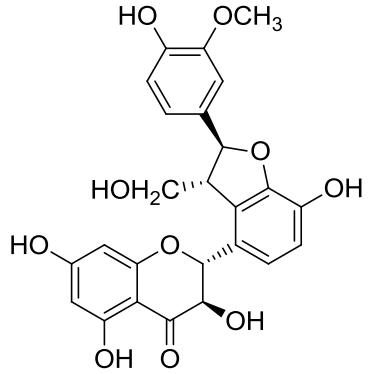

Isosilychristin

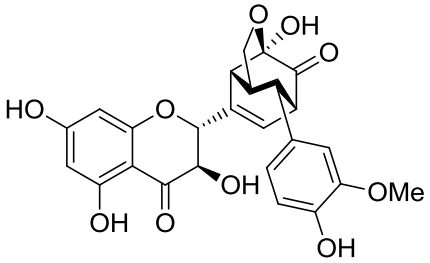

Silydianin

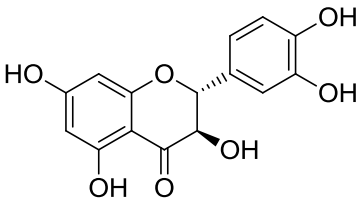

Taxifolin

References

Agarwal R, Agarwal C, Ichikawa H, Singh RP and Aggarwal BB (2006) Anticancer potential of silymarin: from bench to bed side. *Anticancer Res* **26:**4457-4498.

Annaba F, Sarwar Z, Kumar P, Saksena S, Turner JR, Dudeja PK, Gill RK and Alrefai WA (2008) Modulation of ileal bile acid transporter (ASBT) activity by depletion of plasma membrane cholesterol: association with lipid rafts. *Am J Physiol Gastrointest Liver Physiol* **294:**G489-497.

Arnaud O, Koubeissi A, Ettouati L, Terreux R, Alame G, Grenot C, Dumontet C, Di Pietro A, Paris J and Falson P (2010) Potent and fully noncompetitive peptidomimetic inhibitor of multidrug resistance P-glycoprotein. *J Med Chem* **53:**6720-6729.

Beckmann-Knopp S, Rietbrock S, Weyhenmeyer R, Bocker RH, Beckurts KT, Lang W, Hunz M and Fuhr U (2000) Inhibitory effects of silibinin on cytochrome P-450 enzymes in human liver microsomes. *Pharmacol Toxicol* **86:**250-256.

Bent S (2008) Herbal medicine in the United States: review of efficacy, safety, and regulation: grand rounds at University of California, San Francisco Medical Center. *J Gen Intern Med* **23:**854-859.

Bjornsson TD, Callaghan JT, Einolf HJ, Fischer V, Gan L, Grimm S, Kao J, King SP, Miwa G, Ni L, Kumar G, McLeod J, Obach SR, Roberts S, Roe A, Shah A, Snikeris F, Sullivan JT, Tweedie D, Vega JM, Walsh J and Wrighton SA (2003) The conduct of in vitro and in vivo drug-drug interaction studies: a PhRMA perspective. *J Clin Pharmacol* **43:**443-469.

Blumenthal M, Lindstrom A, Lynch M and Rea P (2011) Market Report. Herb Sales Continue Growth -- Up 3.3% in 2010. *HerbalGram* **May-Jul** 4.

Boecker BB (2003) Reference values for basic human anatomical and physiological characteristics for use in radiation protection. *Radiat Prot Dosimetry* **105:**571-574.

Brantley SJ, Oberlies NH, Kroll DJ and Paine MF (2010) Two flavonolignans from milk thistle (*Silybum marianum*) inhibit CYP2C9-mediated warfarin metabolism at clinically achievable concentrations. *Journal of Pharmacology & Experimental Therapeutics* **332:**1081-1087.

Brown RP, Delp MD, Lindstedt SL, Rhomberg LR and Beliles RP (1997) Physiological parameter values for physiologically based pharmacokinetic models. *Toxicol Ind Health* **13:**407-484.

Brownie S (2005) The development of the US and Australian dietary supplement regulations. What are the implications for product quality? *Complement Ther Med* **13:**191-198.

Budzinski JW, Trudeau VL, Drouin CE, Panahi M, Arnason JT and Foster BC (2007) Modulation of human cytochrome P450 3A4 (CYP3A4) and P-glycoprotein (P-gp)

in Caco-2 cell monolayers by selected commercial-source milk thistle and goldenseal products. *Can J Physiol Pharmacol* **85:**966-978.

Camfield DA, Sarris J and Berk M (2011) Nutraceuticals in the treatment of obsessive compulsive disorder (OCD): a review of mechanistic and clinical evidence. *Prog Neuropsychopharmacol Biol Psychiatry* **35:**887-895.

Chang JC, Wu YT, Lee WC, Lin LC and Tsai TH (2009) Herb-drug interaction of silymarin or silibinin on the pharmacokinetics of trazodone in rats. *Chem Biol Interact* **182:**227-232.

Chu X, Bleasby K and Evers R (2013) Species differences in drug transporters and implications for translating preclinical findings to humans. *Expert Opin Drug Metab Toxicol* **9:**237-252.

Clay AT and Sharom FJ (2013) Lipid bilayer properties control membrane partitioning, binding, and transport of p-glycoprotein substrates. *Biochemistry* **52:**343-354.

Davis-Searles PR, Nakanishi Y, Kim NC, Graf TN, Oberlies NH, Wani MC, Wall ME, Agarwal R and Kroll DJ (2005) Milk thistle and prostate cancer: differential effects of pure flavonolignans from *Silybum marianum* on antiproliferative end points in human prostate carcinoma cells. *Cancer Res* **65:**4448-4457.

de Lima Toccafondo Vieira M and Huang SM (2012) Botanical-drug interactions: a scientific perspective. *Planta Med* **78:**1400-1415.

De Smet PA (2005) Herbal medicine in Europe--relaxing regulatory standards. *N Engl J Med* **352:**1176-1178.

Deng JW, Shon JH, Shin HJ, Park SJ, Yeo CW, Zhou HH, Song IS and Shin JG (2008) Effect of silymarin supplement on the pharmacokinetics of rosuvastatin. *Pharm Res* **25:**1807-1814.

DiCenzo R, Shelton M, Jordan K, Koval C, Forrest A, Reichman R and Morse G (2003) Coadministration of milk thistle and indinavir in healthy subjects. *Pharmacotherapy* **23:**866-870.

Doehmer J, Tewes B, Klein KU, Gritzko K, Muschick H and Mengs U (2008) Assessment of drug-drug interaction for silymarin. *Toxicol In Vitro* **22:**610-617.

Doehmer J, Weiss G, McGregor GP and Appel K (2011) Assessment of a dry extract from milk thistle (Silybum marianum) for interference with human liver cytochrome-P450 activities. *Toxicol In Vitro* **25:**21-27.

Efferth T and Koch E (2011) Complex interactions between phytochemicals. The multi-target therapeutic concept of phytotherapy. *Curr Drug Targets* **12:**122-132.

El-Kamary SS, Shardell MD, Abdel-Hamid M, Ismail S, El-Ateek M, Metwally M, Mikhail N, Hashem M, Mousa A, Aboul-Fotouh A, El-Kassas M, Esmat G and Strickland GT (2009) A randomized controlled trial to assess the safety and efficacy of

silymarin on symptoms, signs and biomarkers of acute hepatitis. *Phytomedicine* **16:**391-400.

Etheridge AS, Black SR, Patel PR, So J and Mathews JM (2007) An in vitro evaluation of cytochrome P450 inhibition and P-glycoprotein interaction with goldenseal, Ginkgo biloba, grape seed, milk thistle, and ginseng extracts and their constituents. *Planta Med* **73:**731-741.

European Medicines Agency (2012) Guideline on the investigation of drug interactions, London, UK.

Flaig TW, Gustafson DL, Su LJ, Zirrolli JA, Crighton F, Harrison GS, Pierson AS, Agarwal R and Glode LM (2007) A phase I and pharmacokinetic study of silybin-phytosome in prostate cancer patients. *Invest New Drugs* **25:**139-146.

Forte JS and Raman A (2000) Regulatory issues relating to herbal products-part 1: legislation in the European union, north america, and australia. *J Med Food* **3:**23-39.

Fried MW, Navarro VJ, Afdhal N, Belle SH, Wahed AS, Hawke RL, Doo E, Meyers CM and Reddy KR (2012) Effect of silymarin (milk thistle) on liver disease in patients with chronic hepatitis C unsuccessfully treated with interferon therapy: a randomized controlled trial. *JAMA* **308:**274-282.

Fuhr U, Beckmann-Knopp S, Jetter A, Luck H and Mengs U (2007) The effect of silymarin on oral nifedipine pharmacokinetics. *Planta Med* **73:**1429-1435.

Gagnier J, Boon H, Rochon P, Barnes J, Moher D and Bombardier C (2006) Improving the quality of reporting of randomized controlled trials evaluating herbal interventions: implementing the CONSORT statement [corrected]. *Explore (NY)* **2:**143-149.

Gardiner P, Graham RE, Legedza AT, Eisenberg DM and Phillips RS (2006) Factors associated with dietary supplement use among prescription medication users. *Arch Intern Med* **166:**1968-1974.

Gharagozloo M, Moayedi B, Zakerinia M, Hamidi M, Karimi M, Maracy M and Amirghofran Z (2009) Combined therapy of silymarin and desferrioxamine in patients with beta-thalassemia major: a randomized double-blind clinical trial. *Fundam Clin Pharmacol* **23:**359-365.

Goldman P (2001) Herbal medicines today and the roots of modern pharmacology. *Ann Intern Med* **135:**594-600.

Gordon A, Hobbs DA, Bowden DS, Bailey MJ, Mitchell J, Francis AJ and Roberts SK (2006) Effects of Silybum marianum on serum hepatitis C virus RNA, alanine aminotransferase levels and well-being in patients with chronic hepatitis C. *J Gastroenterol Hepatol* **21:**275-280.

Graf TN, Wani MC, Agarwal R, Kroll DJ and Oberlies NH (2007) Gram-scale purification of flavonolignan diastereoisomers from *Silybum marianum* (milk thistle) extract in

support of preclinical in vivo studies for prostate cancer chemoprevention. *Planta Med* **73:**1495-1501.

Grimm SW, Einolf HJ, Hall SD, He K, Lim HK, Ling KH, Lu C, Nomeir AA, Seibert E, Skordos KW, Tonn GR, Van Horn R, Wang RW, Wong YN, Yang TJ and Obach RS (2009) The conduct of in vitro studies to address time-dependent inhibition of drug-metabolizing enzymes: a perspective of the pharmaceutical research and manufacturers of America. *Drug Metab Dispos* **37:**1355-1370.

Gunaratna C and Zhang T (2003) Application of liquid chromatography-electrospray ionization-ion trap mass spectrometry to investigate the metabolism of silibinin in human liver microsomes. *J Chromatogr B Analyt Technol Biomed Life Sci* **794:**303-310.

Gurley B, Hubbard MA, Williams DK, Thaden J, Tong Y, Gentry WB, Breen P, Carrier DJ and Cheboyina S (2006a) Assessing the clinical significance of botanical supplementation on human cytochrome P450 3A activity: comparison of a milk thistle and black cohosh product to rifampin and clarithromycin. *J Clin Pharmacol* **46:**201-213.

Gurley BJ (2012) Pharmacokinetic herb-drug interactions (part 1): origins, mechanisms, and the impact of botanical dietary supplements. *Planta Med* **78:**1478-1489.

Gurley BJ, Barone GW, Williams DK, Carrier J, Breen P, Yates CR, Song PF, Hubbard MA, Tong Y and Cheboyina S (2006b) Effect of milk thistle (*Silybum marianum*) and black cohosh (*Cimicifuga racemosa*) supplementation on digoxin pharmacokinetics in humans. *Drug Metabolism & Disposition* **34:**69-74.

Gurley BJ, Gardner SF, Hubbard MA, Williams DK, Gentry WB, Carrier J, Khan IA, Edwards DJ and Shah A (2004) In vivo assessment of botanical supplementation on human cytochrome P450 phenotypes: Citrus aurantium, Echinacea purpurea, milk thistle, and saw palmetto. *Clinical Pharmacology & Therapeutics* **76:**428-440.

Gurley BJ, Swain A, Hubbard MA, Williams DK, Barone G, Hartsfield F, Tong Y, Carrier DJ, Cheboyina S and Battu SK (2008) Clinical assessment of CYP2D6-mediated herb-drug interactions in humans: effects of milk thistle, black cohosh, goldenseal, kava kava, St. John's wort, and Echinacea. *Mol Nutr Food Res* **52:**755-763.

Han HK (2011) Role of transporters in drug interactions. *Arch Pharm Res* **34:**1865-1877.

Han Y, Guo D, Chen Y, Tan ZR and Zhou HH (2009a) Effect of continuous silymarin administration on oral talinolol pharmacokinetics in healthy volunteers. *Xenobiotica*.

Han Y, Guo D, Chen Y, Tan ZR and Zhou HH (2009b) Effect of silymarin on the pharmacokinetics of losartan and its active metabolite E-3174 in healthy Chinese volunteers. *Eur J Clin Pharmacol* **65:**585-591.

Harper JN and Wright SH (2013) Multiple mechanisms of ligand interaction with the human organic cation transporter, OCT2. *Am J Physiol Renal Physiol* **304:**F56-67.

Health Canada (2006) Evidence for Safety and Efficacy of Finished Natural Health Products, Ottawa, ON.

Hewitt NJ, Lecluyse EL and Ferguson SS (2007) Induction of hepatic cytochrome P450 enzymes: methods, mechanisms, recommendations, and in vitro-in vivo correlations. *Xenobiotica* **37:**1196-1224.

Hollenberg PF (2002) Characteristics and common properties of inhibitors, inducers, and activators of CYP enzymes. *Drug Metab Rev* **34:**17-35.

Huang SM (2012) PBPK as a tool in regulatory review. *Biopharm Drug Dispos* **33:**51-52.

Huseini HF, Larijani B, Heshmat R, Fakhrzadeh H, Radjabipour B, Toliat T and Raza M (2006) The efficacy of Silybum marianum (L.) Gaertn. (silymarin) in the treatment of type II diabetes: a randomized, double-blind, placebo-controlled, clinical trial. *Phytother Res* **20:**1036-1039.

Jancova P, Anzenbacherova E, Papouskova B, Lemr K, Luzna P, Veinlichova A, Anzenbacher P and Simanek V (2007) Silybin is metabolized by cytochrome P450 2C8 in vitro. *Drug Metabolism & Disposition* **35:**2035-2039.

Jancova P, Siller M, Anzenbacherova E, Kren V, Anzenbacher P and Simanek V (2011) Evidence for differences in regioselective and stereoselective glucuronidation of silybin diastereomers from milk thistle (Silybum marianum) by human UDP-glucuronosyltransferases. *Xenobiotica* **41:**743-751.

Jutabha P, Wempe MF, Anzai N, Otomo J, Kadota T and Endou H (2010) Xenopus laevis oocytes expressing human P-glycoprotein: probing trans- and cis-inhibitory effects on [3H]vinblastine and [3H]digoxin efflux. *Pharmacol Res* **61:**76-84.

Kalgutkar AS, Obach RS and Maurer TS (2007) Mechanism-based inactivation of cytochrome P450 enzymes: chemical mechanisms, structure-activity relationships and relationship to clinical drug-drug interactions and idiosyncratic adverse drug reactions. *Curr Drug Metab* **8:**407-447.

Kato M, Chiba K, Horikawa M and Sugiyama Y (2005) The quantitative prediction of in vivo enzyme-induction caused by drug exposure from in vitro information on human hepatocytes. *Drug Metab Pharmacokinet* **20:**236-243.

Kennedy J, Wang CC and Wu CH (2008) Patient Disclosure about Herb and Supplement Use among Adults in the US. *Evid Based Complement Alternat Med* **5:**451-456.

Khalil F and Laer S (2011) Physiologically based pharmacokinetic modeling: methodology, applications, and limitations with a focus on its role in pediatric drug development. *J Biomed Biotechnol* **2011:**907461.

Kim CS, Choi SJ, Park CY, Li C and Choi JS (2010) Effects of silybinin on the pharmacokinetics of tamoxifen and its active metabolite, 4-hydroxytamoxifen in rats. *Anticancer Res* **30:**79-85.

Kim E, Sy-Cordero A, Graf TN, Brantley SJ, Paine MF and Oberlies NH (2011) Isolation and identification of intestinal CYP3A inhibitors from cranberry (Vaccinium macrocarpon) using human intestinal microsomes. *Planta Med* **77:**265-270.

Kim NC, Graf TN, Sparacino CM, Wani MC and Wall ME (2003a) Complete isolation and characterization of silybins and isosilybins from milk thistle (Silybum marianum). *Org Biomol Chem* **1:**1684-1689.

Kim YC, Kim EJ, Lee ED, Kim JH, Jang SW, Kim YG, Kwon JW, Kim WB and Lee MG (2003b) Comparative bioavailability of silibinin in healthy male volunteers. *Int J Clin Pharmacol Ther* **41:**593-596.

Kis E, Ioja E, Nagy T, Szente L, Heredi-Szabo K and Krajcsi P (2009) Effect of membrane cholesterol on BSEP/Bsep activity: species specificity studies for substrates and inhibitors. *Drug Metab Dispos* **37:**1878-1886.

Köck K, Xie Y, Oberlies NH, Hawke RL and Brouwer KL (2013) Interaction of Silymarin Flavonolignans with Organic Anion Transporting Polypeptides (OATPs). *Drug Metab Dispos*. (in press)

Kosina P, Maurel P, Ulrichova J and Dvorak Z (2005) Effect of silybin and its glycosides on the expression of cytochromes P450 1A2 and 3A4 in primary cultures of human hepatocytes. *J Biochem Mol Toxicol* **19:**149-153.

Kroll DJ, Shaw HS and Oberlies NH (2007) Milk thistle nomenclature: why it matters in cancer research and pharmacokinetic studies. *Integr Cancer Ther* **6:**110-119.

Kunze KL, Eddy AC, Gibaldi M and Trager WF (1991) Metabolic enantiomeric interactions: the inhibition of human (S)-warfarin-7-hydroxylase by (R)-warfarin. *Chirality* **3:**24-29.

Ladas EJ, Kroll DJ, Oberlies NH, Cheng B, Ndao DH, Rheingold SR and Kelly KM (2010) A randomized, controlled, double-blind, pilot study of milk thistle for the treatment of hepatotoxicity in childhood acute lymphoblastic leukemia (ALL). *Cancer* **116:**506-513.

Lee JI, Hsu BH, Wu D and Barrett JS (2006a) Separation and characterization of silybin, isosilybin, silydianin and silychristin in milk thistle extract by liquid chromatography-electrospray tandem mass spectrometry. *J Chromatogr A* **1116:**57-68.

Lee JY, Duke RK, Tran VH, Hook JM and Duke CC (2006b) Hyperforin and its analogues inhibit CYP3A4 enzyme activity. *Phytochemistry* **67:**2550-2560.

Lee KS, Chae SW, Park JH, Choi JM, Rhie SJ and Lee HJ (2013) Effects of single or repeated silymarin administration on pharmacokinetics of risperidone and its major metabolite, 9-hydroxyrisperidone in rats. *Xenobiotica* **43:**303-310.

Lin JH and Lu AY (1998) Inhibition and induction of cytochrome P450 and the clinical implications. *Clin Pharmacokinet* **35:**361-390.

Martignoni M, Groothuis GM and de Kanter R (2006) Species differences between mouse, rat, dog, monkey and human CYP-mediated drug metabolism, inhibition and induction. *Expert Opin Drug Metab Toxicol* **2:**875-894.

McBride A, Augustin KM, Nobbe J and Westervelt P (2012) Silybum marianum (milk thistle) in the management and prevention of hepatotoxicity in a patient undergoing reinduction therapy for acute myelogenous leukemia. *J Oncol Pharm Pract* **18:**360-365.

Menez C, Mselli-Lakhal L, Foucaud-Vignault M, Balaguer P, Alvinerie M and Lespine A (2012) Ivermectin induces P-glycoprotein expression and function through mRNA stabilization in murine hepatocyte cell line. *Biochem Pharmacol* **83:**269-278.

Mengs U, Pohl RT and Mitchell T (2012) Legalon(R) SIL: the antidote of choice in patients with acute hepatotoxicity from amatoxin poisoning. *Curr Pharm Biotechnol* **13:**1964-1970.

Mills E, Wilson K, Clarke M, Foster B, Walker S, Rachlis B, DeGroot N, Montori VM, Gold W, Phillips E, Myers S and Gallicano K (2005) Milk thistle and indinavir: a randomized controlled pharmacokinetics study and meta-analysis. *Eur J Clin Pharmacol* **61:**1-7.

Mohamed ME and Frye RF (2011) Inhibitory effects of commonly used herbal extracts on UDP-glucuronosyltransferase 1A4, 1A6, and 1A9 enzyme activities. *Drug Metab Dispos* **39:**1522-1528.

Mohamed MF, Tseng T and Frye RF (2010) Inhibitory effects of commonly used herbal extracts on UGT1A1 enzyme activity. *Xenobiotica* **40:**663-669.

Molina H, Azocar L, Ananthanarayanan M, Arrese M and Miquel JF (2008) Localization of the Sodium-Taurocholate cotransporting polypeptide in membrane rafts and modulation of its activity by cholesterol in vitro. *Biochim Biophys Acta* **1778:**1283-1291.

Molto J, Valle M, Miranda C, Cedeno S, Negredo E and Clotet B (2012) Effect of milk thistle on the pharmacokinetics of darunavir-ritonavir in HIV-infected patients. *Antimicrob Agents Chemother* **56:**2837-2841.

Nguyen H, Zhang S and Morris ME (2003) Effect of flavonoids on MRP1-mediated transport in Panc-1 cells. *J Pharm Sci* **92:**250-257.

Novak RF and Woodcroft KJ (2000) The alcohol-inducible form of cytochrome P450 (CYP 2E1): role in toxicology and regulation of expression. *Arch Pharm Res* **23:**267-282.

Obach RS (2000) Inhibition of human cytochrome P450 enzymes by constituents of St. John's Wort, an herbal preparation used in the treatment of depression. *J Pharmacol Exp Ther* **294:**88-95.

Okey AB (1990) Enzyme induction in the cytochrome P-450 system. *Pharmacol Ther* **45:**241-298.

Paine MF and Oberlies NH (2007) Clinical relevance of the small intestine as an organ of drug elimination: drug-fruit juice interactions. *Expert Opin Drug Metab Toxicol* **3:**67-80.

Patel J, Buddha B, Dey S, Pal D and Mitra AK (2004) In vitro interaction of the HIV protease inhibitor ritonavir with herbal constituents: changes in P-gp and CYP3A4 activity. *Am J Ther* **11:**262-277.

Payer BA, Reiberger T, Rutter K, Beinhardt S, Staettermayer AF, Peck-Radosavljevic M and Ferenci P (2010) Successful HCV eradication and inhibition of HIV replication by intravenous silibinin in an HIV-HCV coinfected patient. *J Clin Virol* **49:**131-133.

Piscitelli SC, Formentini E, Burstein AH, Alfaro R, Jagannatha S and Falloon J (2002) Effect of milk thistle on the pharmacokinetics of indinavir in healthy volunteers. *Pharmacotherapy* **22:**551-556.

Post-White J, Ladas EJ and Kelly KM (2007) Advances in the use of milk thistle (Silybum marianum). *Integr Cancer Ther* **6:**104-109.

Poulin P and Theil FP (2000) A priori prediction of tissue:plasma partition coefficients of drugs to facilitate the use of physiologically-based pharmacokinetic models in drug discovery. *J Pharm Sci* **89:**16-35.

Rambaldi A, Jacobs BP and Gluud C (2007) Milk thistle for alcoholic and/or hepatitis B or C virus liver diseases. *Cochrane Database Syst Rev***:**CD003620.

Rao BN, Srinivas M, Kumar YS and Rao YM (2007) Effect of silymarin on the oral bioavailability of ranitidine in healthy human volunteers. *Drug Metabol Drug Interact* **22:**175-185.

Raucy JL, Lasker J, Ozaki K and Zoleta V (2004) Regulation of CYP2E1 by ethanol and palmitic acid and CYP4A11 by clofibrate in primary cultures of human hepatocytes. *Toxicol Sci* **79:**233-241.

Rodgers T and Rowland M (2007) Mechanistic approaches to volume of distribution predictions: understanding the processes. *Pharm Res* **24:**918-933.

Roth M, Araya JJ, Timmermann BN and Hagenbuch B (2011) Isolation of modulators of the liver-specific organic anion-transporting polypeptides (OATPs) 1B1 and 1B3 from Rollinia emarginata Schlecht (Annonaceae). *J Pharmacol Exp Ther* **339:**624-632.

Rousseaux CG and Schachter H (2003) Regulatory issues concerning the safety, efficacy and quality of herbal remedies. *Birth Defects Res B Dev Reprod Toxicol* **68:**505-510.

Rowland M, Peck C and Tucker G (2011) Physiologically-based pharmacokinetics in drug development and regulatory science. *Annu Rev Pharmacol Toxicol* **51:**45-73.

Sayyah M, Boostani H, Pakseresht S and Malayeri A (2010) Comparison of Silybum marianum (L.) Gaertn. with fluoxetine in the treatment of Obsessive-Compulsive Disorder. *Prog Neuropsychopharmacol Biol Psychiatry* **34:**362-365.

Schandalik R, Gatti G and Perucca E (1992) Pharmacokinetics of silybin in bile following administration of silipide and silymarin in cholecystectomy patients. *Arzneimittelforschung* **42:**964-968.

Schandalik R and Perucca E (1994) Pharmacokinetics of silybin following oral administration of silipide in patients with extrahepatic biliary obstruction. *Drugs Exp Clin Res* **20:**37-42.

Schrieber SJ, Wen Z, Vourvahis M, Smith PC, Fried MW, Kashuba AD and Hawke RL (2008) The pharmacokinetics of silymarin is altered in patients with hepatitis C virus and nonalcoholic Fatty liver disease and correlates with plasma caspase-3/7 activity. *Drug Metabolism & Disposition* **36:**1909-1916.

Seeff LB, Curto TM, Szabo G, Everson GT, Bonkovsky HL, Dienstag JL, Shiffman ML, Lindsay KL, Lok AS, Di Bisceglie AM, Lee WM and Ghany MG (2008) Herbal product use by persons enrolled in the hepatitis C Antiviral Long-Term Treatment Against Cirrhosis (HALT-C) Trial. *Hepatology* **47:**605-612.

Silano V, Coppens P, Larranaga-Guetaria A, Minghetti P and Roth-Ehrang R (2011) Regulations applicable to plant food supplements and related products in the European Union. *Food Funct* **2:**710-719.

Silverman RB and Daniel LP (1995) [10] Mechanism-based enzyme inactivators, in: *Methods in Enzymology*, pp 240-283, Academic Press.

Song JH and Choi HJ (2011) Silymarin efficacy against influenza A virus replication. *Phytomedicine* **18:**832-835.

Sridar C, Goosen TC, Kent UM, Williams JA and Hollenberg PF (2004) Silybin inactivates cytochromes P450 3A4 and 2C9 and inhibits major hepatic glucuronosyltransferases. *Drug Metabolism & Disposition* **32:**587-594.

Tamaki H, Satoh H, Hori S, Ohtani H and Sawada Y (2010) Inhibitory effects of herbal extracts on breast cancer resistance protein (BCRP) and structure-inhibitory potency relationship of isoflavonoids. *Drug Metab Pharmacokinet* **25:**170-179.

Tatsis EC, Boeren S, Exarchou V, Troganis AN, Vervoort J and Gerothanassis IP (2007) Identification of the major constituents of Hypericum perforatum by LC/SPE/NMR and/or LC/MS. *Phytochemistry* **68:**383-393.

Tyler VE (2000) Herbal medicine: from the past to the future. *Public Health Nutr* **3:**447-452.

US Food and Drug Administration (2012) Draft Guidance: Drug interaction studies-study desig, data analysis, implications for dosing, and labeling recommendations, Rockville, MD.

van Erp NP, Baker SD, Zhao M, Rudek MA, Guchelaar HJ, Nortier JW, Sparreboom A and Gelderblom H (2005) Effect of milk thistle (Silybum marianum) on the pharmacokinetics of irinotecan. *Clin Cancer Res* **11:**7800-7806.

Venkatakrishnan K, Obach RS and Rostami-Hodjegan A (2007) Mechanism-based inactivation of human cytochrome P450 enzymes: strategies for diagnosis and drug-drug interaction risk assessment. *Xenobiotica* **37:**1225-1256.

Venkataramanan R, Ramachandran V, Komoroski BJ, Zhang S, Schiff PL and Strom SC (2000) Milk thistle, a herbal supplement, decreases the activity of CYP3A4 and uridine diphosphoglucuronosyl transferase in human hepatocyte cultures. *Drug Metabolism & Disposition* **28:**1270-1273.

Vidlar A, Vostalova J, Ulrichova J, Student V, Krajicek M, Vrbkova J and Simanek V (2010) The safety and efficacy of a silymarin and selenium combination in men after radical prostatectomy - a six month placebo-controlled double-blind clinical trial. *Biomed Pap Med Fac Univ Palacky Olomouc Czech Repub* **154:**239-244.

Weber CC, Kressmann S, Fricker G and Muller WE (2004) Modulation of P-glycoprotein function by St John's wort extract and its major constituents. *Pharmacopsychiatry* **37:**292-298.

Wei F, Liu SK, Liu XY, Li ZJ, Li B, Zhou YL, Zhang HY and Li YW (2012) Meta-analysis: silymarin and its combination therapy for the treatment of chronic hepatitis B. *Eur J Clin Microbiol Infect Dis*.

Wen Z, Dumas TE, Schrieber SJ, Hawke RL, Fried MW and Smith PC (2008) Pharmacokinetics and metabolic profile of free, conjugated, and total silymarin flavonolignans in human plasma after oral administration of milk thistle extract. *Drug Metabolism & Disposition* **36:**65-72.

Weyhenmeyer R, Mascher H and Birkmayer J (1992) Study on dose-linearity of the pharmacokinetics of silibinin diastereomers using a new stereospecific assay. *Int J Clin Pharmacol Ther Toxicol* **30:**134-138.

Wienkers LC and Heath TG (2005) Predicting in vivo drug interactions from in vitro drug discovery data. *Nat Rev Drug Discov* **4:**825-833.

Winslow LC and Kroll DJ (1998) Herbs as medicines. *Arch Intern Med* **158:**2192-2199.

Won CS, Oberlies NH and Paine MF (2012) Mechanisms underlying food-drug interactions: inhibition of intestinal metabolism and transport. *Pharmacol Ther* **136:**186-201.

Wu JW and Tsai TH (2007) Effect of silibinin on the pharmacokinetics of pyrazinamide and pyrazinoic acid in rats. *Drug Metab Dispos* **35:**1603-1610.

Zhang S and Morris ME (2003a) Effect of the flavonoids biochanin A and silymarin on the P-glycoprotein-mediated transport of digoxin and vinblastine in human intestinal Caco-2 cells. *Pharm Res* **20:**1184-1191.

Zhang S and Morris ME (2003b) Effects of the flavonoids biochanin A, morin, phloretin, and silymarin on P-glycoprotein-mediated transport. *J Pharmacol Exp Ther* **304:**1258-1267.

Zhang S, Yang X and Morris ME (2004) Combined effects of multiple flavonoids on breast cancer resistance protein (ABCG2)-mediated transport. *Pharm Res* **21:**1263-1273.

Zhao P, Rowland M and Huang SM (2012) Best practice in the use of physiologically based pharmacokinetic modeling and simulation to address clinical pharmacology regulatory questions. *Clin Pharmacol Ther* **92:**17-20.

Zuber R, Modriansky M, Dvorak Z, Rohovsky P, Ulrichova J, Simanek V and Anzenbacher P (2002) Effect of silybin and its congeners on human liver microsomal cytochrome P450 activities. *Phytother Res* **16:**632-638.

Chapter 2

Two Flavonolignans from Milk Thistle (*Silybum marianum*) Inhibit CYP2C9-Mediated Warfarin Metabolism at Clinically Achievable Concentrations[1,2]

Overview

Milk thistle (*Silybum marianum*) is a popular herbal product used for hepatoprotection and chemoprevention. Two commercially available formulations are the crude extract, silymarin, and the semi-purified product, silibinin. Silymarin consists of at least seven flavonolignans, of which the most prevalent are the diastereoisomers silybin A and silybin B; silibinin consists only of silybin A and silybin B. Based on a recent clinical study showing an interaction between a silymarin product and the CYP2C9 substrate losartan, the CYP2C9 inhibition properties of silybin A and silybin B, and corresponding regioisomers, isosilybin A and isosilybin B, were evaluated using human liver microsomes (HLM), recombinant CYP2C9 (rCYP2C9) enzymes, and the clinically relevant probe, (*S*)-warfarin. Silybin B was the most potent inhibitor in HLM, followed by silybin A, isosilybin B, and isosilybin A (IC_{50} of 8.2, 18, 74, and >100 μM, respectively). Next, silybin A and silybin B were selected for further characterization. As with HLM, silybin B was more potent than silybin A towards rCYP2C9*1 (6.7 vs. 12 μM),

---

[1] Brantley SJ, Oberlies NH, Kroll DJ and Paine MF (2010) Two flavonolignans from milk thistle (*Silybum marianum*) inhibit CYP2C9-mediated warfarin metabolism at clinically achievable concentrations. *J Pharmacol Exp Ther* **332**:1081-1087.

rCYP2C9*2 (9.3 vs. 19 μM), and rCYP2C9*3 (2.4 *vs*. 9.3 μM). Using a matrix of 5 substrate (1-15 μM) and 6 inhibitor (1-80 μM) concentrations and HLM, both diastereoisomers inhibited (*S*)-warfarin 7-hydroxylation in a manner described best by a mixed-type inhibition model (K_i of 4.8 and 10 μM for silybin B and silybin A, respectively). These observations, combined with the high systemic silibinin concentrations (>5-75 μM) achieved in a phase I study involving prostate cancer patients, prompt clinical evaluation of a potential warfarin-milk thistle interaction.

Introduction

Milk thistle [*Silybum marianum* (L.) Gaertn] is a resilient and sometimes noxious plant that has been valued for its medicinal qualities for over 2000 years (Kroll et al., 2007; Post-White et al., 2007). In modern herbal compendia, milk thistle is used to self-treat hepatic disorders, including hepatitis C and cirrhosis, and as a hepatoprotectant, particularly for mushroom poisoning. Milk thistle is available mainly as an extract prepared from the seeds of the plant. The two most common commercial preparations are termed silymarin and silibinin. Silymarin, a crude extract, is a complex mixture of at least seven flavonolignans and one flavonoid (taxifolin) (Kroll et al., 2007). The most abundant flavonolignans are the diastereoisomers silybin A and silybin B (Fig. 2.1). The diastereoisomers isosilybin A and isosilybin B (Fig. 2.1) also are present and are regioisomers of silybin A and silybin B. The remaining three flavonolignans are silychristin, isosilychristin, and silydianin, all of which are constitutional isomers of the aforementioned compounds. Silibinin is a semi-purified extract, representing approximately a 1:1 mixture of silybin A and silybin B. Because silymarin and silibinin are mixtures of compounds derived from a natural source, batch-to-batch variation in bioactive ingredient composition occurs, which can confound the interpretation of study results (Kroll et al., 2007). Fortuitously, methods have been developed to isolate and purify gram quantities of each flavonolignan from milk thistle extract, permitting delineation of the disposition and action of single constituents (Kim et al., 2001; Graf et al., 2007).

Milk thistle has garnered attention since the 1990s for its chemopreventive properties, particularly for prostate cancer (Agarwal et al., 2006; Gazak et al., 2007; Kroll et al., 2007). With the advent of single components from silymarin, the antiproliferative effects of each flavonolignan, as well silymarin and silibinin, were compared using human prostate cancer cell lines; at concentrations ranging from 15-90 μM, isosilybin B

was consistently the most potent of all the individual components and mixtures examined (Davis-Searles et al., 2005). In rodent models of prostate cancer, dietary feeding of silymarin and silibinin has been shown, respectively, to decrease the incidence of 3,2'-dimethyl-4-aminobiphenyl-induced prostatic adenocarcinoma (Kohno et al., 2005) and to inhibit prostate tumor growth (Ramasamy and Agarwal, 2008; Singh et al., 2008). The latter studies set the target systemic concentration of silibinin at 10-15 μM.

Clinical studies have indicated that both silymarin and silibinin have poor oral bioavailability due to extensive first-pass conjugation via UDP-glucuronosyl transferases and sulfotransferases (Flaig et al., 2007; Schrieber et al., 2008; Wen et al., 2008). As such, at typical "doses", systemic concentrations of unconjugated flavonolignans >1 μM are rarely achieved. The first study to demonstrate systemic concentrations of unconjugated silibinin in the purported therapeutic range was a phase I dose-escalation study involving prostate cancer patients (Flaig et al., 2007). These patients were administered 2.5 to 20 g/day of a silibinin-phosphatidylcholine complex (Siliphos®), which has improved absorption characteristics, and presumably an improved bioavailability, compared to non-complexed silibinin (Flaig et al., 2007). Average peak plasma concentrations of unconjugated silibinin ranged from 5-75 μM. Moreover, these high doses were well-tolerated, and several patients experienced prolonged stable disease, prompting a phase II study that is currently underway.

Herbal products often are taken concomitantly with medications, which could potentially lead to dangerous interactions (Hu et al., 2005; Wu et al., 2009). Clinical studies involving milk thistle extracts to date have shown minimal to no drug interaction liability, at least with drugs that are considered probe substrates for CYP1A2, CYP2D6, CYP2E1, CYP3A, and the efflux transporter P-glycoprotein (Gurley et al., 2004; Gurley et al., 2006a; Gurley et al., 2006b; Gurley et al., 2008). A caveat to these studies is that

a low total daily "dose" (<1 g) of extract (silymarin) was given, which is much less than that postulated to have clinical benefit, at least for prostate cancer. However, a recent healthy volunteer study demonstrated an interaction between the antihypertensive agent and CYP2C9/CYP3A substrate losartan and silymarin, the latter of which was given as a low total daily dose (420 mg) (Han et al., 2009). Relative to placebo, in *CYP2C9*1* carriers, silymarin decreased the AUC ratio of the CYP2C9-mediated active metabolite, E-3174, to that of losartan, by ~50% ($p<0.05$), suggesting inhibition of hepatic CYP2C9 by one or more components of silymarin. These observations, coupled with the high systemic concentrations observed in the dose-escalation study, prompted a systematic evaluation of the inhibitory effects of individual components from silymarin on the CYP2C9-mediated metabolism of another clinically relevant substrate, (*S*)-warfarin, the more pharmacologically active enantiomer of the widely prescribed oral anticoagulant warfarin. Specifically, the inhibitory potency of four key flavonolignans (silybin A, silybin B, isosilybin A, isosilybin B) toward (*S*)-warfarin 7-hydroxylation were compared using human liver microsomes and recombinant CYP2C9 enzymes. To the authors' knowledge, this work represents the first evaluation of the drug interaction liability of single, purified constituents from milk thistle.

Materials and Methods

Chemicals and reagents. Human liver microsomes (HLM; pooled from 50 donors, mixed gender) were purchased from Xenotech, LLC (Lenexa, KS). Baculovirus-insect cell-expressed CYP2C9*1, CYP2C9*2, CYP2C9*3 (supplemented with cDNA-expressed reductase but not cytochrome b_5), tienilic acid, and 7-hydroxywarfarin were purchased from BD Biosciences (San Jose, CA). (*S*)-warfarin, chlorowarfarin, NADPH, and HPLC grade water, methanol, ammonium acetate, and 1-propanol were purchased from Sigma-Aldrich (St. Louis, MO). Silybin A, silybin B, isosilybin A, and isosilybin B were isolated from milk thistle extract as described previously (Graf et al., 2007); all flavonolignans were >97% pure as determined by HPLC.

Evaluation of silymarin flavonolignans as inhibitors of CYP2C9 activity. The inhibitory effects of each flavonolignan on (*S*)-warfarin 7-hydroxylation were evaluated using pooled HLMs and recombinant CYP2C9 (rCYP2C9). (*S*)-Warfarin and sulfaphenazole were dissolved in methanol to yield a working concentration of 10 mM and 1 mM, respectively. Each flavonolignan was dissolved in methanol to yield a working concentration of 50 mM. NADPH was dissolved fresh in potassium phosphate buffer (0.1 M, pH 7.4) to yield a working concentration of 4 mM. Incubation mixtures were prepared in 96-well plates. Under all experimental conditions, the amount of 7-hydroxywarfarin formed was linear with respect to incubation time and mass/amount of microsomal protein or rCYP2C9 (data not shown). *Initial testing.* Incubation mixtures consisted of HLMs (0.1 mg/mL microsomal protein), (*S*)-warfarin (4 μM), flavonolignan (1, 10, and 100 μM), and potassium phosphate buffer (100 mM, pH 7.4). As a positive control for CYP2C9 inhibition, incubation mixtures contained sulfaphenazole (1 μM) in place of flavonolignan. Control incubation mixtures contained 0.75% methanol (v/v) in place of flavonolignan/sulfaphenazole. The plates were placed on a dry heat block, and the mixtures were equilibrated for 5 minutes at 37°C before initiating the reactions with

NADPH (1 mM final concentration) to yield a final volume of 200 µL. After 30 minutes, the reactions were quenched with 400 µL of cold methanol containing 3.33 nM chlorowarfarin as the internal standard. After centrifugation (1350 x *g* for 10 minutes at 4°C), the supernatant (8 µL) was analyzed for 7-hydroxywarfarin by LC-MS/MS (described below). *K_i determination for silybin A and silybin B using HLMs*. Incubation mixtures were prepared in a similar manner as described above using a 5 x 6 matrix of substrate (1-15 µM) and flavonolignan (1-80 µM) concentrations. The reaction mixtures were processed further and analyzed for 7-hydroxywarfarin as described above. *IC_{50} determination for silybin A and silybin B using rCYP2C9 enzymes.* Incubation mixtures consisting of rCYP2C9 (12.5 pmol/mL), (*S*)-warfarin (4 µM), flavonolignan (0.5-100 µM), and potassium phosphate buffer were equilibrated for 5 minutes at 37°C before initiating the reactions with NADPH. After 30 (rCYP2C9*1, rCYP2C9*2) or 60 (rCYP2C9*3) minutes, the reactions were quenched and processed as described above. *Testing of silybin A and silybin B as mechanism-based inhibitors of CYP2C9 using HLMs.* IC_{50} shift experiments (Obach et al., 2007) were utilized to determine whether silybin A and silybin B are mechanism-based inhibitors of hepatic CYP2C9 activity. Primary incubation mixtures consisting of HLMs (1 mg/mL), flavonolignan (0.1-1000 µM), and potassium phosphate buffer were equilibrated for 5 minutes at 37°C before initiating the reactions with NADPH. Control primary reaction mixtures were identical except that NADPH was absent. As a positive control for mechanism based inhibition, incubation mixtures contained tienilic acid (1.0-500 µM) in place of flavonolignan. After 30 minutes, an aliquot (20 µL) was removed and diluted 10-fold into a secondary incubation mixture containing (*S*)-warfarin (4 µM) and NADPH (1 mM). After an additional 30 minutes, the secondary reactions were quenched and processed as described above.

Analysis of microsomal incubations for 7-hydroxywarfarin. 7-Hydroxywarfarin was quantified by LC-MS/MS using a Shimadzu solvent delivery system

(Columbia, MD) and a Leap HTC Pal thermostated autosampler (Carrboro, NC) connected to an Applied Biosystems (Foster City, CA) API 4000 triple quadruple mass spectrometer equipped with a TurboSpray® ion source. Tuning, operation, integration, and data analysis were carried out in negative mode using multiple reaction monitoring (Analyst® software v.1.4.1, Applied Biosystems). Analytes (7-hydroxywarfarin, chlorowarfarin), as well as other metabolites, were separated using a Gemini® C_{18} column (30 x 2.0 mm, 5 µm particle size; Phenomenex, Torrance, CA) and a solvent flow rate of 0.75 mL/min. Initial gradient conditions were 100% 10 mM ammonium acetate, which were held for 0.7 min while the eluent was directed to waste. From 0.7 min to 4.5 min, the mobile phase composition increased linearly to 60% methanol, and the eluent was directed to the mass spectrometer. At 5.0 min, the eluent was directed again to waste, and the column was flushed with 80% methanol for 0.4 min. From 6.0 to 6.5 min, the system was equilibrated with 100% 10 mM ammonium acetate. Total run time, including equilibration, was 6.5 minutes per injection. Duplicate ten-point calibration curves for 7-hydroxywarfarin (0.2 to 100 nM) were constructed using the peak area ratio of 7-hydroxywarfarin (323.06→176.8; retention time, 3.34 min) to chlorowarfarin (341.2→160.9; retention time, 4.24 min). Interday accuracy and precision ranged from 99-110% and from 9.0-12%, respectively, for all quality controls (0.23, 1.5, 15 pmol).

Data analysis. *Apparent IC_{50} determination.* Initial estimates of apparent IC_{50} values were derived from linear regression of the velocity vs. natural logarithm of flavonolignan concentration data. Apparent IC_{50} values were determined by fitting the following equation with untransformed data using WinNonlin (v5.0.1, Pharsight, Mountain View, CA):

$$v = \frac{v_0}{1 + \left(\frac{I}{IC_{50}} \right)} \qquad \text{(Eq. 1)}$$

where I denotes the concentration of inhibitor, and v_0 and v denote the velocity of 7-hydroxywarfarin formation in the absence and presence of flavonolignan, respectively. *Apparent K_i determination.* Initial estimates of apparent K_m and V_{max} were derived from Eadie-Hofstee plots of the velocity vs. velocity/[substrate] data in the absence of flavonolignan. Initial estimates of apparent K_i values were derived from Dixon plots of velocity^{-1} vs. flavonolignan concentration data. Kinetic parameters (K_m, V_{max}, K_i) were obtained by fitting the following inhibition equations for a unienzyme system with untransformed data:

Competitive

$$v = \frac{V_{max} * S}{K_m\left(1+\left(\frac{I}{K_i}\right)\right)+S} \qquad \text{(Eq. 2)}$$

Non-competitive

$$v = \frac{V_{max} * S}{K_m\left(1+\left(\frac{I}{K_i}\right)\right)+S\left(1+\frac{I}{K_i}\right)} \qquad \text{(Eq. 3)}$$

Mixed-type

$$v = \frac{V_{max} * S}{K_m\left(1+\left(\frac{I}{K_i}\right)\right)+S\left(1+\frac{I}{\alpha K_i}\right)} \qquad \text{(Eq. 4)}$$

where S denotes the concentration of (*S*)-warfarin, I denotes the concentration of inhibitor, and α (Eq. 4) denotes a parameter to describe the affinity change of the enzyme-substrate and enzyme-inhibitor complexes (Geng, 2003). When α =1, Eq. 4 simplifies to the pure non-competitive inhibition model (Eq. 3); when α is very large (approaches infinity), Eq. 4 simplifies to the pure competitive inhibition model (Eq. 2). The best-fit equation was assessed from visual inspection of the observed vs. predicted data, randomness of the residuals, Akaike information criteria, and standard errors of the parameter estimates. Apparent intrinsic clearance (Cl_{int}) was calculated as the ratio of V_{max} to K_m.

Statistical analysis. All statistical analyses were carried out using SigmaStat (v3.5, Systat Software, Inc., San Jose, CA). Data are presented as means ± SDs of triplicate determinations, unless indicated otherwise. Concentration-dependent inhibition of each flavonolignan in HLMs was evaluated by 1-way ANOVA; post-hoc comparisons were made using Tukey's test when an overall difference resulted ($p<0.05$). Enzyme kinetic parameters are presented as the estimates ± SEs. Statistical differences between the calculated IC_{50} for silybin A and silybin B within an enzyme source was evaluated by a Student's *t*-test of 2 independent samples; a *p*-value <0.05 was considered significant. Statistical differences between the calculated IC_{50} for a given inhibitor among enzyme sources was evaluated by 1-way ANOVA; post-hoc comparisons were made using Tukey's test when an overall difference resulted ($p<0.05$).

Results

Selected flavonolignans differentially inhibit CYP2C9-mediated warfarin metabolism. Each flavonolignan inhibited the 7-hydroxylation of (*S*)-warfarin in a concentration-dependent manner, with the diastereoisomer pair, silybin A and silybin B, showing greater potency than their regioisomer counterparts, isosilybin A and isosilybin B (Fig. 2.2). Within each diastereoisomer pair, the B forms were slightly more potent than the A forms. As reflected by the IC_{50} values, silybin B was the most potent of the flavonolignans tested, followed by silybin A, isosilybin B, and isosilybin A (Table 2.1). Isosilybin A and isosilybin B were not evaluated further due the relative lack of inhibitory potency.

Silybin B is a more potent inhibitor of CYP2C9-mediated warfarin metabolism than silybin A. The apparent K_i for silybin A and silybin B towards (*S*)-warfarin 7-hydroxylation was determined using a 5 x 6 matrix of substrate-inhibitor concentrations and HLMs (Fig. 2.3). The simple linear mixed-type inhibition model (Eq. 3) best described the data for both silybin A and silybin B. In the absence of inhibitor, 7-hydroxywarfarin formation was consistent with classic Michaelis-Menten unienzyme kinetics, as evidenced by linear Eadie-Hofstee plots (not shown). The K_m and V_{max} of 7-hydroxywarfarin formation were, respectively, 4.0 ± 0.5 μM and 7.7 ± 0.5 pmol/min/mg protein (silybin A) or 3.4 ± 0.4 μM and 9.1 ± 0.6 pmol/min/mg protein (silybin B). Cl_{int} values were 1.9 and 2.7 μL/min/mg, respectively. The K_i for silybin A was twice that for silybin B (Fig. 2.3). The α value for silybin A and silybin B was 5 and 8, respectively. As observed with HLMs, silybin B was more potent than silybin A with all recombinant enzyme variants (Fig. 2.4). At the lowest flavonolignan concentration tested, the velocity for CYP2C9*1 was approximately twice that of CYP2C9*2, which was approximately twice that of CYP2C9*3. For a given inhibitor, the calculated IC_{50} value for CYP2C9*3 was significantly lower than that for HLM, CYP2C9*1, and CYP2C9*2 (Table 2.1).

Silybin A and silybin B appear not to be mechanism-based inhibitors of (*S*)-warfarin 7-hydroxylation. IC_{50} shift experiments with HLMs were carried out to determine whether silybin A and silybin B are mechanism-based inhibitors of hepatic CYP2C9. When NADPH was absent from the primary incubation mixture, the calculated IC_{50} values for each flavonolignan agreed with those from initial experiments (Table 2.1). When NADPH was present in the primary reaction mixture, IC_{50} values remained unchanged (Fig. 2.5). The calculated IC_{50} values for the positive control, tienilic acid, shifted from 12 ± 0.9 μM in the absence of NADPH to 1.7 ± 0.1 μM in the presence of NADPH.

Discussion

Warfarin is a widely prescribed oral anticoagulant used to treat thromboembolic disorders (Rettie and Tai, 2006). Despite over 50 years of clinical experience, optimal warfarin therapy remains challenging due to a narrow therapeutic window and large inter-patient differences in anticoagulant response. As such, the daily therapeutic warfarin dose varies by more than an order of magnitude in a given population (Rettie and Tai, 2006). The clinically available formulation of warfarin is a racemic mixture, with the *S*-enantiomer having an estimated five-fold greater pharmacologic potency than the *R*-enantiomer (Jonas and McLeod, 2009). (*S*)-Warfarin is eliminated from the body almost exclusively via hepatic metabolism by CYP2C9, with 7-hydroxylation representing the major metabolic pathway (Jonas and McLeod, 2009). Accordingly, any process that significantly impairs CYP2C9 activity would be expected to decrease the clearance of (*S*)-warfarin and increase anticoagulant response. Indeed, a number of clinically used CYP2C9 inhibitors, e.g., fluconazole, amiodarone, and trimethoprim/sulfamethoxazole, have been associated with serious bleeding events in patients receiving warfarin (Thi et al., 2009).

Whereas specific drugs have been identified as CYP2C9 inhibitors, such is not the case for herbal products, which continue to increase in popularity as complementary and alternative medicines for health maintenance, disease prevention, and even disease treatment (Ulbricht et al., 2008). The fact that herbal products are derived from natural sources has led to the widespread notion that they are safe. As such, these products often are taken with conventional medications, raising the potential for dangerous drug-herb interactions. Moreover, unlike most drug products, herbal products typically contain multiple bioactive ingredients that vary in composition between batches and manufacturers, precluding between-study comparisons, as well as accurate predictions of drug interaction liability (Paine and Oberlies, 2007). A recent dose-escalation study

involving prostate cancer patients showed that oral gram doses of a crude/semi-purified extract of milk thistle, silibinin (2.5-20 g/day), were well-tolerated with minimal side effects; based on these encouraging results, a phase II study is underway (Flaig et al., 2007; Kroll et al., 2007; Post-White et al., 2007). Taken together, the goal of the current work was to characterize, systematically, the CYP2C9 inhibition properties of single constituents from milk thistle. Based on previous studies that compared the antiproliferative effects of individual flavonolignans in prostate cancer cell lines, as well as to discern whether changes in stereo- and regiochemistry alter metabolic inhibition, four key flavonolignans (silybin A, silybin B, isosilybin A, isosilybin B) were selected for evaluation.

Similar to the differential effects of individual flavonolignans observed in prostate cancer cell models (Davis-Searles et al., 2005), individual flavonolignans differentially inhibited the 7-hydroxylation of (*S*)-warfarin. Whereas isosilybin A and isosilybin B were the most potent antiproliferative compounds, silybin A and silybin B were the most potent CYP2C9 inhibitors. Based on the greater than 4-fold difference in IC_{50} values between silybin A/silybin B and isosilybin A/isosilybin B (<20 μM vs. >70 μM), the latter two flavonolignans were not evaluated further. To determine the mode of CYP2C9 inhibition by silybin A and silybin B, reversible inhibition design experiments were undertaken that involved a range of substrate and flavonolignan concentrations. The mixed-type model best described the data for compounds, producing K_i values of 4.8 and 10 μM, respectively. The lack of mechanism-based inhibition, as evidenced from the IC_{50} shift experiments, is inconsistent with results obtained by Sridar et al. (2004), who reported a K_I of 5 μM and a k_{inact} of 0.14 min^{-1}. These investigators used the semi-purified mixture, silibinin (termed silybin), a reconstituted enzyme system, and a fluorescent probe substrate, any or all of which could account for this between-laboratory discrepancy.

Xenobiotics, including drugs, herbal products, and dietary substances, are considered to have a high drug interaction liability when the ratio of in vivo inhibitor concentration to K_i is greater than unity (Bachmann and Lewis, 2005). The average plasma, and presumably total (i.e., bound + unbound) concentrations of unconjugated silybin A/silybin B achieved in the prostate cancer patient dose-escalation study (Flaig et al., 2007) were at least five-fold greater than the apparent K_i values measured in the current work. It should be noted that the systemic concentrations reported for these patients represented the sum of silybin A and silybin B. Although dosed as a ~1:1 mixture (i.e., silibinin), systemic concentrations cannot be considered 1:1 due to differential clearance (Kroll et al., 2007; Wen et al., 2008). Despite this limitation, the low K_i values for both compounds compared to the high concentration of the mixture in plasma would necessitate caution when milk thistle products are taken with warfarin. The potential inter-product variation in milk thistle constituents in commercial products, along with the recent clinical study involving losartan and a silymarin product further support this contention.

Two common single nucleotide polymorphisms in the coding region of the *CYP2C9* gene, *CYP2C9*2* (Arg144Cys) and *CYP2C9*3* (Ile359Leu), are known to influence warfarin anticoagulant response. Both of the corresponding proteins have lower catalytic activity (approximately 50% and less than 10%, respectively) compared to the protein encoded by the reference allele, *CYP2C9*1*, and carriers of these variants often require a lower daily dose of warfarin (Jonas and McLeod, 2009). *CYP2C9*2* and *CYP2C9*3* carriers also may require a longer period of time to become stabilized on warfarin therapy (Rettie and Tai, 2006). Consistent with previous reports, in the absence of inhibitor, the velocity of 7-hydroxywarfarin formation with rCYP2C9*2 and rCYP2C9*3 were roughly 50% and 25%, respectively, than that of rCYP2C9*1 (8.0, 3.6, and 15 pmol/min/nmol, respectively). Among the different recombinant enzyme preparations,

CYP2C9*3 was significantly more sensitive to inhibition by both silybin A and silybin B. These observations, coupled with the increased time to stabilize warfarin therapy and the increased bleeding risk that is associated with this variant, may suggest that co-administration of warfarin and silymarin could further complicate therapy in *CYP2C9*3* carriers. Despite the increased sensitivity of rCYP2C9*3, the relatively potent inhibition potential of these compounds toward rCYP2C9*1 and rCYP2C9*2 would not exclude *CYP2C9*1* and *CYP2C9*2* carriers from being at risk for a potential warfarin-milk thistle interaction.

In summary, unlike drug products, dietary/natural products are not consistently regulated, and accordingly, are not required to undergo strict pre-clinical or clinical testing prior to marketing. Patients often take these products with their medications, sometimes unbeknownst to their physicians and/or pharmacists, which can lead to potentially dangerous adverse events. The current observations, combined with the reported interaction between silymarin and losartan (Han et al., 2009) and the inter-product variation in milk thistle composition, prompts a clinical study with a standardized milk thistle product and warfarin. Finally, the current work provides impetus to revisit P450-mediated drug-milk thistle interactions using purified single constituents.

Legends to Figures

Fig. 2.1. Structures of the four selected flavonolignans from milk thistle.

Fig. 2.2. Inhibitory effects of selected flavonolignans on (*S*)-warfarin 7-hydroxylation activity in human liver microsomes. Human liver microsomes (0.1 mg/ml) were incubated with (*S*)-warfarin (4 μM) and flavonolignan (1, 10, or 100 μM; hatched, solid, and checkered bars, respectively) for 30 minutes. Reactions were initiated by the addition of NADPH (1 mM). (*S*)-Warfarin 7-hydroxylation activity in the presence of vehicle control (0.75% methanol, v/v) was 5.8 ± 0.1 pmol/min/mg microsomal protein. Bars and error bars denote means and standard deviations, respectively, of triplicate incubations. $^{*}p < 0.05$ *vs.* flavonolignan at 10 μM; $^{\#}p < 0.05$ *vs*. flavonolignan at 1 μM (2-way ANOVA, followed by Tukey's test).

Fig. 2.3. Dixon plots showing the inhibition of (*S*)-warfarin 7-hydroxylation by silybin A (**A**) and silybin B (**B**) in human liver microsomes (HLMs). HLMs (0.1 mg/ml) were incubated with (*S*)-warfarin (1-15 μM) and flavonolignan (1-80 μM silybin A or 1-50 μM silybin B) for 30 minutes. Reactions were initiated by the addition of NADPH (1 mM). Symbols denote means of duplicate incubations. Solid lines denote regression lines through values generated from a simple mixed-type inhibition model using WinNonlin (v5.0.1).

Fig. 2.4. Inhibitory effects of silybin A and silybin B on (*S*)-warfarin 7-hydroxylation activity in recombinant CYP2C9 enzymes. Recombinant enzymes (12.5 pmol/ml) were incubated with (*S*)-warfarin (4 μM) and a range of concentrations (1-100 μM) of silybin A (boxes) or silybin B (triangles) for 30 (CYP2C9*1, CYP2C9*2) or 60 (CYP2C9*3) minutes. Reactions were initiated by the addition of NADPH (1 mM). (*S*)-Warfarin 7-hydroxylation activity in the presence of vehicle control (0.75% methanol, v/v) was, respectively, 15 ± 1.3, 8.0 ± 0.4, and 3.6 ± 0.3 pmol/min/nmol recombinant enzyme.

Symbols and error bars denote means and standard deviations, respectively, of triplicate incubations. Solid (silybin A) and dashed (silybin B) curves denote nonlinear least-squares regression of observed values using WinNonlin (v5.0.1).

Fig. 2.5. IC_{50} shift plot for silybin A and silybin B. Human liver microsomes (0.1 mg/ml) were incubated first with silybin A (boxes) or silybin B (triangles) (0.1-1000 μM) (**A**) and tienilic acid (circles) (1-500 μM) (**B**) in the presence (closed symbols) or absence (open symbols) of NADPH (1 mM). The primary reaction mixture was diluted ten-fold to initiate the secondary reaction, which contained NADPH (1 mM) and (*S*)-warfarin (4 μM). (*S*)-warfarin 7-hydroxylation activity in the presence of vehicle control (0.75% methanol, v/v) was 1.5 and 1.6 pmol/min/mg microsomal protein in the absence and presence, respectively, of NADPH. Symbols denote means of duplicate incubations. Open symbols denote observed values when NADPH was absent from the primary reaction mixture; solid symbols denote observed values when NADPH was present in the primary reaction mixture. Curves denote nonlinear least-squares regression of observed values using WinNonlin (v5.0.1).

Table 2.1. Comparison of IC_{50} values (μM) for four key flavonolignans from milk thistle using (*S*)-warfarin 7-hydroxylation as an index of CYP2C9 activity.

Values represent the estimate ± SE.

Enzyme Source	Silybin A	Silybin B	Isosilybin A	Isosilybin B
Reversible inhibition experimental design				
HLM	18 ± 2.2	8.2 ± 1.4[a]	>100	74 ± 11
CYP2C9*1	12 ± 0.9	6.7 ± 0.5[a]	ND	ND
CYP2C9*2	19 ± 1.7	9.3 ± 0.9[a]	ND	ND
CYP2C9*3	9.3 ± 2.0[b]	2.4 ± 0.6[ab]	ND	ND
IC_{50} shift experimental design				
HLM (-NADPH)[c]	18 ±0.7	7.8 ± 0.5	ND	ND
HLM (+NADPH)[d]	17 ± 0.7	7.9 ± 0.9	ND	ND

[a]*Significantly different than the IC_{50} for silybin A ($p<0.05$, Student's t-test of two independent samples).*

[b]*Significantly different than the IC_{50} obtained with HLM, CYP2C9*1, and CYP2C9*2 ($p<0.05$, 1-way ANOVA, followed by Tukey's test) for a given inhibitor.*

[c]*NADPH was absent during the primary incubation.*

[d]*NADPH was present during the primary incubation.*

Figure 2.1

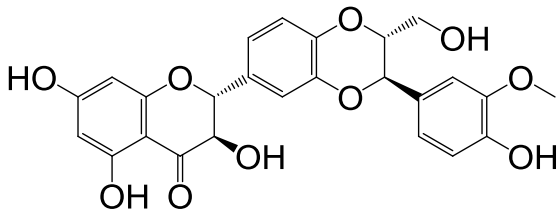

Silybin A

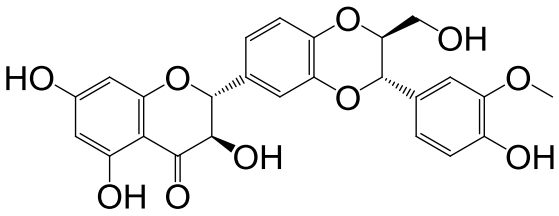

Silybin B

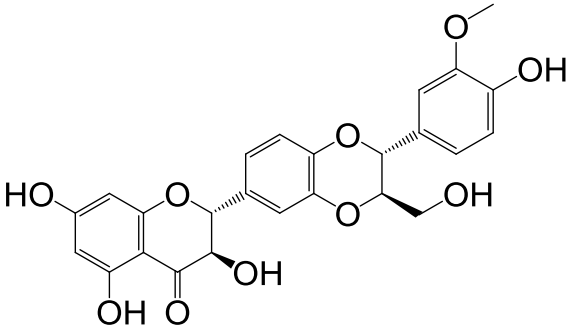

Isosilybin A

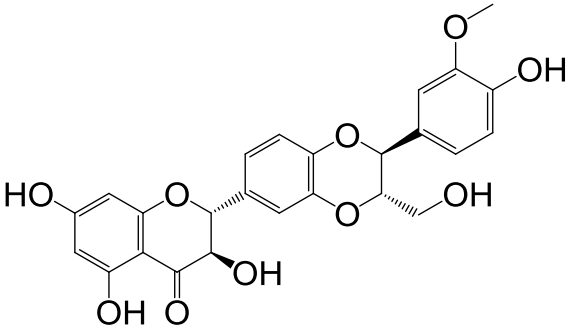

Isosilybin B

Figure 2.2

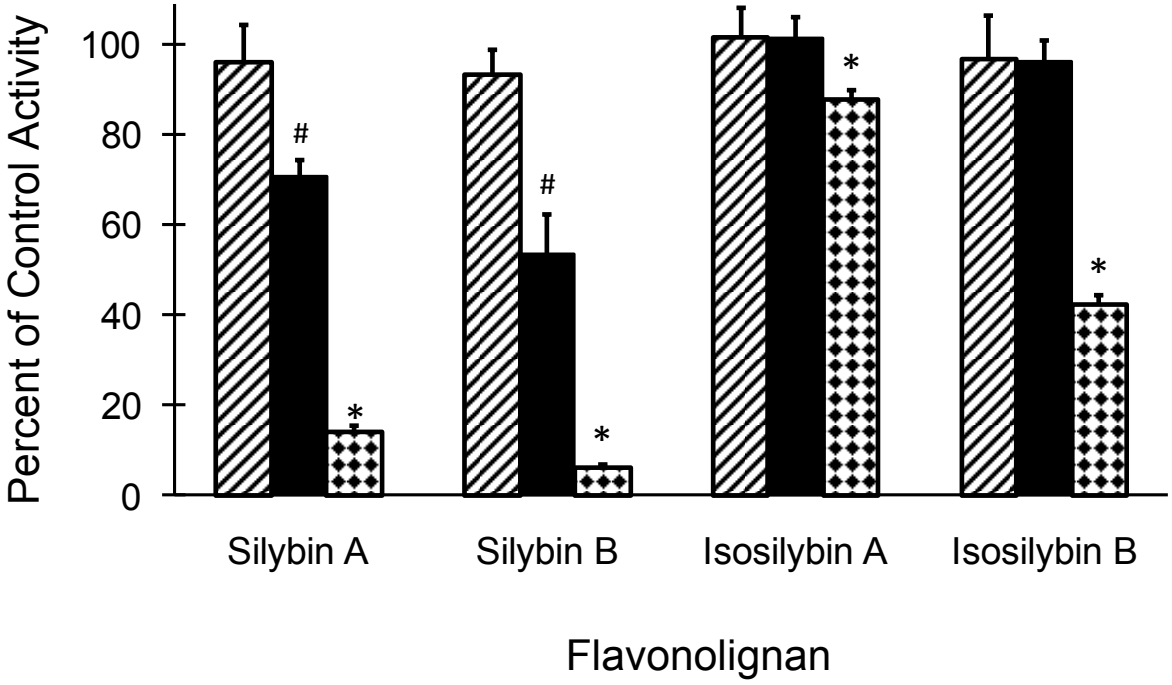
Percent of Control Activity
100
80
60
40
20
0
#
#
*
*
*
*
Silybin A
Silybin B
Isosilybin A
Isosilybin B
Flavonolignan

Figure 2.3

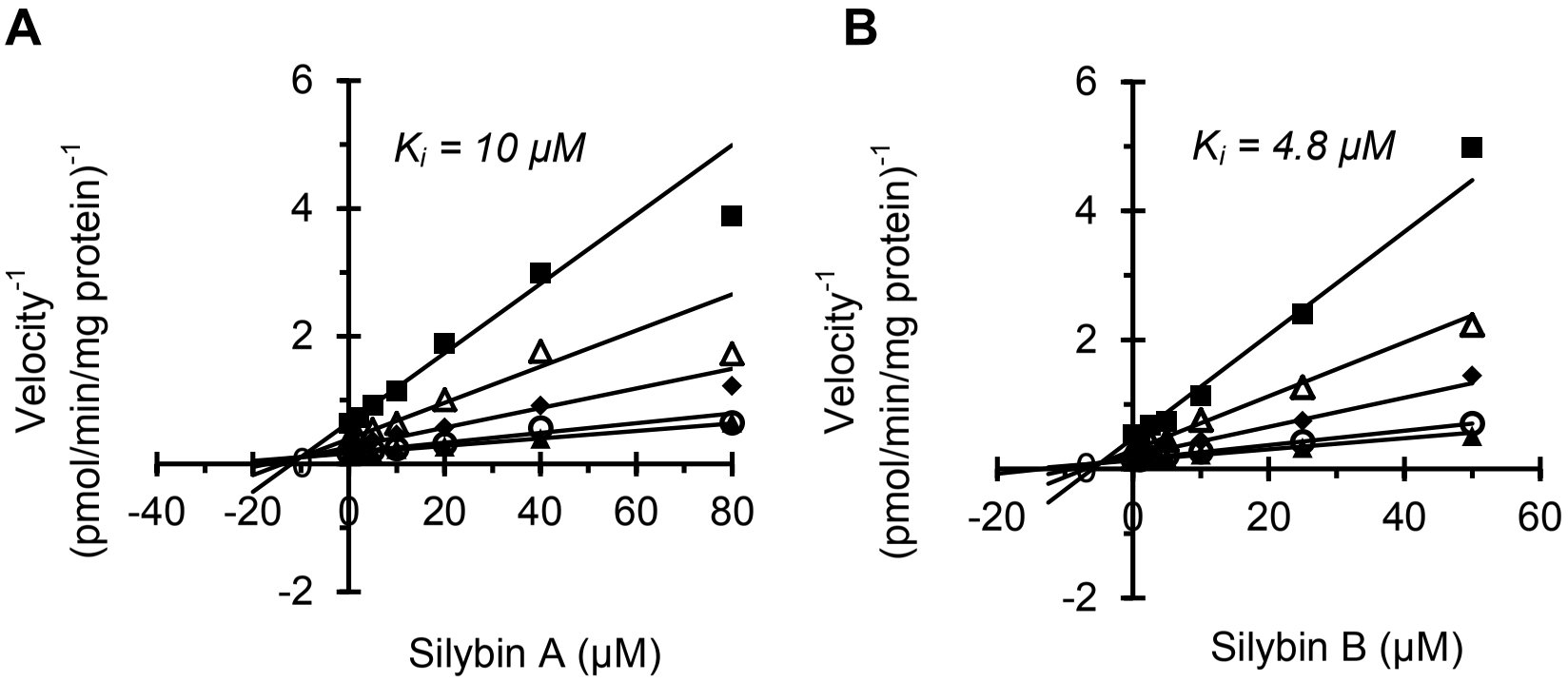
A
K_i = 10 μM
Velocity^{-1} (pmol/min/mg protein)$^{-1}$
Silybin A (μM)
B
K_i = 4.8 μM
Velocity^{-1} (pmol/min/mg protein)$^{-1}$
Silybin B (μM)

Figure 2.4

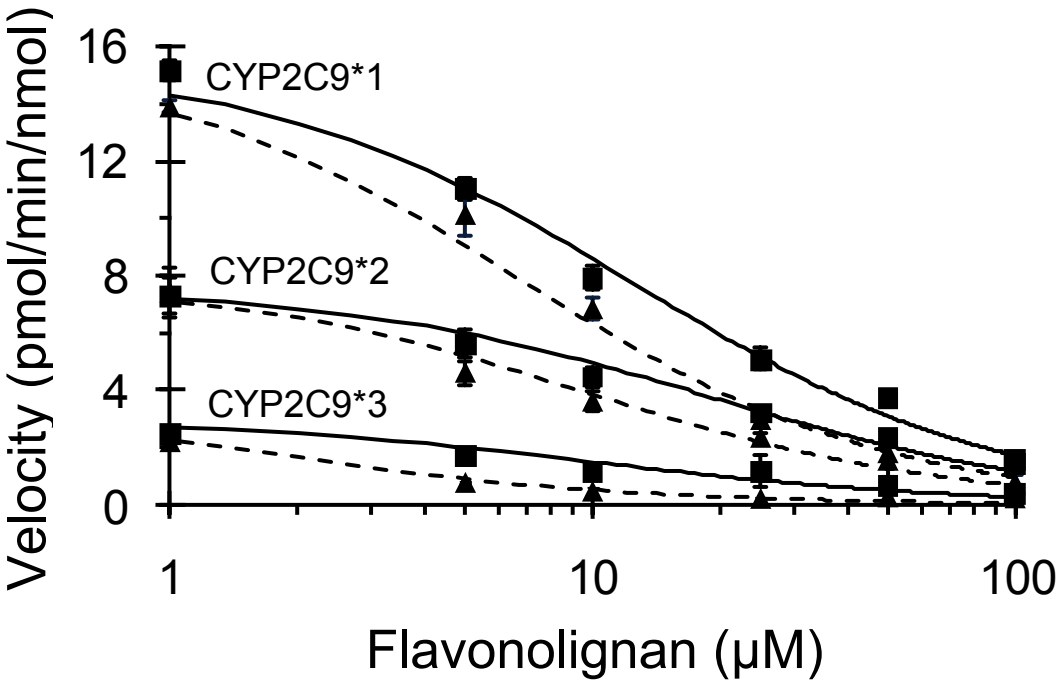
Velocity (pmol/min/nmol)
16
12
8
4
0
CYP2C9*1
CYP2C9*2
CYP2C9*3
1
10
100
Flavonolignan (μM)

Figure 2.5

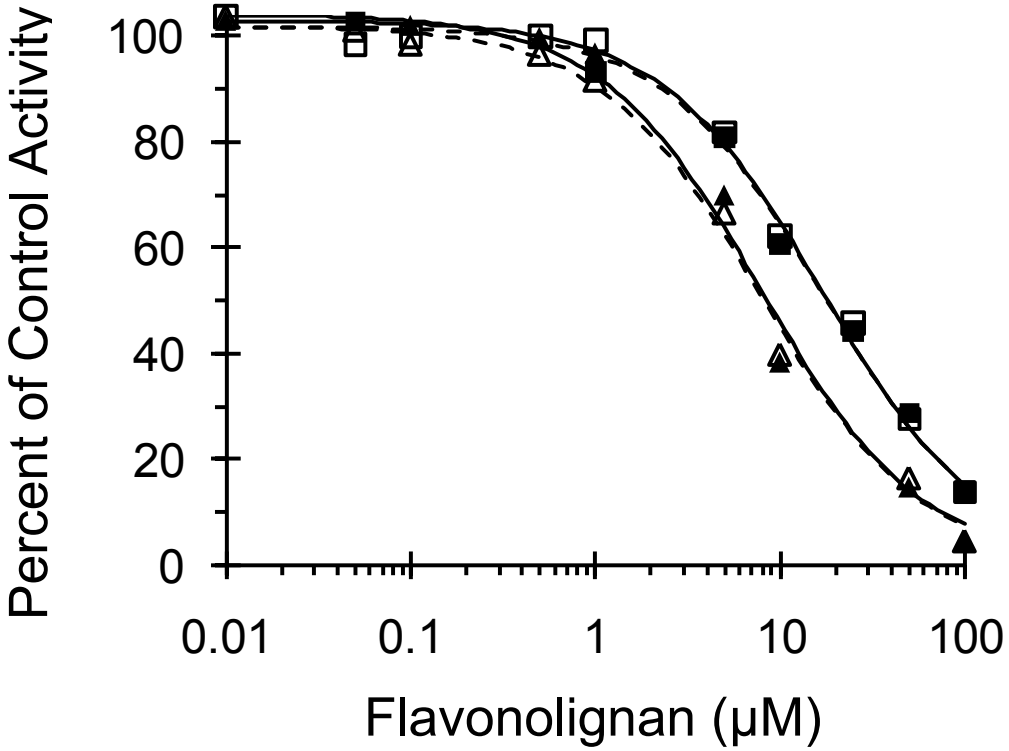
Percent of Control Activity
100
80
60
40
20
0
0.01
0.1
1
10
100
Flavonolignan (μM)

References

Agarwal R, Agarwal C, Ichikawa H, Singh RP and Aggarwal BB (2006) Anticancer potential of silymarin: from bench to bed side. *Anticancer Res* **26**:4457-4498.

Bachmann KA and Lewis JD (2005) Predicting inhibitory drug-drug interactions and evaluating drug interaction reports using inhibition constants. *Ann Pharmacother* **10**:10.

Davis-Searles PR, Nakanishi Y, Kim NC, Graf TN, Oberlies NH, Wani MC, Wall ME, Agarwal R and Kroll DJ (2005) Milk thistle and prostate cancer: differential effects of pure flavonolignans from *Silybum marianum* on antiproliferative end points in human prostate carcinoma cells. *Cancer Res* **65**:4448-4457.

Flaig TW, Gustafson DL, Su LJ, Zirrolli JA, Crighton F, Harrison GS, Pierson AS, Agarwal R and Glode LM (2007) A phase I and pharmacokinetic study of silybin-phytosome in prostate cancer patients. *Invest New Drugs* **25**:139-146.

Gazak R, Walterova D and Kren V (2007) Silybin and silymarin--new and emerging applications in medicine. *Curr Med Chem* **14**:315-338.

Geng W (2003) A method for identification of inhibition mechanism and estimation of Ki in in vitro enzyme inhibition study. *Drug Metab Dispos* **31**:1456-1457.

Graf TN, Wani MC, Agarwal R, Kroll DJ and Oberlies NH (2007) Gram-scale purification of flavonolignan diastereoisomers from Silybum marianum (Milk Thistle) extract in support of preclinical in vivo studies for prostate cancer chemoprevention. *Planta Med* **73**:1495-1501.

Gurley B, Hubbard MA, Williams DK, Thaden J, Tong Y, Gentry WB, Breen P, Carrier DJ and Cheboyina S (2006a) Assessing the clinical significance of botanical supplementation on human cytochrome P450 3A activity: comparison of a milk thistle and black cohosh product to rifampin and clarithromycin. *J Clin Pharmacol* **46**:201-213.

Gurley BJ, Barone GW, Williams DK, Carrier J, Breen P, Yates CR, Song PF, Hubbard MA, Tong Y and Cheboyina S (2006b) Effect of milk thistle (Silybum marianum) and black cohosh (Cimicifuga racemosa) supplementation on digoxin pharmacokinetics in humans. *Drug Metabolism & Disposition* **34**:69-74.

Gurley BJ, Gardner SF, Hubbard MA, Williams DK, Gentry WB, Carrier J, Khan IA, Edwards DJ and Shah A (2004) In vivo assessment of botanical supplementation on human cytochrome P450 phenotypes: Citrus aurantium, Echinacea purpurea, milk thistle, and saw palmetto. *Clinical Pharmacology & Therapeutics* **76**:428-440.

Gurley BJ, Swain A, Hubbard MA, Williams DK, Barone G, Hartsfield F, Tong Y, Carrier DJ, Cheboyina S and Battu SK (2008) Clinical assessment of CYP2D6-mediated herb-drug interactions in humans: effects of milk thistle, black cohosh, goldenseal, kava kava, St. John's wort, and Echinacea. *Mol Nutr Food Res* **52**:755-763.

Han Y, Guo D, Chen Y, Tan ZR and Zhou HH (2009) Effect of silymarin on the pharmacokinetics of losartan and its active metabolite E-3174 in healthy Chinese volunteers. *Eur J Clin Pharmacol* **65**:585-591.

Hu Z, Yang X, Ho PC, Chan SY, Heng PW, Chan E, Duan W, Koh HL and Zhou S (2005) Herb-drug interactions: a literature review. *Drugs* **65**:1239-1282.

Jonas DE and McLeod HL (2009) Genetic and clinical factors relating to warfarin dosing. *Trends Pharmacol Sci* **30**:375-386.

Kim NC, Oberlies NH, Brine DR, Handy RW, Wani MC and Wall ME (2001) Isolation of symlandine from the roots of common comfrey (*Symphytum officinale*) using countercurrent chromatography. *J Nat Prod* **64**:251-253.

Kohno H, Suzuki R, Sugie S, Tsuda H and Tanaka T (2005) Dietary supplementation with silymarin inhibits 3,2'-dimethyl-4-aminobiphenyl-induced prostate carcinogenesis in male F344 rats. *Clin Cancer Res* **11**:4962-4967.

Kroll DJ, Shaw HS and Oberlies NH (2007) Milk thistle nomenclature: why it matters in cancer research and pharmacokinetic studies. *Integr Cancer Ther* **6**:110-119.

Obach RS, Walsky RL and Venkatakrishnan K (2007) Mechanism-based inactivation of human cytochrome p450 enzymes and the prediction of drug-drug interactions. *Drug Metabolism & Disposition* **35**:246-255.

Paine MF and Oberlies NH (2007) Clinical relevance of the small intestine as an organ of drug elimination: drug-fruit juice interactions. *Expert Opin Drug Metab Toxicol* **3**:67-80.

Post-White J, Ladas EJ and Kelly KM (2007) Advances in the use of milk thistle (Silybum marianum). *Integr Cancer Ther* **6**:104-109.

Ramasamy K and Agarwal R (2008) Multitargeted therapy of cancer by silymarin. *Cancer Lett* **269**:352-362.

Rettie AE and Tai G (2006) The pharmocogenomics of warfarin: closing in on personalized medicine. *Mol Interv* **6**:223-227.

Schrieber SJ, Wen Z, Vourvahis M, Smith PC, Fried MW, Kashuba AD and Hawke RL (2008) The pharmacokinetics of silymarin is altered in patients with hepatitis C virus and nonalcoholic Fatty liver disease and correlates with plasma caspase-3/7 activity. *Drug Metabolism & Disposition* **36**:1909-1916.

Singh RP, Raina K, Sharma G and Agarwal R (2008) Silibinin inhibits established prostate tumor growth, progression, invasion, and metastasis and suppresses tumor angiogenesis and epithelial-mesenchymal transition in transgenic adenocarcinoma of the mouse prostate model mice. *Clin Cancer Res* **14**:7773-7780.

Thi L, Shaw D and Bird J (2009) Warfarin potentiation: a review of the "FAB-4" significant drug interactions. *Consult Pharm* **24**:227-230.

Ulbricht C, Chao W, Costa D, Rusie-Seamon E, Weissner W and Woods J (2008) Clinical evidence of herb-drug interactions: a systematic review by the natural standard research collaboration. *Curr Drug Metab* **9**:1063-1120.

Wen Z, Dumas TE, Schrieber SJ, Hawke RL, Fried MW and Smith PC (2008) Pharmacokinetics and metabolic profile of free, conjugated, and total silymarin flavonolignans in human plasma after oral administration of milk thistle extract. *Drug Metabolism & Disposition* **36**:65-72.

Wu JW, Lin LC and Tsai TH (2009) Drug-drug interactions of silymarin on the perspective of pharmacokinetics. *J Ethnopharmacol* **121**:185-193.

Chapter 3

Toward a Predictive Herb-Drug Interaction Framework: Evaluation of Milk Thistle Extracts and Eight Purified Constituents as CYP3A4/5 Inhibitors

Overview

Despite increasing recognition of untoward interactions between herbal products and conventional medications, a standard system for prospective assessment of herb-drug interactions remains elusive. This information gap was addressed by evaluating the drug interaction liability of the model herbal product milk thistle (*Silybum marianum*) with the CYP3A4/5 probe substrate midazolam. The inhibitory effects of commercially available milk thistle extracts and purified constituents on midazolam 1'-hydroxylation were screened using human liver and intestinal microsomes. Relative to vehicle, the extract silymarin and purified constituents silybin A, isosilybin A, isosilybin B, and silychristin at 100 μM demonstrated >50% inhibition in at least one microsomal preparation, prompting IC_{50} determination. The IC_{50}s for isosilybin B and silychristin were ~60, and 90 μM, respectively, whereas those for the remaining constituents were >100 μM. Extracts and constituents that contained the 1,4-dioxane moiety demonstrated a >1.5-fold shift in IC_{50} when tested as potential mechanism-based inhibitors. The semi-purified extract, silibinin, and the two associated constituents (silybin A, silybin B) demonstrated mechanism-based inhibition of recombinant CYP3A4 activity, showing similar kinetics (K_I ~100 μM; $k_{,inact}$ ~0.20 min^{-1}). Given that milk thistle extracts have been administered in gram quantities, silybin A and silybin B could achieve concentrations in

the gut near the K_I, providing a basis for clinical evaluation of the drug interaction liability of milk thistle with CYP3A substrates. Application of this herb-drug interaction evaluation framework to other herbal products may assist clinical decision-making and facilitate development of guidelines for quantitative prediction of clinically relevant interactions.

Introduction

An estimated 20% of adults in the US acknowledge taking herbal products (Bent, 2008), with nearly 70% failing to inform their conventional medical practitioner (Gardiner et al., 2006; Kennedy et al., 2008). An herbal product that inhibits one or more drug metabolizing enzymes can perpetrate untoward interactions with conventional medications (Hu et al., 2005; Izzo and Ernst, 2009). Prominent among these enzymes are the cytochromes P450 (P450s). Inhibition of P450 activity by the herbal product can reduce “victim” drug clearance, leading to higher systemic drug concentrations and the potential for adverse effects and toxicity. Dietary substances, including herbal products, are not regulated in the same manner as drug products. Consequently, herbal product drug interaction liability is not evaluated routinely prior to marketing. This information gap prevents both clinicians and consumers from making informed decisions about the risk of adding herbal products to pharmacotherapeutic regimens.

Despite increasing recognition of potential untoward interactions between drugs and herbal products, a standard system for prospective assessment of the drug interaction liability of herbal products remains elusive. One approach to developing such a system is to examine a well-characterized herbal product using traditional drug-drug interaction (DDI) predictive tools. Milk thistle is a top-10 selling herbal product in the US (Blumenthal et al., 2012) used predominately to self-treat hepatic disorders, particularly hepatitis C (Kroll et al., 2007; Post-White et al., 2007; Seeff et al., 2008). Milk thistle represents an ideal model herbal product due to the following key properties: high sales numbers (12.8 million dollars in 2011) indicate that a large number of consumers are at risk for milk thistle-drug interactions (Blumenthal et al., 2012); individual constituents have been identified, isolated, and scaled-up to quantities sufficient for in vitro DDI evaluation (Kim et al., 2003; Graf et al., 2007; Monti et al., 2010; Sy-Cordero et al.,

2012); and the literature indicates inconsistent in vitro-in vivo extrapolation of extant studies (Gurley et al., 2004; Gurley et al., 2006; Han et al., 2009).

Commercial preparations of milk thistle [*Silybum marianum* (L.) Gaertn.] include the crude extract silymarin, consisting of at least seven flavonolignans (Fig. 3.1), the flavonoid taxifolin, and fatty acids, and the semi-purified extract silibinin, consisting of the most prevalent flavonolignans (silybin A and silybin B). These extracts have been shown to inhibit the activity of several P450s in vitro, both reversibly (e.g., CYP2C9, CYP2C19, CYP2D6, CYP2E1, CYP3A4/5) (Beckmann-Knopp et al., 2000; Zuber et al., 2002; Etheridge et al., 2007; Doehmer et al., 2008; Brantley et al., 2010) and irreversibly (e.g., CYP2C9, CYP3A4) (Sridar et al., 2004). Translation to the clinic, however, has been inconsistent. For example, two healthy volunteer studies demonstrated no interaction between the CYP3A4/5 probe substrate midazolam and one silymarin product (Gurley et al., 2004; Gurley et al., 2006), whereas another study demonstrated a different silymarin product to increase significantly the systemic exposure to the CYP2C9/3A4/5 substrate losartan (Han et al., 2009). Explanation of these in vitro-in vivo disconnects requires rigorous characterization of the CYP3A4/5 inhibition properties of individual constituents, as well as commercial preparations.

CYP3A4/5 is responsible for the oxidative metabolism of nearly 50% of the top 200 prescribed medications (Wienkers and Heath, 2005) and is expressed in both the intestine and liver (Thummel et al., 1996). Following oral administration of milk thistle, intestinal CYP3A4/5 likely will be exposed to higher concentrations of the constituents compared to hepatic CYP3A4/5. This difference was demonstrated by the nearly 60-fold higher mean (± SD) concentration in intestinal relative to hepatic tissue in cancer patients administered 1.4 g silibinin (140 ± 170 vs. 2.5 ± 2.4 μM) (Hoh et al., 2006). Such high intestinal concentrations could reduce markedly the intestinal first-pass metabolism of susceptible CYP3A4/5 substrates, thereby increasing systemic drug exposure. Using

milk thistle as an model herbal product, the objectives of this study were to (1) assess the interaction liability of individual constituents towards CYP3A4/5 activity, (2) prioritize constituents for further evaluation, and (3) develop a framework to explain in vitro-in vivo disconnects and predict future herb-drug interactions. This information ultimately may permit clinicians and consumers to gauge the impact of adding herbal products to pharmacotherapeutic regimens.

Materials and Methods

Chemicals and reagents. Human liver (pooled from 50 donors, mixed gender) and intestinal (pooled from 18 donors, mixed gender) microsomes (HLMs, HIMs) were purchased from Xenotech, LLC (Lenexa, KS). Baculovirus insect cell-expressed CYP3A4 (rCYP3A4), supplemented with cDNA-expressed reductase and cytochrome b_5, was purchased from BD Biosciences (San Jose, CA). Midazolam, 1'-hydroxymidazolam, alprazolam, silibinin, ketoconazole, NADPH, glutathione, superoxide dismutase (SOD), catalase, 5,5-dimethyl-1-pyrroline-n-oxide (DMPO), DMSO, HPLC-grade water, methanol, ammonium acetate, and 1-propanol were purchased from Sigma-Aldrich (St. Louis, MO). 6',7'-Dihydroxybergamottin (DHB) was purchased from Cayman Chemical (Ann Arbor, MI). Silymarin was obtained from Euromed S.A. (Barcelona, Spain). Silybin A, silybin B, isosilybin A, isosilybin B, silychristin, isosilychristin, silydianin, and taxifolin were purified as described previously (Graf et al 2007); all milk thistle constituents were >97% pure as determined by high-performance liquid chromatography.

Evaluation of the stability of individual milk thistle constituents*. Stability in potassium phosphate buffer*. Each constituent was dissolved in DMSO to yield a 100 mM solution. Each solution was diluted in potassium phosphate buffer (0.1 M, pH 7.4), supplemented with $MgCl_2$ (3.3 mM), to yield a final concentration of 100 μM. Solutions were placed immediately into a heated (37°C) auto-sampler, and aliquots (0.3 μL) were collected serially from 0-1440 min and analyzed via UPLC-UV (described below). *Metabolic lability of selected constituents.* Silybin A, silybin B, isosilybin A, and isosilybin B were added to potassium phosphate buffer as described above with the addition of HLMs (0.05 mg/mL). Incubation mixtures were placed on a dry heat block and equilibrated for 5 min. Reactions were initiated with the addition of NADPH to yield a final concentration of 1 mM. Aliquots (100 μL) were removed from 0-60 min, and

reactions were terminated with 2 volumes of ice-cold acetonitrile. Each constituent was quantified by UPLC-UV (described below).

Analysis of incubations for milk thistle constituents. Constituents were quantified with an Acquity UPLC system (Empower 2 software; Waters Corp., Milford, MA) at a flow rate of 0.80 (stability study) or 0.75 (lability study) mL/min using an Acquity binary solvent manager and an Acquity HSS-T3 column (1.8 µm, 2.1 × 50 mm; Waters Corp.). The elution gradient for the stability study ranged from 10:90 to 40:60 methanol:water over 0.45 minutes, then from 40:60 to 55:45 over 1.5 minutes. The elution gradient for the lability study ranged from 40:60 to 55:45 methanol:water over 2 minutes. Signals were monitored at UV 288 nm using an Acquity PDA detector, and the volume injected was 0.3 (stability study) or 7.5 (lability study) µL by an Acquity sample manager.

Evaluation of milk thistle constituents as inhibitors of CYP3A4/5 activity. The inhibitory effects of silymarin, silibinin, and individual constituents on midazolam 1'-hydroxylation activity were evaluated using HLMs, HIMs, and rCYP3A4. Midazolam and ketoconazole were dissolved in methanol to yield 10 mM and 1 mM solutions, respectively. Milk thistle constituents were dissolved in DMSO to yield a 200 mM solution. NADPH was prepared fresh in potassium phosphate buffer to yield a 4 mM solution. Under all experimental conditions, the amount of 1'-hydroxymidazolam formed was linear with respect to incubation time and concentration of microsomal or rCYP3A4 protein (data not shown). *Initial testing.* Incubation mixtures consisted of HLMs or HIMs (0.05 mg/mL protein), midazolam (4 µM), milk thistle constituent/extract (1, 10, or 100 µM), and potassium phosphate buffer. Control mixtures contained 0.1% (v/v) DMSO in place of milk thistle constituent/extract. As a positive control for CYP3A4/5 inhibition, mixtures contained ketoconazole (1 µM) in place of milk thistle constituent/extract. The mixtures were equilibrated in a dry heat block at 37°C for 5 min before initiating the

reactions with NADPH (1 mM final concentration) to yield a final volume of 200 µL. After 2 (HLMs) or 4 (HIMs) min, reactions were terminated with 2 volumes of ice-cold acetonitrile containing 20 µg/mL alprazolam as the internal standard. After centrifugation (1350 x g for 10 min at 4°C), supernatants were analyzed for 1'-hydroxymidazolam by HPLC-MS/MS as described previously (Wang et al., 2007; Ngo et al., 2009). Individual constituents demonstrating ≥50% inhibition in either microsomal preparation were selected for further evaluation. *Screening of constituents as reversible inhibitors of CYP3A4/5 activity in HLMs and HIMs.* Incubation mixtures were prepared as described above, only milk thistle constituent/extract concentrations ranged from 0.10-200 µM. Reaction mixtures were processed and analyzed for 1'-hydroxymidazolam as described above. *Screening of constituents as metabolism-dependent inhibitors of CYP3A4/5 activity in HLMs, HIMs, and rCYP3A4.* IC_{50} shift experiments (Obach et al., 2007) were used to screen milk thistle constituents and extracts as potential mechanism-based inhibitors of CYP3A4/5 activity. Primary incubation mixtures consisting of HLMs, HIMs (0.25 mg/mL), or rCYP3A4 (20 pmol/mL), milk thistle constituent/extract (0-1000 µM), and potassium phosphate buffer were equilibrated at 37°C for 5 min before initiating reactions with NADPH (1 mM). Control reactions were identical except NADPH was replaced with potassium phosphate buffer. After 15 min, an aliquot (40 µL) was removed and diluted 5-fold into a secondary incubation mixture containing midazolam (4 µM) and NADPH (1 mM). After 2 (HLMs) or 4 (HIMs and rCYP3A4) min, the secondary reactions were terminated and processed as described above. Individual constituents demonstrating a >1.5-fold shift in IC_{50} were selected for further analysis. *Effect of nucleophilic trapping agents and reactive oxygen species scavengers on CYP3A4/5 inactivation in HLMs.* Primary mixtures consisted of HLMs (0.25 mg/mL), silybin A (0, 30, or 100 µM), potassium phosphate buffer, and trapping agent [DMPO (1 mM), SOD (1,000 U/mL), glutathione (2 mM), or catalase (5,000 U/mL)]. The mixtures were

equilibrated at 37°C for 5 min before initiating reactions with NADPH (1 mM). Control reactions were identical except NADPH was replaced with potassium phosphate buffer. Reactions proceeded as described for the IC_{50} shift experiment. *Determination of mechanism-based inhibition kinetics.* Time- and concentration-dependent inhibition of CYP3A4 was assessed as described previously (Paine et al., 2004). Briefly, primary incubation mixtures consisting of rCYP3A4 (0.2 nmol/mL), milk thistle constituent/extract (0-200 μM), and potassium phosphate buffer were equilibrated at 37°C for 5 min before initiating the primary reactions with NADPH. As a positive control for mechanism-based inhibition, incubation mixtures contained DHB (5 μM) in place of milk thistle constituent/extract (Paine et al., 2004). At designated times (0-15 min), an aliquot (4 μL) was removed and diluted 50-fold into a secondary reaction mixture containing midazolam (8 μM) and NADPH (1 mM). The secondary reactions were terminated and processed as described for the reversible inhibition experiments.

Data analysis. *Determination of apparent IC_{50}.* The apparent IC_{50} of milk thistle constituent/extract was recovered according to previously published methods (Brantley et al., 2010). Briefly, an initial estimate was determined by visual inspection of the velocity of 1'-hydroxymidazolam formation versus the natural logarithm of milk thistle constituent/extract concentration data. Apparent IC_{50} was recovered by fitting equation 1 or 2 to untransformed data using WinNonlin (version 5.3; Pharsight, Mountain View, CA):

$$v = \frac{v_0}{1 + \left(\frac{I}{IC_{50}}\right)} \qquad \text{(Eq. 1)}$$

$$v = \frac{v_0}{1 + \left(\frac{I}{IC_{50}}\right)^h} \qquad \text{(Eq. 2)}$$

where v denotes the velocity of 1'-hydroxymidazolam formation, v_0 denotes the initial velocity of 1'-hydroxymidazolam formation, I denotes the concentration of milk thistle

constituent/extract, and *h* denotes the Hill coefficient. The best-fit equation was assessed from visual inspection of the observed versus predicted data, randomness of the residuals, Akaike information criteria, and SEs of the parameter estimates.

Determination of K_I and k_{inact}. Mechanism-based inhibition (MBI) parameters were recovered according to previously published methods (Paine et al., 2004; Obach et al., 2007). Briefly, the natural logarithm of the percentage of CYP3A4 activity remaining was plotted as a function of primary reaction time. The apparent inactivation rate constant ($k_{inact,app}$) for each inhibitor concentration was determined from the slope of the initial mono-exponential decline in activity. Initial estimates of K_I and k_{inact} were obtained from a Kitz-Wilson plot. Final parameter estimates were obtained by nonlinear least-squares regression using equation 3:

$$k_{inact,app} = k_{zero} + \frac{k_{inact} * I}{K_I + I} \qquad \text{(Eq. 3)}$$

where k_{zero} is the rate of CYP3A4 inactivation in the absence of inhibitor. The efficiency of inactivation was calculated as the ratio of k_{inact} to K_I.

Statistical analysis. Data are presented as means ± SDs of triplicate determinations unless indicated otherwise. Enzyme kinetic parameters are presented as the estimates ± SEs. All statistical comparisons were made according to previously published methods (Brantley et al., 2010). In brief, concentration-dependent inhibition of individual flavonolignans was evaluated by a one-way ANOVA; post-hoc comparisons were made using Tukey's test when an overall significance resulted. Statistical differences between calculated IC_{50} values were evaluated by a Student's *t*-test of two independent samples. A $p<0.05$ was considered significant for all statistical tests.

Results

Selected milk thistle constituents are metabolically stable in HLMs for up to 15 min. All tested constituents were stable (>95% remaining) for 1 h at 37°C in potassium phosphate buffer (data not shown). Metabolic stability experiments determined the optimal primary incubation time such that inhibitor depletion would be ≤20%. All constituents at 10 μM demonstrated ≥50% oxidative depletion by 60 min (Fig. 3.2). Isosilybin A was the least stable, showing 40% depletion by 10 min, whereas the remaining constituents were depleted by <10%. At 100 μM, silybin A was slightly more stable than the other constituents, (~40% vs. 50% depletion by 60 min). Isosilybin A was the least stable, showing 30% depletion by 10 min, whereas the remaining constituents were depleted by <10%. Based on these observations, the primary incubation time of the metabolism- and mechanism-dependent inhibition experiments was limited to 15 min.

Milk thistle constituents differentially inhibit CYP3A4/5-mediated midazolam 1'-hydroxylation. *Initial testing.* All flavonolignans and the two extracts (silibinin, silymarin) inhibited midazolam 1'-hydroxylation in a concentration-dependent manner (100 vs. 10 μM) in HLMs (Fig. 3.3A) and, with the exception of isosilychristin, in HIMs (Fig. 3.3B). The sole flavonoid, taxifolin, showed no concentration-dependent inhibition with either preparation. Only silybin B (HLMs), silychristin (HIMs), and silydianin (HIMs) showed concentration-dependent inhibition from 10 to 1 μM (1 μM data not shown). With HLMs, silybin A at 100 μM was the most potent, followed by silymarin, isosilybin B, and isosilybin A (Fig. 3.3A); with HIMs, silymarin at 100 μM was the most potent, followed by isosilybin A, isosilybin B, and silychristin (Fig. 3.3B). Based on >50% inhibition at 100 μM in at least one microsomal preparation, silybin A, isosilybin A, isosilybin B, and silychristin were selected for IC_{50} determination. Additionally, based on the high concentrations (>140 μM) observed in enterocytes following silibinin

administration to human subjects (Hoh et al 2006), silybin B and silibinin were selected for further evaluation. *Reversible inhibition.* With both HLMs and HIMs, isosilybin B was the most potent constituent, followed by silychristin, silybin B, and silybin A (Table 3.1). Because isosilybin A was not soluble at concentrations >100 μM, a complete IC_{50} curve could not be recovered. *IC_{50} shift*. The IC_{50} for silybin A, silybin B, and silibinin was 73-98% lower in the presence compared to the absence of NADPH in the primary incubation (Table 3.2). rCYP3A4 was more sensitive to inhibition than HLMs and HIMs (Table 3.2, Fig. 3.4). The IC_{50} for silychristin did not decrease in either HLMs or HIMs (Table 3.2), precluding further evaluation of this constituent. Reactive species scavengers did not ameliorate the NADPH-dependent increase in potency of silybin A towards CYP3A4/5 activity (Fig. 3.5).

Silybin A, silybin B, and silibinin demonstrate mechanism-based inactivation of rCYP3A4 activity. The time- and concentration-dependent inhibition of rCYP3A4 activity by silybin A, silybin B, and silibinin was evaluated to derive mechanism-based inhibition kinetics (Fig. 3.6). Because the rate of inactivation for silybin B at 200 μM deviated from linearity (Fig. 3.6B), these data were excluded from further analysis. The kinetics were similar between silybin A and silybin B; the kinetics of the 1:1 mixture of silybin A and silybin B (silibinin) were similar to those recovered for the single constituents (Table 3.3).

Discussion

Herb-drug interactions are a growing concern in clinical practice as consumers turn increasingly to herbal products as a means to self-treat various conditions. Despite increasing recognition of these potential untoward interactions, a standard system for prospective assessment of the drug interaction liability of herbal products remains elusive. Milk thistle was selected as a model herbal product based on the well-characterized nature, market share, and clinical relevance. Milk thistle extracts have been reported to inhibit P450 activity in vitro (Beckmann-Knopp et al., 2000; Zuber et al., 2002; Doehmer et al., 2008); however, translation to the clinic has been inconsistent, particularly with CYP3A4/5-mediated interactions (Gurley et al., 2004; Gurley et al., 2006; Han et al., 2009). Taken together, inhibition of CYP3A4/5 by single constituents was evaluated to address these in vitro-in vivo disconnects, as well as to develop a framework for prospective assessment of herb-drug interactions.

As demonstrated previously with CYP2C9 activity ((*S*)-warfarin 7-hyroxylation) (Brantley et al., 2010), milk thistle constituents differentially inhibited CYP3A4/5 activity (midazolam 1'-hydroxylation) (Fig. 3.3). The crude extract silymarin was consistently one of the most potent inhibitors of CYP3A4/5 activity in microsomal preparations. Among single constituents, the relatively less abundant isosilybin A and isosilybin B were two of the more potent inhibitors in both HLMs and HIMs (Fig. 3.3). Inhibitory kinetic parameters were recovered for isosilybin B, whereas metabolic lability (Fig. 3.2) and insolubility above 100 μM precluded recovery of these parameters for isosilybin A. Inhibition of midazolam 1'-hydroxylation in HLMs by silymarin at 100 μM (47%) was comparable to that by silymarin at approximately 50 μM (43%) in a previous study (Etheridge et al., 2007). With microsomes, silibinin was a more potent inhibitor of both nifedipine dehydrogenation (IC_{50}, 27-60 μM) (Zuber et al., 2002) and testosterone 6β-hydroxylation (IC_{50}, 50 μM) (Jancova et al., 2007) compared to midazolam 1'-

hydroxylation (IC_{50}, 67-120 μM). Substrate-dependent inhibition potencies are well-documented for CYP3A4 due to multiple substrate binding domains (Schrag and Wienkers, 2001; Galetin et al., 2003). As midazolam was the only substrate tested in the current work, the reversible inhibition kinetics for the individual milk thistle constituents can be extrapolated only to CYP3A4/5 substrates that bind to the benzodiazepine binding domain. In addition, the extent of inhibition by silymarin at 100 μM was greater than expected assuming additive inhibition by flavonolignans in aggregate (Fig. 3.3), suggesting that milk thistle flavonolignans may be synergistic inhibitors of CYP3A4/5. Further evaluation is needed to determine the extent, as well as clinical implications, of this potential synergism.

With the exception of silychristin, all constituents and both extracts demonstrated mechanism-based inhibition (MBI) of CYP3A4/5 activity in HLMs and HIMs, as evidenced by a >1.5-fold shift in IC_{50} (Berry and Zhao, 2008). The K_I for silibinin in the current work (110 μM) was within, whereas the k_{inact} (0.20 min^{-1}) was roughly three times faster, than corresponding parameters reported using the CYP3A4/5 substrates 7-benzyloxy-4-(trifluoromethyl) coumarin (32 μM and 0.06 min^{-1}) and testosterone (132 μM and 0.08 min^{-1}) (Sridar et al., 2004). The difference in k_{inact} may reflect different enzyme sources (recombinant vs. reconstituted CYP3A4). Inactivation of CYP3A4 activity in rCYP3A4 was rapid, occurring within the 2-4 min incubation times for the reversible inhibition experiments. As such, some inactivation would be expected under these conditions; however, the presence of midazolam should mitigate inactivation through substrate protection (Silverman and Daniel, 1995).

The major oxidative metabolite of silibinin is reported to be an *O*-demethylated product produced by CYP2C8 and CYP3A4 (Jancova et al., 2007). Further oxidation of the resulting catechol could create a reactive 1,2-benzoquinone moiety. However, inactivation by this mode was unlikely, as MBI was not observed with compounds

containing either the catechol (taxifolin) (data not shown) or the 2-methoxyphenol (silychristin) moiety (Fig. 3.1, Table 3.2). Unlike the 2-methoxyphenol- or catechol-containing constituents, only constituents testing positive for MBI contained a 1,4-dioxane moiety (Fig. 3.1). Oxidation of this region may create reactive oxygen species capable of inactivating CYP3A4. Since inactivation was not abrogated by the trapping agents, the inactivating species exerted their effect before leaving the CYP3A4 active site. If this proposed mode of MBI is verified, this chemical moiety may be considered an addition to the list of structural alerts (Kalgutkar et al., 2007).

The clinical interaction potential for mechanism-based inhibitors is higher than that for reversible inhibitors, as restoration of P450 activity is dependent upon *de novo* protein synthesis, rather than removal of the offending molecule(s) (Watanabe et al., 2007). MBI has been hypothesized as the only means by which fruit juices can elicit clinically significant interactions with CYP3A4/5 substrates (Hanley et al., 2012). The maximum rate of CYP3A4 inactivation by silibinin was roughly half that reported for the mechanism-based inhibitor in grapefruit juice, DHB (0.20 vs. 0.41 min^{-1}) (Paine et al., 2004). The K_I for silybin A and silybin B was approximately one hundred times that for DHB (~100 vs. 1.1 μM). Thus, at equivalent exposures, DHB will inactivate CYP3A4 more efficiently than the milk thistle constituents (370 vs. ~2 μl/min/pmol). However, enteric concentrations as high as 140 μM have been reported following administration of 1.4 g/day of silibinin (Hoh et al., 2006), albeit with large between-subject variability (120% CV). At doses this high, clinically relevant inactivation of CYP3A4/5 might be anticipated, even if only limited to the intestine.

Historically noted for putative hepatoprotective effects, self-administration of milk thistle products is popular among hepatitis C patients, in which an estimated 33% have used milk thistle as part of their therapeutic regimen (Seeff et al., 2008). These patients also may have an increased plasma exposure to milk thistle flavonolignans due to

impaired hepatic function (Schrieber et al., 2008). The disease-related decrease in hepatic function alone could put these patients at increased risk for metabolic DDIs. Adding milk thistle products may provide an additional insult rather than the desired hepatoprotective effect.

In summary, herb-drug interaction predictions are challenging due to the multitude of bioactive constituents typically composing herbal products. As such, identification of individual perpetrators is necessitated. The current work outlines a framework to facilitate prospective evaluation of herb-drug interaction potential using milk thistle as a model herbal product. Of the eight constituents tested, this approach identified two constituents, silybin A and silybin B, which may perpetrate interactions via MBI of CYP3A4/5 activity. Intestinal concentrations of these constituents could achieve those near the K_I (~100 μM), particularly with gram doses of silibinin that have been tested in patient populations. Clinical evaluation at these higher doses is needed to rule out an interaction liability with CYP3A4/5 substrates. Refinement and application of this framework to other herbal products ultimately may assist clinicians and consumers to make informed decisions about the consequences of adding an herbal product to conventional pharmacotherapeutic regimens.

Legends to Figures

Fig. 3.1. Structures of flavonolignans and flavonoid (taxifolin) from milk thistle.

Fig. 3.2. Metabolic lability of selected milk thistle constituents in human liver microsomes. Microsomes (0.05 mg/mL) were incubated with silybin A (solid circle), silybin B (solid diamond), isosilybin A (open circle) or isosilybin B (open diamond) at 10 or 100 μM in potassium phosphate buffer. Incubations were initiated with NADPH (1 mM) and quenched at designated times. Symbols and error bars denote means and SDs, respectively, of triplicate incubations.

Fig. 3.3. Inhibitory effects of flavonolignans on midazolam 1'-hydroxylation activity in human liver microsomes (A) and human intestinal microsomes (B). Microsomes (0.05 mg/mL) were incubated with midazolam (4 μM) and flavonolignan (10 or 100 μM; grey and black bars, respectively) for 2 (HLMs) or 4 (HIMs) min. Reactions were initiated with NADPH (1 mM). Midazolam 1'-hydroxylation activity in the presence of vehicle control [0.1% (v/v) DMSO] was 800 ± 40 pmol/min/mg or 280 ± 16 pmol/min/mg microsomal protein for HLMs and HIMs, respectively. Bars and error bars denote means and SDs, respectively, of triplicate incubations.

Fig. 3.4. IC_{50} shift plot for silybin A, silybin B, and silibinin. Human liver microsomes (A), human intestinal microsomes (B), and cDNA expressed CYP3A4 (C) were incubated with silybin A (circles), silybin B (diamonds) or silibinin (squares) (0.1-200 μM) in the presence (open symbols) or absence (solid symbols) of NADPH (1 mM). The primary reaction mixture was diluted 5-fold to initiate the secondary reaction, which contained NADPH (1 mM) and midazolam (4 μM). Midazolam 1'-hydroxylation activity in the presence of vehicle control [(0.1% (v/v) DMSO)] was 2000 ± 90 pmol/min/mg (HLMs), 350 ± 10 pmol/min/mg (HIMs), and 7.9 ± 1.0 pmol/min/pmol (rCYP3A4). Symbols and error bars denote means and SDs, respectively, of triplicate incubations. Open symbols denote observed data when NADPH was present in the primary incubation; solid

symbols denote observed data when NADPH was absent in the primary incubation. Curves denote nonlinear least-squares regression of observed data using WinNonlin (version 5.3).

Fig. 3.5. Effect of traditional reactive species scavengers. Human liver microsomes were incubated for 15 min with silybin A (100 μM) and traditional reactive species scavengers in the presence or absence of NADPH. The primary reaction mixture was diluted 5-fold to initiate the secondary reaction, which contained NADPH (1 mM) and midazolam (4 μM). Midazolam 1'-hydroxylation activity in the presence of vehicle control [(0.1% (v/v) DMSO] was 1700 ± 46 pmol/min/mg microsomal protein. With the exception of glutathione and catalase (duplicate incubations), bars and error bars denote means and SDs, respectively, of triplicate incubations.

Fig. 3.6. Time- and concentration-dependent plot of CYP3A4/5 activity. cDNA expressed CYP3A4 was incubated with silybin A (A), silybin B (B), and silibinin (C) (0-200 μM). The primary reaction mixture was diluted 50-fold to initiate the secondary reaction, which contained NADPH (1 mM) and midazolam (8 μM), at designated times. Symbols denote means of duplicate incubations. Lines denote linear regression of the initial mono-exponential decline in activity. The inset depicts the rate of CYP3A4 inactivation as a function of inhibitor concentration. Symbols denote observed inactivation rates at each inhibitor concentration. Curves denote nonlinear least-squares regression of observed values using WinNonlin (version 5.3).

Table 3.1. Comparison of IC_{50}s under reversible inhibition experimental design

Values represent the estimate ± S.E. from nonlinear regression using WinNonlin

Enzyme Source	IC_{50} (μM)				
	Silybin A	Silybin B	Isosilybin A	Isosilybin B	Silychristin
HLMs[a]	180 ± 16	150 ± 7.6	N.D.	56 ± 4.4	90 ± 8.8
HIMs[b]	130 ± 12	90 ± 10	N.D.	60 ± 4.8	93 ± 8.7

N.D., not determined due to insolubility at concentrations > 100 μM
[a]Human liver microsomes
[b]Human intestinal microsomes

Table 3.2. Comparison of IC_{50}s under IC_{50} shift experimental design

Values represent the estimate ± S.E. from nonlinear regression using WinNonlin

Constituent/Extract	Enzyme Source								
	HLMs[a]			HIMs[b]			rCYP3A4[c]		
	IC_{50} (μM)		Fold Change	IC_{50} (μM)		Fold Change	IC_{50} (μM)		Fold Change
	- NADPH[d]	+ NADPH[e]		- NADPH	+ NADPH		- NADPH	+ NADPH	
Silybin A	120 ± 4.8	28 ± 3.1	4.3	100 ± 6.9	23 ± 1.7	4.3	53 ± 2.0	1.6 ± 0.2	33
Silybin B	140 ± 5.7	19 ± 2.1	7.4	100 ± 3.8	27 ± 1.9	3.7	63 ± 3.2	1.4 ± 0.2	45
Silibinin	120 ± 5.7	14 ± 2.2	8.6	67 ± 7.9	15 ± 3.0	4.5	45 ± 2.8	1.2 ± 0.2	38
Silychristin	26 ± 3.3	52 ± 5.2	0.5	25 ± 4.2	72 ± 7.7	0.3	N.D.	N.D.	N.D.
Isosilybin B	78 ± 6.2	30 ± 3.3	2.6	54 ± 3.3	23 ± 2.3	2.3	N.D.	N.D.	N.D.
Silymarin	95 ± 12	28 ± 4.5	3.4	29 ± 2.7	7.0 ± 0.8	4.1	N.D.	N.D.	N.D.

N.D., not determined
[a]Human liver microsomes
[b]Human intestinal microsomes
[c]Baculovirus insect cell-expressed CYP3A4
[d]NADPH was absent during the primary incubation
[e]NADPH was present during the primary incubation

Table 3.3. Inactivation kinetics of milk thistle constituents

Values represent the estimate ± S.E. from nonlinear regression using WinNonlin

Constituent/Extract	K_I (μM)	k_{inact} (min^{-1})	k_{inact} / K_I (μl/min/pmol)	$t_{1/2}$ (min)	k_{zero} (min^{-1})
Silybin A	100 ± 27	0.22 ± 0.02	2.2	3.2	0.025 ± 0.005
Silybin B	89 ± 60	0.15 ± 0.04	1.7	4.5	0.023 ± 0.008
Silibinin	110 ± 15	0.20 ± 0.01	1.8	3.5	0.016 ± 0.002

Figure 3.1

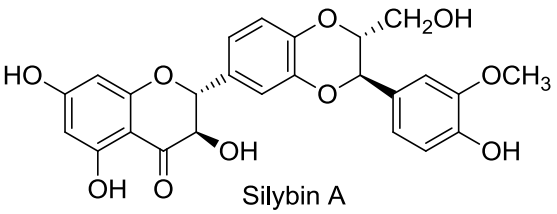

Silybin A

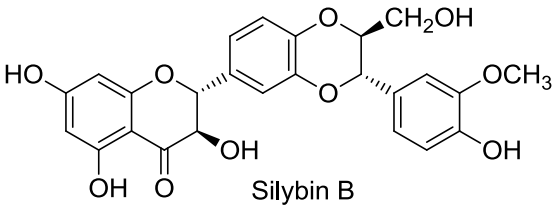

Silybin B

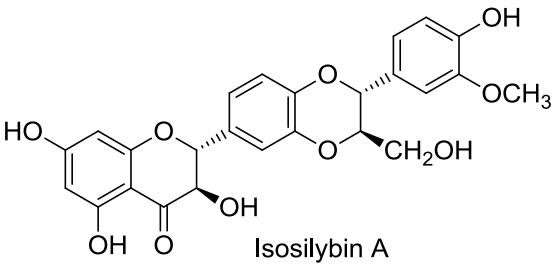

Isosilybin A

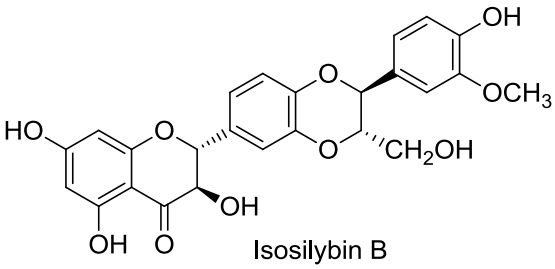

Isosilybin B

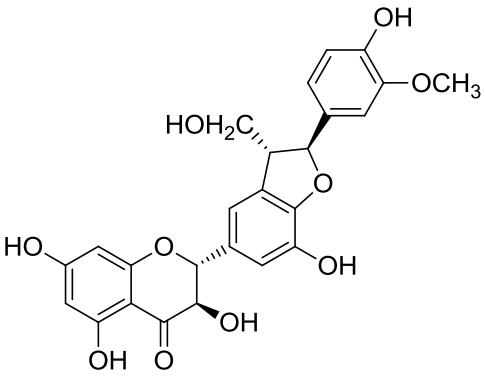

Silychristin

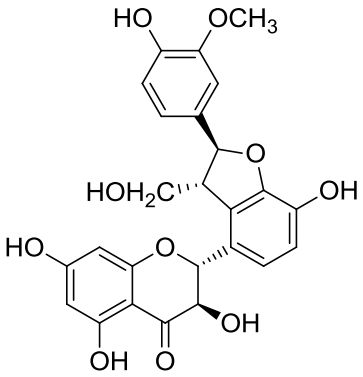

Isosilychristin

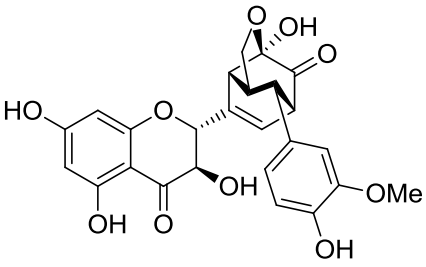

Silydianin

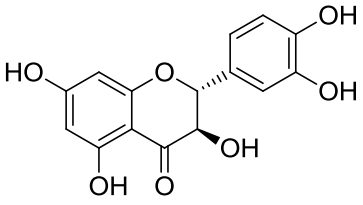

Taxifolin

Figure 3.2

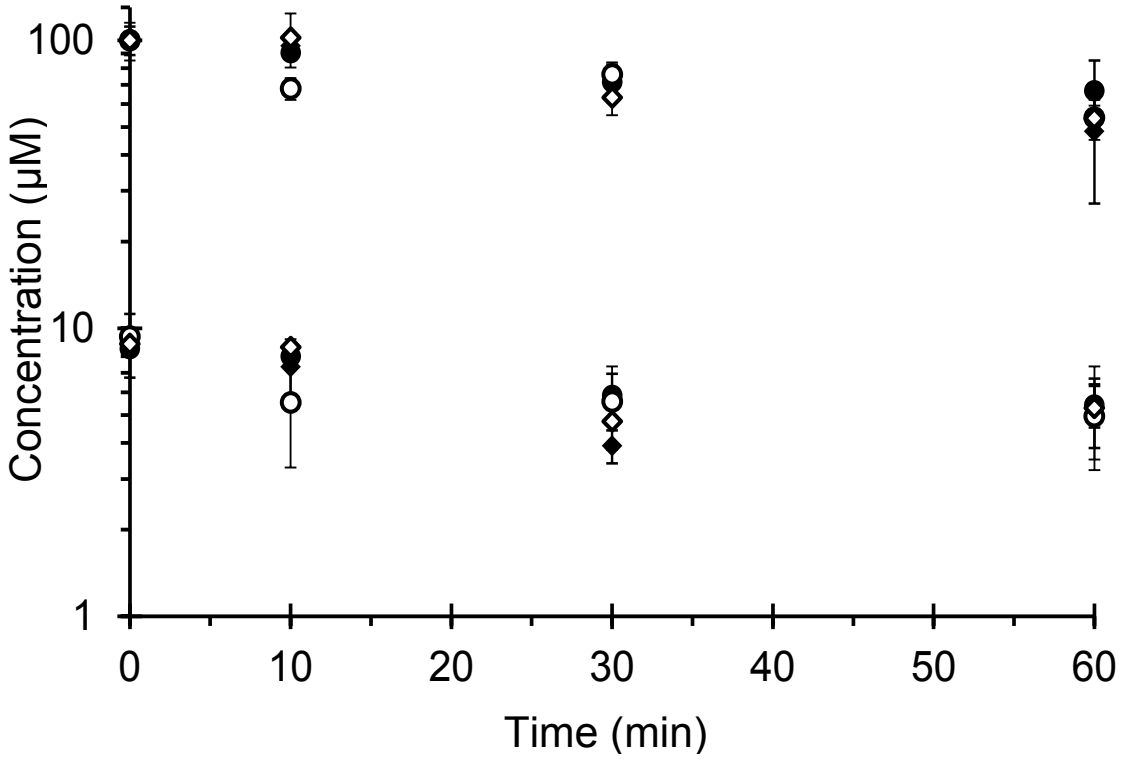

Figure 3.3

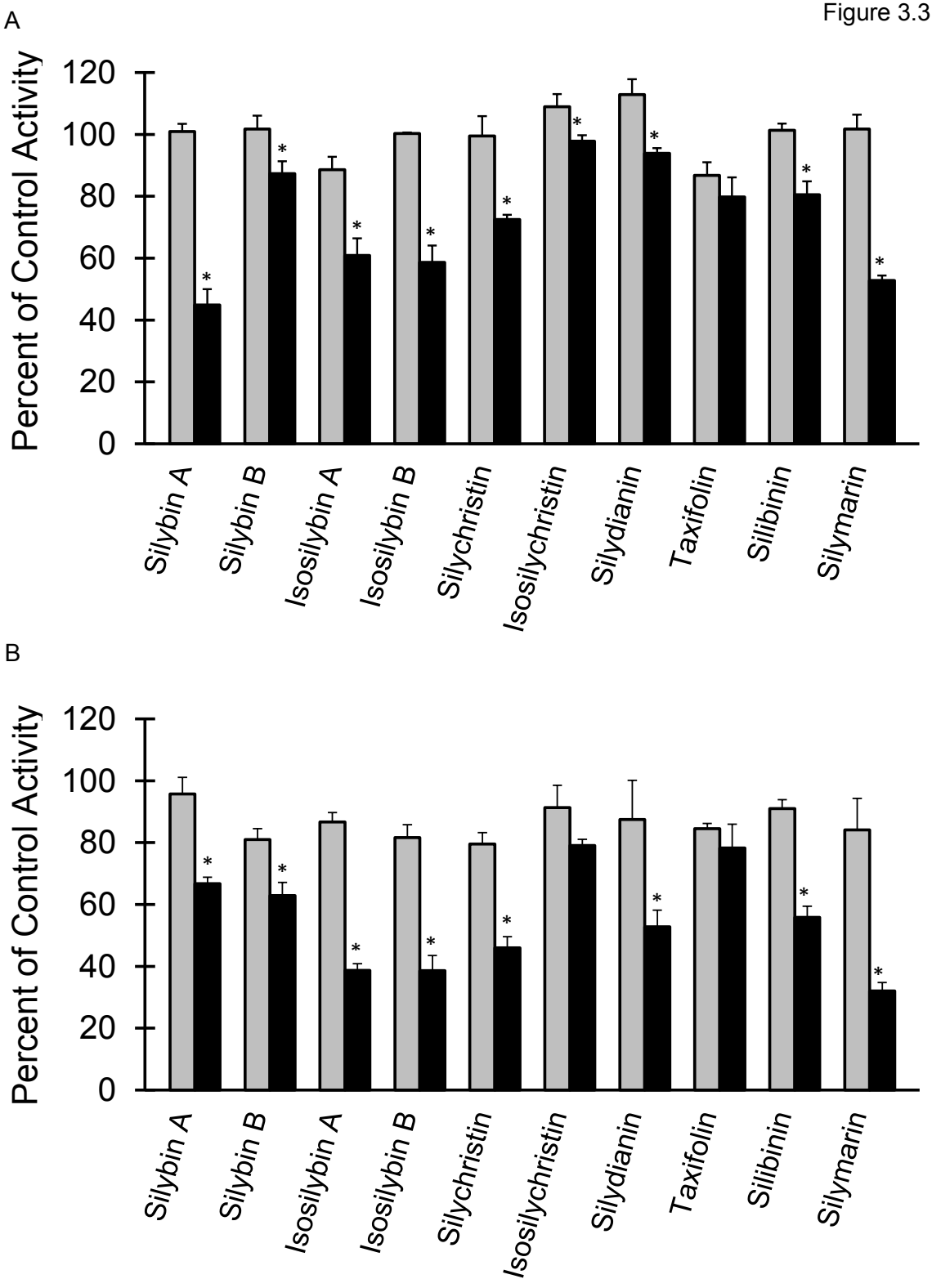
A
Percent of Control Activity
120
100
80
60
40
20
0
*
Silybin A
Silybin B
Isosilybin A
Isosilybin B
Silychristin
Isosilychristin
Silydianin
Taxifolin
Silibinin
Silymarin
B
Percent of Control Activity
120
100
80
60
40
20
0
*
Silybin A
Silybin B
Isosilybin A
Isosilybin B
Silychristin
Isosilychristin
Silydianin
Taxifolin
Silibinin
Silymarin

Figure 3.4

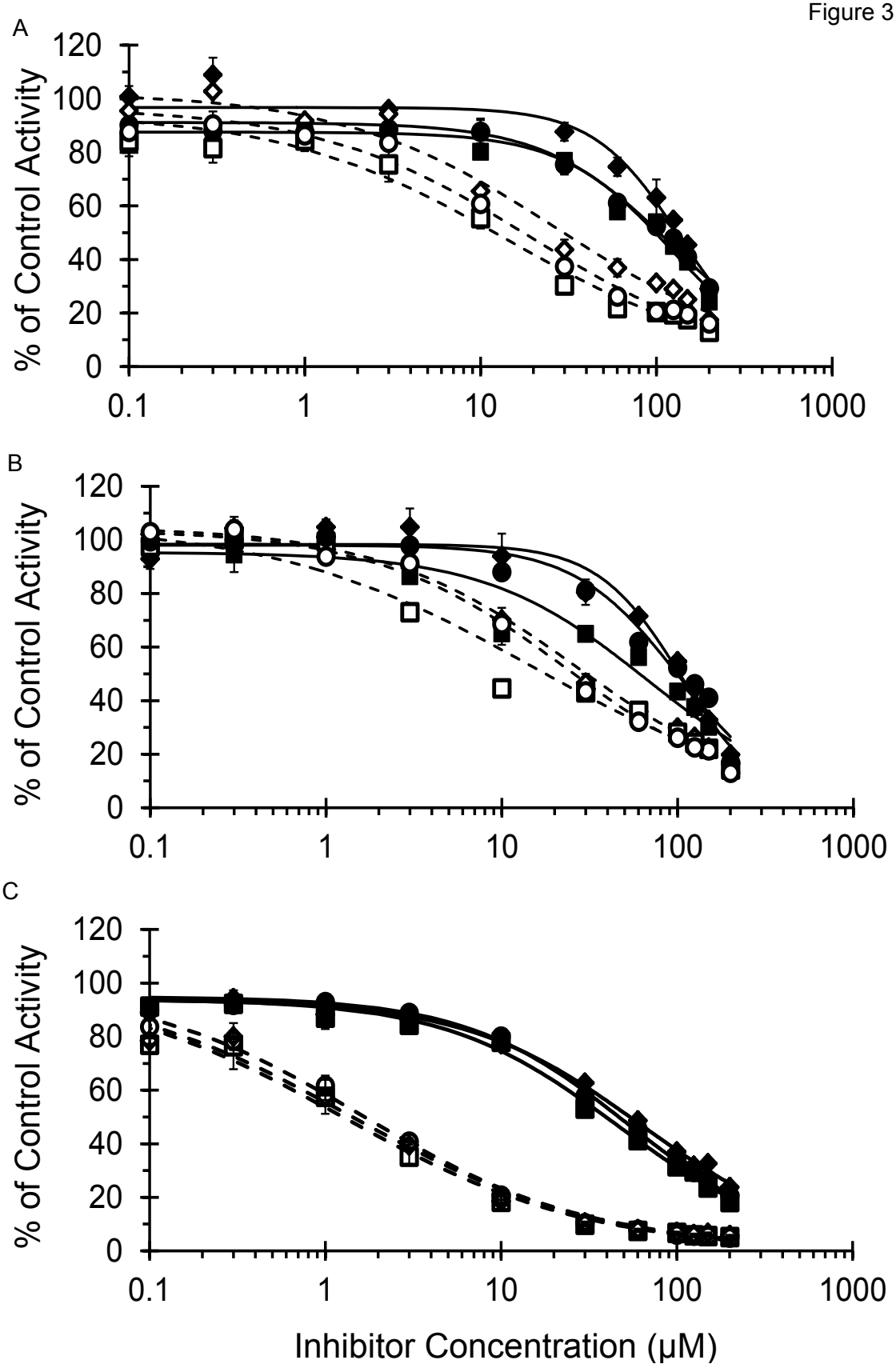
A
B
C
% of Control Activity
120
100
80
60
40
20
0
0.1
1
10
100
1000
Inhibitor Concentration (μM)

Figure 3.5

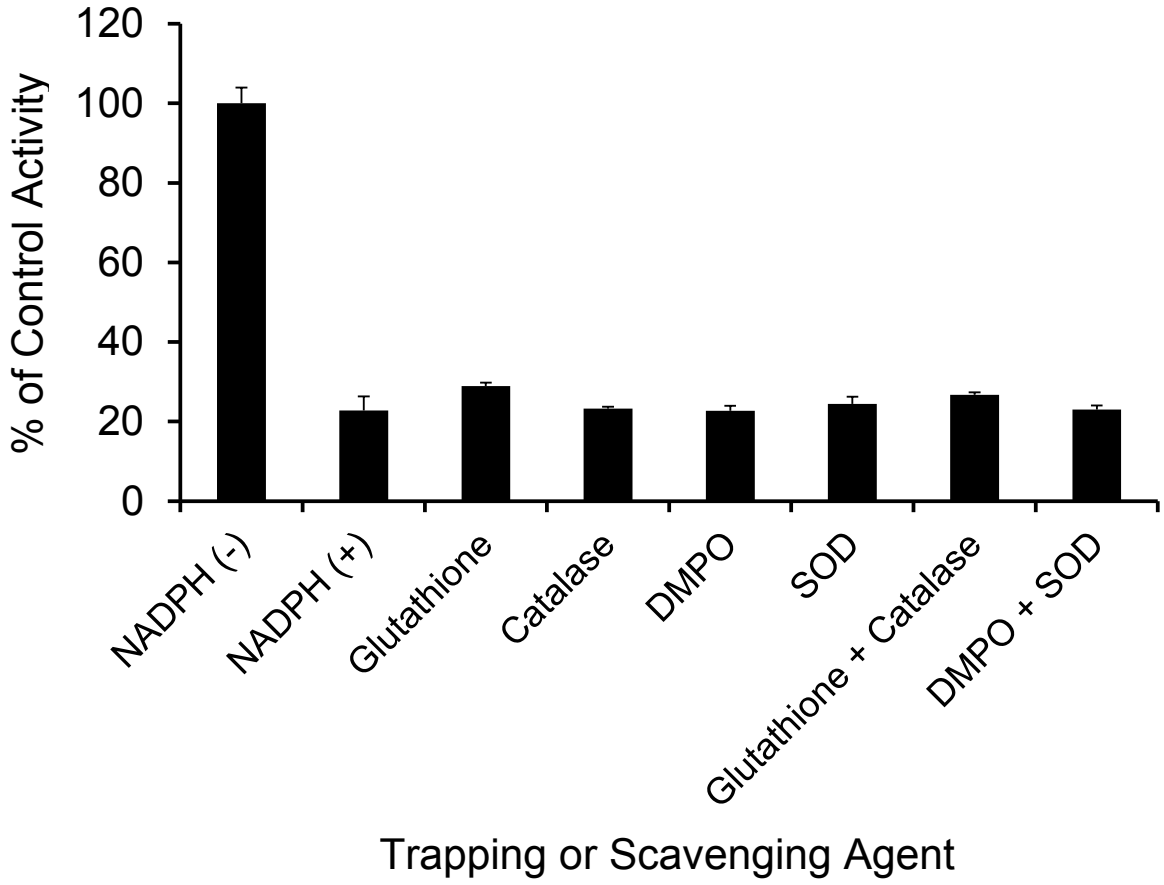
120
100
80
60
40
20
0
% of Control Activity
NADPH (-)
NADPH (+)
Glutathione
Catalase
DMPO
SOD
Glutathione + Catalase
DMPO + SOD
Trapping or Scavenging Agent

Figure 3.6

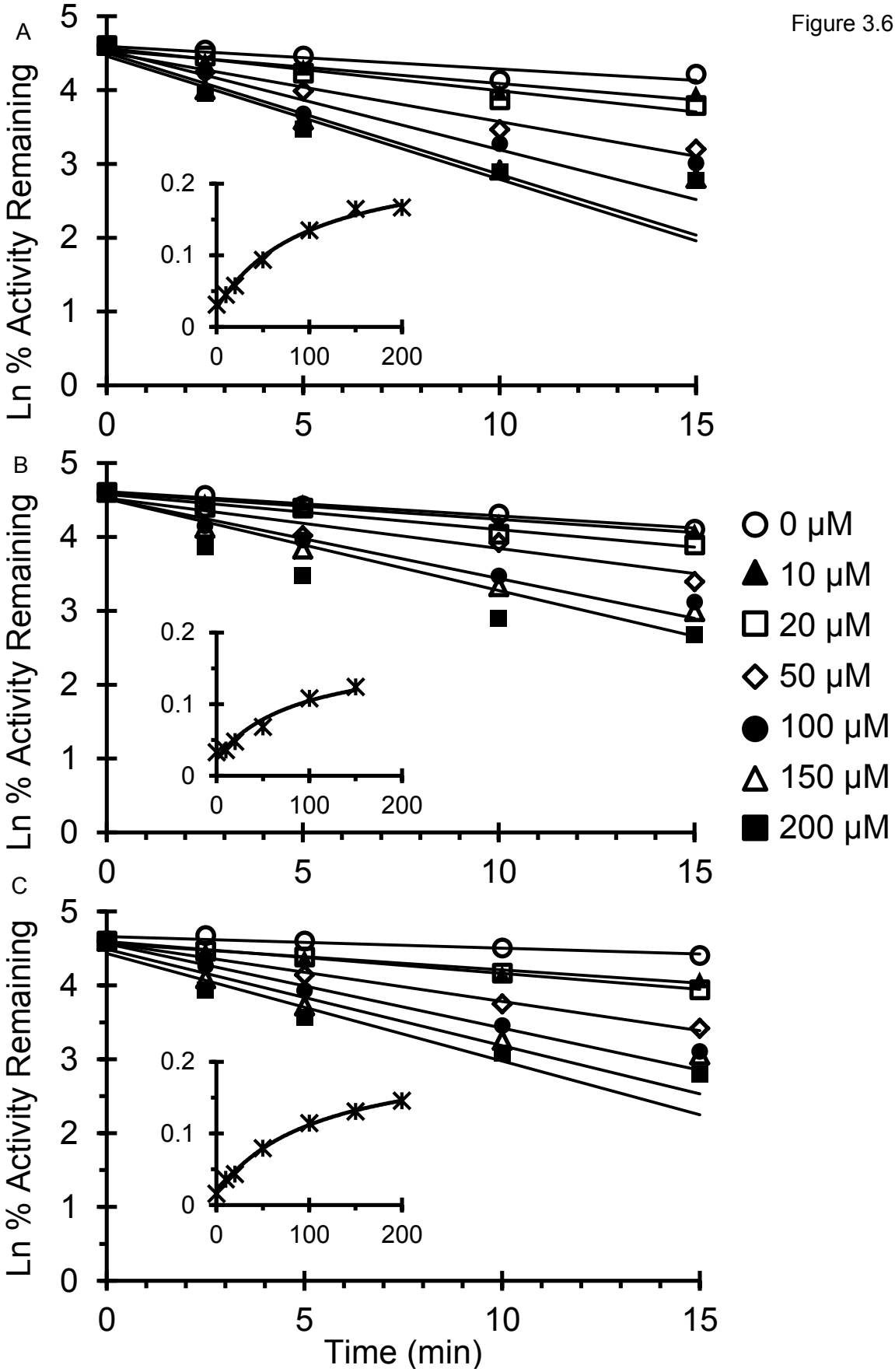
A
B
C
Ln % Activity Remaining
Time (min)
0 μM
10 μM
20 μM
50 μM
100 μM
150 μM
200 μM

References

Beckmann-Knopp S, Rietbrock S, Weyhenmeyer R, Bocker RH, Beckurts KT, Lang W, Hunz M and Fuhr U (2000) Inhibitory effects of silibinin on cytochrome P-450 enzymes in human liver microsomes. *Pharmacol Toxicol* **86**:250-256.

Bent S (2008) Herbal medicine in the United States: review of efficacy, safety, and regulation: grand rounds at University of California, San Francisco Medical Center. *J Gen Intern Med* **23**:854-859.

Berry LM and Zhao Z (2008) An examination of IC50 and IC50-shift experiments in assessing time-dependent inhibition of CYP3A4, CYP2D6 and CYP2C9 in human liver microsomes. *Drug Metab Lett* **2**:51-59.

Blumenthal M, Lindstrom A, Ooyen C and Lynch ME (2012) Herb supplement sales increase 4.5% in 2011. *HerbalGram* **95**: 60-64.

Brantley SJ, Oberlies NH, Kroll DJ and Paine MF (2010) Two flavonolignans from milk thistle (*Silybum marianum*) inhibit CYP2C9-mediated warfarin metabolism at clinically achievable concentrations. *J Pharmacol Exp Ther* **332**:1081-1087.

Doehmer J, Tewes B, Klein KU, Gritzko K, Muschick H and Mengs U (2008) Assessment of drug-drug interaction for silymarin. *Toxicol In Vitro* **22**:610-617.

Etheridge AS, Black SR, Patel PR, So J and Mathews JM (2007) An in vitro evaluation of cytochrome P450 inhibition and P-glycoprotein interaction with goldenseal, Ginkgo biloba, grape seed, milk thistle, and ginseng extracts and their constituents. *Planta Med* **73**:731-741.

Galetin A, Clarke SE and Houston JB (2003) Multisite kinetic analysis of interactions between prototypical CYP3A4 subgroup substrates: midazolam, testosterone, and nifedipine. *Drug Metab Dispos* **31**:1108-1116.

Gardiner P, Graham RE, Legedza AT, Eisenberg DM and Phillips RS (2006) Factors associated with dietary supplement use among prescription medication users. *Arch Intern Med* **166**:1968-1974.

Gurley BJ, Barone GW, Williams DK, Carrier J, Breen P, Yates CR, Song PF, Hubbard MA, Tong Y and Cheboyina S (2006) Effect of milk thistle (*Silybum marianum*) and black cohosh (*Cimicifuga racemosa*) supplementation on digoxin pharmacokinetics in humans. *Drug Metab Dispos* **34**:69-74.

Gurley BJ, Gardner SF, Hubbard MA, Williams DK, Gentry WB, Carrier J, Khan IA, Edwards DJ and Shah A (2004) In vivo assessment of botanical supplementation on human cytochrome P450 phenotypes: Citrus aurantium, Echinacea purpurea, milk thistle, and saw palmetto. *Clin Pharmacol Ther* **76**:428-440.

Han Y, Guo D, Chen Y, Tan ZR and Zhou HH (2009) Effect of silymarin on the pharmacokinetics of losartan and its active metabolite E-3174 in healthy Chinese volunteers. *Eur J Clin Pharmacol* **65**:585-591.

Hanley MJ, Masse G, Harmatz JS, Court MH and Greenblatt DJ Pomegranate juice and pomegranate extract do not impair oral clearance of flurbiprofen in human volunteers: divergence from in vitro results. *Clin Pharmacol Ther* **92**:651-657.

Hoh C, Boocock D, Marczylo T, Singh R, Berry DP, Dennison AR, Hemingway D, Miller A, West K, Euden S, Garcea G, Farmer PB, Steward WP and Gescher AJ (2006) Pilot study of oral silibinin, a putative chemopreventive agent, in colorectal cancer patients: silibinin levels in plasma, colorectum, and liver and their pharmacodynamic consequences. *Clin Cancer Res* **12**:2944-2950.

Hu Z, Yang X, Ho PC, Chan SY, Heng PW, Chan E, Duan W, Koh HL and Zhou S (2005) Herb-drug interactions: a literature review. *Drugs* **65**:1239-1282.

Izzo AA and Ernst E (2009) Interactions between herbal medicines and prescribed drugs: an updated systematic review. *Drugs* **69**:1777-1798.

Jancova P, Anzenbacherova E, Papouskova B, Lemr K, Luzna P, Veinlichova A, Anzenbacher P and Simanek V (2007) Silybin is metabolized by cytochrome P450 2C8 in vitro. *Drug Metab Dispos* **35**:2035-2039.

Kalgutkar AS, Obach RS and Maurer TS (2007) Mechanism-based inactivation of cytochrome P450 enzymes: chemical mechanisms, structure-activity relationships and relationship to clinical drug-drug interactions and idiosyncratic adverse drug reactions. *Curr Drug Metab* **8**:407-447.

Kennedy J, Wang CC and Wu CH (2008) Patient Disclosure about Herb and Supplement Use among Adults in the US. *Evid Based Complement Alternat Med* **5**:451-456.

Monti D, Gazak R, Marhol P, Biedermann D, Purchartova K, Fedrigo M, Riva S and Kren V Enzymatic kinetic resolution of silybin diastereoisomers. *J Nat Prod* **73**:613-619.

Ngo N, Yan Z, Graf TN, Carrizosa DR, Kashuba AD, Dees EC, Oberlies NH and Paine MF (2009) Identification of a cranberry juice product that inhibits enteric CYP3A-mediated first-pass metabolism in humans. *Drug Metab Dispos* **37**:514-522.

Obach RS, Walsky RL and Venkatakrishnan K (2007) Mechanism-based inactivation of human cytochrome p450 enzymes and the prediction of drug-drug interactions. *Drug Metab Dispos* **35**:246-255.

Paine MF, Criss AB and Watkins PB (2004) Two major grapefruit juice components differ in intestinal CYP3A4 inhibition kinetic and binding properties. *Drug Metab Dispos* **32**:1146-1153.

Schrag ML and Wienkers LC (2001) Covalent alteration of the CYP3A4 active site: evidence for multiple substrate binding domains. *Arch Biochem Biophys* **391**:49-55.

Schrieber SJ, Wen Z, Vourvahis M, Smith PC, Fried MW, Kashuba AD and Hawke RL (2008) The pharmacokinetics of silymarin is altered in patients with hepatitis C

virus and nonalcoholic Fatty liver disease and correlates with plasma caspase-3/7 activity. *Drug Metab Dispos* **36**:1909-1916.

Seeff LB, Curto TM, Szabo G, Everson GT, Bonkovsky HL, Dienstag JL, Shiffman ML, Lindsay KL, Lok AS, Di Bisceglie AM, Lee WM and Ghany MG (2008) Herbal product use by persons enrolled in the hepatitis C Antiviral Long-Term Treatment Against Cirrhosis (HALT-C) Trial. *Hepatology* **47**:605-612.

Silverman RB and Daniel LP (1995) [10] Mechanism-based enzyme inactivators, in *Methods in Enzymology* pp 240-283, Academic Press.

Sridar C, Goosen TC, Kent UM, Williams JA and Hollenberg PF (2004) Silybin inactivates cytochromes P450 3A4 and 2C9 and inhibits major hepatic glucuronosyltransferases. *Drug Metab Dispos* **32**:587-594.

Sy-Cordero AA, Day CS and Oberlies NH Absolute Configuration of Isosilybin A by X-ray Crystallography of the Heavy Atom Analogue 7-(4-Bromobenzoyl)isosilybin A. *J Nat Prod*.

Thummel KE, O'Shea D, Paine MF, Shen DD, Kunze KL, Perkins JD and Wilkinson GR (1996) Oral first-pass elimination of midazolam involves both gastrointestinal and hepatic CYP3A-mediated metabolism. *Clin Pharmacol Ther* **59**:491-502.

Wang MZ, Wu JQ, Bridges AS, Zeldin DC, Kornbluth S, Tidwell RR, Hall JE and Paine MF (2007) Human enteric microsomal CYP4F enzymes O-demethylate the antiparasitic prodrug pafuramidine. *Drug Metab Dispos* **35**:2067-2075.

Watanabe A, Nakamura K, Okudaira N, Okazaki O and Sudo K (2007) Risk assessment for drug-drug interaction caused by metabolism-based inhibition of CYP3A using automated in vitro assay systems and its application in the early drug discovery process. *Drug Metab Dispos* **35**:1232-1238.

Wienkers LC and Heath TG (2005) Predicting in vivo drug interactions from in vitro drug discovery data. *Nat Rev Drug Discov* **4**:825-833.

Zuber R, Modriansky M, Dvorak Z, Rohovsky P, Ulrichova J, Simanek V and Anzenbacher P (2002) Effect of silybin and its congeners on human liver microsomal cytochrome P450 activities. *Phytother Res* **16**:632-638.

Chapter 4

Physiologically-Based Pharmacokinetic Interaction Modeling Framework for Quantitative Predictions of Metabolic Herb-Drug Interactions

Overview

Herb-drug interaction predictions remain challenging. Physiologically-based pharmacokinetic (PBPK) modeling was used to improve prediction accuracy and assist clinical trial design of potential herb-drug interactions using the semi-purified milk thistle preparation, silibinin, as an exemplar herbal product. Interactions between silibinin constituents and the probe substrates warfarin (CYP2C9) and midazolam (CYP3A) were modeled. A low silibinin dose (160 mg/day x 14 days) was predicted to increase midazolam AUC by 1%, as corroborated with external data; a higher dose (1440 mg/day x 7 days) was predicted to increase midazolam and (*S*)-warfarin AUC by 5% and 4%, respectively. Clinical evaluation confirmed minimal interactions between silibinin and both midazolam and (*S*)-warfarin (9 and 13% increase in AUC, respectively). (*R*)-warfarin AUC was decreased (by 15%) but unlikely to be clinically relevant. Application of this PBPK modeling approach to other herb-drug interactions could facilitate development of guidelines for quantitative prediction of clinically relevant interactions and aid in informed decisions about adding herbal products to conventional pharmacotherapy.

Introduction

Current US FDA oversight of herbal products does not include evaluation of drug interaction liability prior to marketing. Consequently, herb-drug interactions typically are investigated following case reports of adverse events. Although interactions caused by St. John's Wort are well-publicized (Gurley et al., 2012; Hermann and von Richter, 2012), consumers remain hesitant to discuss herbal product usage with health care practitioners. An estimated 20% of adults in the US consume herbal products (Bent, 2008), and less than one-third inform their health care practitioners (Gardiner et al., 2006; Kennedy et al., 2008). Taken together, herbal products remain understudied perpetrators of potential drug interactions.

Drug interaction liability assessment is more challenging for herbal products than conventional drugs because unlike drug products, herbal products typically are mixtures of bioactive constituents that vary substantially between preparations (de Lima Toccafondo Vieira and Huang, 2012; Gurley, 2012; Hermann and von Richter, 2012). Compounding this complexity is the often scant knowledge of the specific causative constituents or the systemic exposure of such constituents. Due to incomplete absorption and extensive pre-systemic clearance, herbal products may only reach sufficient concentrations in the intestine and liver to inhibit first-pass metabolism of sensitive substrates (Paine and Oberlies, 2007). Isolation and purification of individual constituents permit testing of herbal products akin to that for conventional drugs. Recent drug-drug interaction (DDI) guidelines suggest dynamic modeling and simulation approaches to predict complex interactions (US FDA, 2012; European Medicines Agency, 2012). Extension of this approach to herb-drug interactions is a logical step to facilitate prospective evaluation of such interactions. As with DDIs (Fahmi et al., 2009; Huang and Rowland, 2012), physiologically-based pharmacokinetic (PBPK) modeling may be used to improve predictions of herb-drug interaction liability. In vitro kinetic

parameters for individual constituents, as well as estimates of systemic constituent exposure, are needed to develop robust models.

Milk thistle preparations are top-ten selling herbal products in the US (Blumenthal et al., 2011). The crude extract, silymarin, contains at least seven flavonolignans and one flavonoid (Kroll et al., 2007). The semi-purified product silibinin contains roughly a 1:1 mixture of the flavonolignans silybin A and silybin B and represents an exemplar herbal product for initial model development. First, silybin A and silybin B have been purified in quantities sufficient to recover requisite in vitro parameters (Graf et al., 2007; Monti et al., 2010). Second, in vitro studies have demonstrated both reversible and irreversible inhibition of the key drug metabolizing enzymes CYP2C9 (Zuber et al., 2002; Sridar et al., 2004; Brantley et al., 2010) and CYP3A4 (Zuber et al., 2002; Sridar et al., 2004). Third, in vitro-in vivo extrapolation has been inconsistent (Gurley et al., 2004; Gurley et al., 2006; Han et al., 2009). Based on these observations, the objective of this study was to improve the mechanistic understanding of this herb-drug interaction using PBPK modeling and simulation with warfarin and midazolam as probe substrates. The models were evaluated through a proof-of-concept clinical study in healthy volunteers. Results could help develop guidelines for prospective evaluation of herb-drug interaction liability.

Methods

PBPK model development. The base model structure was adapted from the literature (Bjorkman et al., 2001) (Figure 4.1), incorporating physiologic parameters obtained from the International Commission on Radiological Protection (ICRP) (Boecker, 2003). Warfarin partition coefficients (K_ps) (Luecke et al., 1994) and plasma protein binding parameters (Chan et al., 1994) were obtained from the literature (Table 4.1). The absorption rate constant (k_a) and saturable clearance parameters (K_m, V_{max}) for warfarin were obtained by fitting the PBPK model to previously reported concentration-time profiles (Ngo et al., 2010). Midazolam K_ps and k_a were obtained from the literature (Langlois et al., 1987; Bjorkman et al., 2001) (Table 4.1). Intestinal and hepatic midazolam clearance parameters were extrapolated from in vitro experiments (Brantley et al., 2009) according to previously published methods (Barter et al., 2007; Obach, 2011). K_ps for silybin A and silybin B were predicted from physicochemical properties (Poulin et al., 2001) using GastroPlus (version 8.0; Simulations Plus Inc., Lancaster, CA). Silibinin plasma binding parameters were obtained from the literature (Deng et al., 2008) and clearance parameters were generated by fitting the PBPK model to concentration-time data from hepatitis C patients receiving silymarin (Hawke et al., 2010) (Table 1). Silybin A and silybin B reversible and mechanism-based inhibition kinetic parameters associated with CYP2C9 and CYP3A4 were obtained from the literature (Brantley et al., 2010) or generated in-house (unpublished observations). Competitive inhibition of CYP2C9 activity by (*R*)-warfarin was obtained from the literature (Kunze et al., 1991).

PBPK interaction model simulations. PBPK models were constructed for midazolam, (*R*)-warfarin, (*S*)-warfarin, silybin A, and silybin B using Berkeley Madonna (version 8.3; University of California at Berkeley, Berkeley, CA) with code compiled in MEGen (Loizou and Hogg, 2011) (version 0.5; UK Health & Safety Laboratory, Buxton,

UK) (Table 4.S.1). The PBPK model for perpetrator (silybin A and silybin B) and victim (warfarin or midazolam) were linked through the reversible or mechanism-based inhibition of victim substrate. Initial simulations used doses of probe substrates and milk thistle products as reported in previous studies. Following initial model evaluation, simulations were conducted with higher doses of silibinin (1440 mg/day) to determine the maximal expected interaction. Pharmacokinetic outcomes from the simulated profiles were recovered via non-compartmental analysis using Phoenix Winnonlin (version 6.3; Pharsight Corp., Mountain View, CA).

Analysis of silibinin product. Siliphos® capsules (n=28) (Thorne Research, Dover, ID) were analyzed individually using a modification of previously described methods (Kim et al., 2003; Davis-Searles et al., 2005; Ladas et al., 2010) to ensure purity and content. The contents of each capsule was weighed and extracted with 2 mL of acetone. The extract was vortexed, centrifuged at 13,000 x *g* for 2 min, and the supernatant was transferred to a new vial. The pellet was extracted a second time using an identical method, and the acetone supernatants were combined and dried. Aliquots of these extracts were prepared at 10 mM (presuming a molecular weight of 482.1 g/mol) in DMSO (42, 43) then diluted to 100 µM in 30:70 MeOH:H2O for analysis. Samples were quantitated on an Acquity UPLC system with an HSS-T3 1.8 µm (2.1 x 100 mm) Acquity column using Empower 3 software (Waters, Milford, MA). Standards and Siliphos® capsule extracts were analyzed utilizing a gradient from 30:70 to 55:45 MeOH:H2O (0.1% formic acid) over 5.0 min at a flow rate of 0.6 mL/min at 50°C, with peaks detected at 288 nm.

Proof-of-Concept Clinical Study Design. Twelve healthy volunteers (six nonpregnant women) were enrolled in an open-label, fixed sequence crossover drug interaction study conducted at the UNC Clinical and Translational Research Center (CTRC). The study protocol was approved by the University of North Carolina Office of

Human Research Ethics Biomedical Institutional Review Board and the CTRC Advisory Committee. Eligibility to participate was based on screening evaluation and according to inclusion/exclusion criteria (Table 4.S.2). Written informed consent was obtained from each subject prior to enrollment.

The first (control) phase consisted of administration of 10 mg warfarin (Coumadin®; Bristol Meyers Squibb, Princeton, NJ), 10 mg vitamin K (Mephyton®; Aton Pharma, Lawrenceville, NJ), and 5 mg midazolam syrup (Ranbaxy; Jacksonville, FL). Women of childbearing potential were administered a pregnancy test; a negative result was required before drug administration. Vital signs (blood pressure, temperature, respiratory rate, pulse, oxygen saturation) were obtained at baseline and every 15 minutes for the first 2 hours. All subjects underwent an INR with PT. Blood (7 mL) was collected through an intravenous line before drug administration and at 0.25, 0.5, 1, 1.5, 2, 3, 4, 6, 8, and 12 hours thereafter. Subjects continued to fast until after the 4-hour blood collection, when meals and snacks, devoid of fruit juices and caffeinated beverages, were provided. Subjects returned to the CTRC 24 and 48 hours post-drug administration for blood collection. Optimal study design simulations (Ma et al., 2004) of previously reported clinical data (Ngo et al., 2009) demonstrated that a 0-48 hour collection was an effective surrogate of the total systemic exposure ($AUC_{0\text{-}inf}$) for warfarin. Plasma was separated from blood cells by centrifugation and stored at -80°C pending analysis by HPLC/MS-MS.

Following at least 14 days of washout, the subjects received 480 mg silibinin (based on labeled content) three times daily for 7 days. Subjects returned on day 7 for concomitant administration of silibinin, warfarin, vitamin K, and midazolam. Each subject received his/her silibinin in a blister pack and was asked to complete a pill diary documenting the time of administration. Subjects were contacted at least twice during

the week of silibinin self-administration to monitor compliance and adverse events, which were graded using a validated Adverse Events Scale.

Pharmacokinetic analysis. Pharmacokinetic outcomes were recovered by noncompartmental analysis using Phoenix Winnonlin (version 6.3; Pharsight Corp., Mountain View, CA). Concentrations below the limit of quantification were excluded. The terminal elimination rate constant (λ_z) was estimated by linear regression of the terminal portion of the log-transformed concentration-time profile using at least three data points. The terminal half-life ($t_{1/2}$) was calculated as $\ln(2)/\lambda_z$. The maximum observed concentration (C_{max}), time to reach C_{max} (t_{max}), and last measured concentration (C_{last}) were recovered directly from the concentration-time profile. Area under the curve from time zero to C_{last} ($AUC_{0\text{-}last}$) was determined using the trapezoidal rule with linear up/log down interpolation. $AUC_{0\text{-}inf}$ was calculated as the sum of $AUC_{0\text{-}last}$ and the ratio of C_{last} to λ_z.

Statistical analysis. All statistical analyses were conducted using SAS (version 9.2; SAS Institute Inc, Cary, NC). The primary endpoints were the test/reference ratio of log-transformed $AUC_{0\text{-}48}$ (warfarin) or $AUC_{0\text{-}inf}$ (midazolam) and C_{max} (warfarin and midazolam) (US Food and Drug Administration, 2012; European Medicines Agency, 2012). The two treatment groups were considered bioequivalent if the respective means were within 25% of each other and the calculated 90% confidence interval for the ratio of means lay between 0.75 and 1.33. The sample size (n=12 evaluable subjects) was calculated based on 80% power to detect a 25% change in the primary outcomes with a Type I error of 0.05. Intra-individual variability in midazolam and warfarin AUC and C_{max} were assumed to be approximately 20% (Kashuba et al., 1998; Kharasch et al., 1999; Yacobi et al., 2000). Secondary outcomes such as oral clearance (Cl/F), $t_{1/2}$, and t_{max} were evaluated using a paired two-tailed Student's *t*- test on log-transformed data or

Wilcoxon signed-rank test as appropriate. A *p*-value <0.05 was considered statistically significant.

Analysis of plasma for (R)- and (S)-warfarin and midazolam. Concentrations of (*R*)- and (*S*)-warfarin and midazolam were quantified using a Sciex (Framingham, MA) API4000Qtrap HPLC/MS/MS triple quadrupole mass spectrometer fitted with a Turbo ionspray interface operated in the positive ion mode. Plasma was treated with acetonitrile (6 volumes) containing the internal standard warfarin-d_5 (Toronto Research Chemicals; Toronto, Canada) or 1'-hydroxymidazolam-d_4 (Cerilliant; Round Rock, TX), centrifuged (3000 x *g*), and the supernatant was injected into the HPLC-MS/MS system. Warfarin enantiomers were separated on a Supelco Astec Chirobiotic V 15 cm x 2.1mm 5 micron chiral column (Sigma Aldrich; St Louis, MO) and eluted with an isocratic mixture consisting of 75% 5 mM ammonium acetate containing 0.01% (v/v) formic acid and 25% acetonitrile (flow rate, 0.4 mL/min). Midazolam was eluted with a binary gradient mixture consisting of 10 mM ammonium formate containing 1% (v/v) isopropyl alcohol and 0.1% (v/v) formic acid and methanol on a Varian Polaris C18-A 20 cm x 2.0 mm 5 micron column (Agilent; Santa Clara, CA) (flow rate, 0.65 mL/min). Analyte concentration was determined by interpolation from a linear standard curve with an assay dynamic range of 0.5-10,000 nM for (*R*)- and (*S*)-warfarin and 0.5-5,000 nM for midazolam.

Analysis of plasma for silybin A and B. Concentrations of silybin A and silybin B were quantified using a Sciex mass spectrometer as described for warfarin and midazolam. Samples were eluted with an isocratic mixture consisting of 44% water with 0.1% (v/v) formic acid (solvent A) and 56% methanol with 0.1% (v/v) formic acid on an Agilent Zorbax XDB C18 15 cm x 3.0 mm 3.5 micron column (Agilent) (flow rate, 0.7 mL/min). Analyte concentrations were determined by interpolation from linear standard

curves with a dynamic range of the assay ranging from 0.5-5,000 nM for both silybin A and silybin B.

Analytical methods were validated according to US Food and Drug Administration (FDA) guidelines (US Food and Drug Administration, 2001). Inter- and intra-day variability for all analytes was less than 10%.

Results

Modeling and simulation. *PBPK model generation and evaluation.* Simulated probe substrate concentrations closely approximated previously published pharmacokinetic outcomes (Table 4.2). The terminal half-life for both (*R*)- and (*S*)-warfarin was underestimated, whereas maximum concentration (C_{max}), systemic exposure (AUC), and oral clearance (Cl/F) were predicted accurately. Simulated midazolam AUC was overestimated at the higher silibinin dose, whereas C_{max} was underestimated at the lower silibinin dose. As anticipated, simulated silybin A and silybin B concentrations were less accurate than those for warfarin and midazolam. The C_{max} for silybin A was underpredicted by roughly three-fold, whereas that for silybin B was underpredicted by roughly two-fold (Table 4.2). The AUC of silybin A was underpredicted by roughly 15%, whereas that for silybin B was overpredicted by roughly two-fold.

Prediction of silibinin-drug interaction magnitude. Simulations of the silibinin-warfarin interaction showed negligible changes (<5%) in all pharmacokinetic outcomes (Table 4.3). Likewise, simulations of a previously reported milk thistle-midazolam interaction (Gurley et al., 2006), assuming reversible CYP3A inhibition solely due to silybin A and silybin B, demonstrated negligible changes in pharmacokinetic outcomes (Figure 4.2). Incorporation of mechanism-based CYP3A inhibition showed a 60% and 30% increase in midazolam AUC and C_{max}, respectively (Figure 4.2). Increases of 3% and 6% in midazolam AUC and C_{max}, respectively, were reported (Figure 4.2). Simulations with a higher silibinin dose (1440 mg/day) predicted a 5% increase in midazolam AUC when incorporating reversible inhibition and a 5-fold increase in AUC when incorporating mechanism-based inhibition (Table 4.3).

Clinical evaluation. *Silibinin content in test product.* A single lot (#304090) of Siliphos® capsules was used. The capsules were labeled to contain 60 mg of silibinin and 120 mg of phosphatidyl choline, totaling 180 mg. The Siliphos® capsules were

overfilled with silibinin consistently, containing 69.1 ± 4.28 mg silibinin represented as 30.3 ± 1.88 mg silybin A and 38.9 ± 2.39 mg silybin B. The capsules were contaminated slightly with the minor constituents isosilybin A (1.55 ± 0.09 mg) and isosilybin B (0.94 ± 0.06 mg). Stability of >98% has been reported at 21 months (Ladas et al., 2010), but the capsules were used within six months of receipt.

Clinical study subjects. All enrolled subjects (n=12) completed both phases of the study. All study drugs and silibinin generally were well-tolerated. One subject experienced mild gastrointestinal upset following the first dose of silibinin. The effect was deemed likely to be drug-related by the study physician but was transient and did not limit the subject's continued participation in the study. During study visits to the CTRC, 4 subjects (2 in both phases) reported mild headaches attributed to caffeine withdrawal. No INR elevations from baseline were observed following warfarin administration.

Effects of high-dose silibinin on midazolam and warfarin pharmacokinetics. The effects of high-dose silibinin (1440 mg/day) were compared to baseline oral pharmacokinetics of midazolam and warfarin. Due to the reported mechanism-based inhibition of CYP3A *in vitro* (Sridar et al., 2004), silibinin was administered three times daily for 6 days prior to administration of the probe substrates. Silibinin constituents were not expected to accumulate during the administration period due to short reported half-lives (<4 hour) (Wen et al., 2008). One subject demonstrated poor goodness-of-fit statistics for the $t_{1/2}$ of both warfarin enantiomers in both phases ($R^2 < 0.85$). Accordingly, data from this subject were excluded from analysis of $t_{1/2}$ and Cl/F.

Warfarin enantiomers were absorbed rapidly during both study phases, with median time to peak concentration (t_{max}) occurring at 1.25 and 1.5 hours for (*R*)- and (*S*)-warfarin, respectively (Table 4.3; Fig. 4.3). Co-administration with silibinin did not alter the absorption of (*S*)-warfarin but delayed median (*R*)-warfarin t_{max} by 15 minutes. Relative to control, silibinin decreased the geometric mean AUC_{0-48} of (*R*)-warfarin by

15%. (*R*)-warfarin AUC decreased in all subjects, by 2-28% (Table 4.3; Fig. 4.4A). (*R*)-warfarin geometric mean C_{max} similarly decreased (by 17%); C_{max} decreased in 10 subjects by 12-32% (Fig. 4.4B). Silibinin increased the geometric mean AUC_{0-48} of (*S*)-warfarin by 13%; AUC_{0-48} decreased in four subjects (by 6-17%) and increased in the remaining subjects (by 1-62%) (Table 4.3; Fig. 4.4C). In three subjects (*S*)-warfarin AUC_{0-48} increased to outside the no effect range (by 36-62%). (*S*)-Warfarin geometric C_{max} decreased by 2%; C_{max} decreased in eight subjects (by 3-16%) and increased in four subjects (by 8-31%) (Fig. 4.4D). The 90% confidence intervals for all warfarin primary outcomes lay within the no effect range (0.75-1.33) (Table 4.3).

The rapid absorption of midazolam was unaltered by co-administration with silibinin, with median t_{max} occurring at 0.5 hours (Table 4.3; Fig. 4.3). Relative to control, geometric mean midazolam AUC_{0-inf} increased by 8% following silibinin administration (Table 4.3; Fig. 4.4E). Except for one subject (2.3-fold increase), treatment/control ratios of AUC_{0-inf} lay within the pre-defined no effect range (0.75-1.33). Relative to control, five subjects demonstrated marked (>50%) increases in C_{max}, whereas one subject demonstrated a marked (>50%) decrease in C_{max}. The 90% confidence interval for midazolam treatment-to-control ratio of AUC_{0-inf} lay within, whereas that of C_{max} extended above, the no effect range (Table 4.3; Fig. 4.4F).

The sampling strategy was not optimized for recovery of silybin A and silybin pharmacokinetic outcomes; as such, these outcomes were interpreted for qualitative rather than quantitative purposes. The median t_{max} of silybin A and silybin B following the initial administration of silibinin (3 and 3.5 hours, respectively) nearly coincided with the second administration of silibinin (Table 4.3; Fig. 4.3). Geometric mean C_{max} for silybin A was nearly double that for silybin B (Table 4.3). Geometric mean $t_{1/2}$ of both silybin A and silybin B was approximately 5 hours.

Discussion

Although herbal product usage continues to increase, current US regulatory guidelines do not request pre-market evaluation of herb-drug interaction liability. Investigations into such liabilities are fraught with inconsistent results due to the lack of a standard system for evaluation, high compositional variation between herbal products, and uncertainty about causative constituents. Unlike conventional drug products, the relative composition of a given herbal product may vary widely depending on weather conditions, product collection and storage methods, and processing procedures (Paine and Oberlies, 2007). Accurate predictions of herb-drug interaction liability require not only identification and quantification of causative constituents, but also measures of exposure in organs with metabolic capability. Silibinin was selected as an exemplar herbal product due to a well-characterized composition, availability of inhibitory kinetic parameters from individual constituents, and disparate impact of milk thistle products on victim drug pharmacokinetics in previous herb-drug interaction clinical studies. A PBPK modeling and simulation approach was used to address the challenges inherent to investigation of herb-drug interaction liability.

Warfarin is a widely used oral anticoagulant with a narrow therapeutic window. Warfarin is associated with a notoriously complicated pharmacotherapy due in part to myriad drugs and herbal products that interfere with warfarin's metabolism or anticoagulant activity. As the clearance of the more pharmacologically active (*S*)-enantiomer is mediated primarily by CYP2C9, inhibition of this enzyme can lead to increased risk of bleeding. Silymarin was shown previously to increase systemic exposure to the CYP2C9/3A substrate losartan (Han et al., 2009), prompting evaluation of the interaction potential between milk thistle and warfarin. Of the milk thistle constituents whose CYP2C9 interaction liability has been evaluated in vitro, silybin A and silybin B were the most potent (Brantley et al., 2010). These observations lead to

the selection of silibinin, which consists largely of these two constituents, for clinical evaluation.

Relative to control, silibinin unexpectedly decreased both the geometric mean $AUC_{0\text{-last}}$ and C_{max} of (*R*)-warfarin. Clinical manifestation of the previously reported CYP1A2 induction by a milk thistle extract in vitro (Doehmer et al., 2011) is consistent with this decrease in exposure. In contrast to the doubling of losartan exposure following administration of silymarin, high-dose silibinin did not increase geometric mean (*S*)-warfarin exposure to a clinically relevant extent. However, increases above 33% were observed in three subjects, indicating that the CYP2C9 interaction potential of silibinin cannot be disregarded completely.

Modeling and simulation of the silibinin-warfarin interaction demonstrated that the rapid clearance of the silibinin constituents precluded marked inhibition of warfarin clearance. Sensitivity analysis of this interaction potential demonstrated that ten-fold increases in silybin A or silybin B inhibition potency would lead to roughly 15% increases in (*S*)-warfarin exposure (Fig. 4.S.1). Extensive intestinal and hepatic conjugation of silybin A and silybin B followed by rapid elimination likely would limit the interaction potential to first-pass clearance of sensitive substrates. Warfarin is not sensitive to first-pass elimination and is cleared only upon subsequent passes through the liver, at which time the interaction potential of silybin A and silybin B is abated. In contrast, losartan has a low bioavailability (33%) that is limited, in part, to first-pass elimination (Lo et al., 1995). This observation, coupled with the differences in study population and herbal product tested, could explain the difference between the reported interaction with losartan (Han et al., 2009) and the lack of interaction with warfarin in the present study. Collectively, these observations suggest examination of other CYP2C9 substrates sensitive to first-pass elimination, such as fluvastatin, to understand fully the milk thistle-CYP2C9 interaction potential.

Midazolam is a gold standard CYP3A probe substrate metabolized extensively by intestinal and hepatic enzymes. Inhibition of CYP3A at either site can increase systemic exposure to midazolam; inhibition of hepatic CYP3A also can impact (increase) the $t_{1/2}$. Milk thistle constituents, including silybin A and silybin B, have been shown to be reversible and irreversible inhibitors of CYP3A activity in both human intestinal and liver microsomes; however, the mechanism of clinical inhibition has not been determined. Previous interaction studies with midazolam (Gurley et al., 2004; Gurley et al., 2006) have demonstrated limited interaction potential with the milk thistle product silymarin, albeit the doses administered were not sufficient to determine the difference between reversible and irreversible inhibition of CYP3A (Fig. 4.2). The 'supratherapeutic' silibinin dose in the current study was selected to provide a large range between the predicted interaction based on reversible and irreversible inhibition of CYP3A and to maximize the ability to observe a clinical interaction. The lack of an interaction observed in all but one subject indicated that the CYP3A interaction potential is low for silibinin and is more consistent with reversible inhibition than mechanism-based inhibition. As such, the mechanism-based inhibition observed with recombinant and purified enzymes (Sridar et al., 2004) likely represent false-positives due to the highly reactive nature of these enzyme systems, rather than indicating actual clinical liability.

Modeling and simulation of the silibinin-midazolam interaction indicated that the low interaction potential is due, in part, to the decreased potency of the silibinin constituents toward CYP3A compared to CYP2C9. Ten-fold increases in inhibition potency of silybin A and silybin B toward CYP3A activity increased midazolam exposure by roughly 25% (Fig. 4.S.1). These observations indicated that at the predicted exposures, the constituents would need to be ten-fold more potent to demonstrate any clinically relevant interaction with CYP3A. The large predicted increase in midazolam exposure following mechanism-based inhibition further supported the hypothesis that

products with limited systemic exposure (first posed with fruit juices (Hanley et al., 2012)) need to be mechanism-based inhibitors of CYP enzymes to demonstrate clinically relevant interactions.

The current approach is limited due to recovery of silybin A and silybin B clearance parameters by fitting the model to data obtained from hepatitis C patients who were administered a product (silymarin) that contained additional constituents not measured in silibinin (Hawke et al., 2010). In vitro determination of silibinin clearance parameters would provide a true bottom-up modeling approach and reduce complexities inherent to pharmacokinetic data from patients with hepatic disease.

Prospective evaluation of herb-drug interactions, consistent with those for pharmaceutical agents, largely has been ignored due to substantial compositional variability inherent to herbal products, multiple inhibitory constituents, and varying inhibitory mechanisms. The PBPK interaction model developed in the current study permits accurate interaction potential predictions for herbal products by incorporating in vitro inhibition kinetic parameters and estimates of systemic exposure of individual constituents. Modeling of the silibinin-warfarin and silibinin-midazolam interaction accurately predicted minimal clinical interaction liability. Application of this framework with other combinations of herbal products and conventional drugs could identify potential clinically significant herb-drug interactions, predict the extent of those interactions, and ultimately help guide pharmacotherapeutic decisions.

Study Highlights

What is the current knowledge on the topic?

Despite increasing recognition of herb-drug interactions in clinical practice, robust information about the causative ingredients and mechanisms underlying these interactions remains limited. As a consequence, evidence-based recommendations about adding herbal products to existing pharmacotherapeutic regimens frequently are nonexistent.

What question did this study address?

This study addressed the utility of a PBPK modeling approach to predict the drug interaction liability of an herbal product. This approach was tested using the exemplar herbal product silibinin and the widely used cytochrome P450 probe substrates warfarin and midazolam.

What this study adds to our knowledge?

A PBPK modeling approach accurately predicted the minimal interaction potential of chronic exposure to high-'dose' silibinin and two FDA-recommended probe substrates. Sensitivity analysis demonstrated that silibinin constituents are cleared too rapidly to influence the systemic metabolism of warfarin and that the inhibitory potency towards CYP3A is not sufficient for clinical interactions with midazolam.

How this might change clinical pharmacology and therapeutics?

A PBPK modeling and simulation approach could facilitate prospective evaluation of herb-drug interactions, as well as evidence-based recommendations regarding addition of herbal products to conventional drug regimens.

Figure Legends

Figure 4.1. Base PBPK model structure. Model structure was modified from the literature (Bjorkman et al., 2001). Organ weights and blood flows were obtained from ICRP values (Boecker, 2003). Following oral administration, drug transfer from dosing compartment to intestine is driven by the oral absorption rate (k_a). Drug clearance (Cl) is mediated by metabolic processes in the intestine and liver. The pancreas and spleen were combined into a hybrid "organ" identified as PSP.

Figure 4.2. Mean concentration-time profile (0-6 hours) of midazolam in 19 healthy volunteers following an 8 mg oral midazolam dose given alone (open symbols) or following a 14-day treatment with milk thistle product (solid symbols) (21). Lines denote PBPK model simulations of the midazolam concentration-time profile when given alone (grey) or with milk thistle (black). The dotted line denotes incorporation of reversible inhibition of CYP3A, whereas the dashed line denotes incorporation of mechanism-based inhibition of CYP3A. Symbols and error bars denote means and SDs, respectively.

Figure 4.3. Geometric mean concentration-time profile of warfarin (A), midazolam (B), and silibinin (C) in 12 healthy volunteers following a 10 mg oral dose of warfarin or 5 mg oral dose of midazolam given alone (open symbols) or following a 7-treatment with silibinin (solid symbols). Lines denote PBPK model simulations of the concentration-time profiles when the probe substrates were given alone (solid) or with silibinin (dashed). Symbols and error bars denote geometric means and upper limits of the 90% confidence interval, respectively.

Figure 4.4. Effects of silibinin (1440 mg/day for 7 days) on the exposure (A, C, E) and peak concentration (B, D, F) of (*R*)-warfarin (A, B), (*S*)-warfarin (C, D), and midazolam (E, F) in 12 healthy volunteers following oral administration of warfarin (10 mg) and

midazolam (5 mg). Open symbols connected by solid lines denote individual values. Solid symbols connected by dashed lines denote geometric means.

Table 4.1. Model input parameters

	Victim Drug			Perpetrator Compound	
Parameter	(*R*)-Warfarin	(*S*)-Warfarin	Midazolam	Silybin A	Silybin B
Physicochemical/Binding					
Molecular weight	308.33	308.33	325.78	482.44	482.44
Fraction absorbed	1.0[a]	1.0[a]	1.0[a]	0.77[b]	0.77[b]
K_a (h^{-1})	3.0[c]	3.0[c]	1.17[d]	0.50[b]	0.50[b]
Blood/plasma ratio	1.0[e]	1.0[e]	0.80[f]	0.58[b]	0.58[b]
Unbound fraction in plasma	0.006[g]	0.006[g]	0.02[f]	0.04[h]	0.04[h]
Metabolism					
Intestinal K_m (μM)	-	-	3.7[i]	22[c]	8.5[c]
Intestinal V_{max} (μmol/h)	-	-	1,100[i]	2,700[c]	2,600[c]
Hepatic K_m (μM)	-	6.5[e]	6.0[i]	54[c]	57[c]
Hepatic V_{max} (μmol/h)	-	260[c]	18,000[i]	2,300[c]	2,700[c]
Hepatic Cl_{int} (l/h)	30.4[c]	-	-	-	-
Inhibition					
CYP2C9 K_i (μM)	6.5[j]	-	-	10[k]	4.8[k]
CYP2C9 α	-	-	-	5[k]	8[k]
CYP3A4 K_i (μM)	-	-	-	26.5[l]	31.5[l]
CYP3A4 k_{inact} (min^{-1})	-	-	-	0.22[l]	0.15[l]
CYP3A4 K_I (μM)	-	-	-	100[l]	89[l]

K_a, absorption rate constant; α, affinity change of the enzyme-substrate and enzyme-inhibitor complexes

[a]Assumed
[b]Predicted based on physicochemical properties
[c]Obtained by fitting the model to clinical data
[d]Kanglois et al., 1987
[e]Luecke et al., 1994
[f]Bjorkman et al., 2001
[g]Chan et al., 2004
[h]Deng et al., 2008
[i]Extrapolated from in vitro data
[j]Kunze et al., 1991
[k]Brantley et al., 2010
[l]Generated in-house

Table 4.2. Model evaluation

Measure	Observed (CV)	Predicted
(*R*)-Warfarin (5 mg)		
$t_{½}$ (h)	42 (18)	29
t_{max} (h) [median (range)]	2.0 (0.5-12)	1.6
C_{max} (µM)	1.7 (22)	2.1
$AUC_{0\text{-}inf}$ (µM *h)	93 (21)	91
Cl/F (l/h)	0.18 (21)	0.18
(*S*)-Warfarin (5 mg)		
$t_{½}$ (h)	32 (26)	22
t_{max} (h) [median (range)]	2 (0.5-4)	1.5
C_{max} (µM)	2.0 (29)	2.1
$AUC_{0\text{-}inf}$ (µM *h)	65 (30)	70
Cl/F (l/h)	0.25 (31)	0.23
Midazolam (5 mg)		
$t_{½}$ (h)	2.9 (41)	3.5
t_{max} (h) [median (range)]	0.5 (0.25-1.5)	0.6
C_{max} (nM)	88 (44)	70
$AUC_{0\text{-}inf}$ (nM *h)	215 (33)	212
Cl/F (l/h)	71 (33)	72
Midazolam (8 mg)		
$t_{½}$ (h)	4.22 (29)	3.5
t_{max} (h) [mean (SD)]	0.47 (51)	0.6
C_{max} (µM)	114 (49)	112
$AUC_{0\text{-}inf}$ (nM *h)	295 (44)	342
Cl/F (l/h)	95.3 (35)	72
Silybin A (92.8 mg)		
$t_{½}$ (h)	1.6	1.4
t_{max} (h) [median (range)]	1.5 (1-2)	1.3
C_{max} (µM)	0.84 (89)	0.27
$AUC_{0\text{-}inf}$ (µM *h)	1.3	1.1
Cl/F (l/h)	150	170
Silybin B (128 mg)		
$t_{½}$ (h)	1.1	1.4
t_{max} (h) [median (range)]	1.5 (0.5-2)	1.1
C_{max} (µM)	0.27 (120)	0.16
$AUC_{0\text{-}inf}$ (µM *h)	0.28	0.63
Cl/F (l/h)	948	407

$t_{1/2}$, terminal elimination half-life; t_{max}, time to maximal concentration; C_{max}, maximal concentration; AUC, area under the concentration-time curve; Cl/F, oral clearance

Table 4.3. Evaluation of predicted interaction with clinical data

Measure	Observed			Predicted (Reversible Inhibition)			Predicted (Mechanism-Based Inhibition)		
	Geometric Mean			Geometric Mean			Geometric Mean		
	Control	Treatment	Treatment/Control Ratio	Control	Treatment	Treatment/Control Ratio	Control	Treatment	Treatment/Control Ratio
(*R*)-Warfarin									
$t_{1/2}$ (h)	52.0 (28)	61.2 (27)	1.14	29.0	29.0	1.00	-	-	-
C_{max} (µM)	1.92 (30)	1.60 (29)	0.83 (0.77 – 0.90)	2.08	2.08	1.00	-	-	-
AUC_{0-48} (µM *h)	55.0 (24)	47.0 (23)	0.85 (0.81 – 0.90)	61.6	61.5	1.00	-	-	-
Cl/F (l/h)	0.13 (37)	0.14 (40)	1.07	0.18	0.18	1.00	-	-	-
(*S*)-Warfarin									
$t_{1/2}$ (h)	29.6 (25)	30.3 (20)	0.97	22.2	22.4	1.01	-	-	-
C_{max} (µM)	2.01 (32)	1.97 (27)	0.98 (0.91 – 1.05)	2.06	2.08	1.01	-	-	-
AUC_{0-48} (µM *h)	37.4 (41)	42.3 (34)	1.13 (1.01 – 1.26)	53.8	56.0	1.04	-	-	-
Cl/F (l/h)	0.30 (44)	0.26 (39)	0.92	0.23	0.22	0.96	-	-	-
Midazolam									
$t_{1/2}$ (h)	5.17 (36)	4.90 (48)	0.95	3.55	3.54	1.00	3.55	5.30	1.49
C_{max} (nM)	74.2 (43)	89.5 (39)	1.20 (0.96 – 1.51)	70	73	1.04	70	150	2.11
AUC_{0-inf} (nM*h)	198 (42)	216 (36)	1.09 (0.93 – 1.25)	210	220	1.05	210	1070	5.05
Cl/F (l/h)	73 (42)	68 (36)	0.93	72	69	0.96	72	13	0.18
Silybin A									
C_{max} (µM)	-	0.97 (91)	-	-	0.76	-	-	-	-
$t_{1/2}$ (h)	-	5.1 (34)	-	-	1.4	-	-	-	-
Silybin B									
C_{max} (µM)	-	0.40 (110)	-	-	0.43	-	-	-	-
$t_{1/2}$ (h)	-	5.1 (56)	-	-	1.4	-	-	-	-

$t_{1/2}$, terminal elimination half-life; C_{max}, maximal concentration; AUC, area under the concentration-time curve; Cl/F, oral clearance

Figure 4.1. PBPK model structure

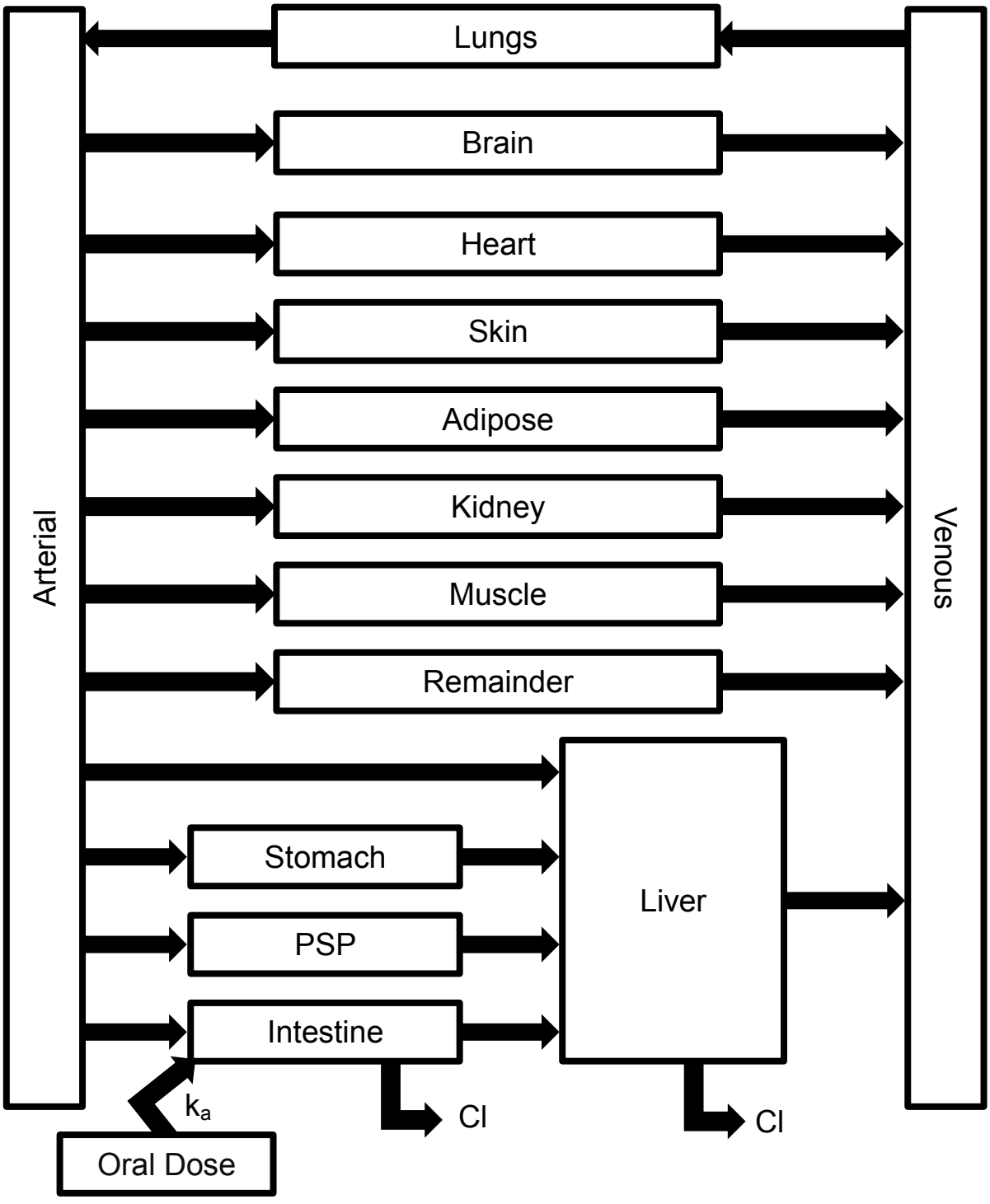

Figure 4.2.

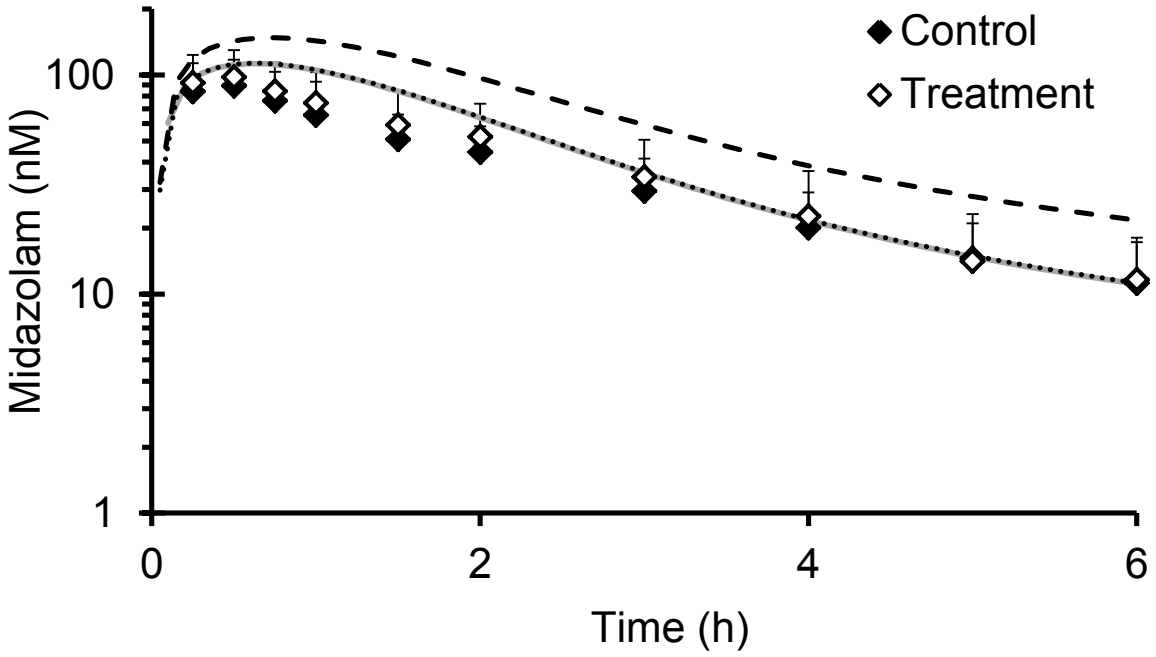

Figure 4.3.

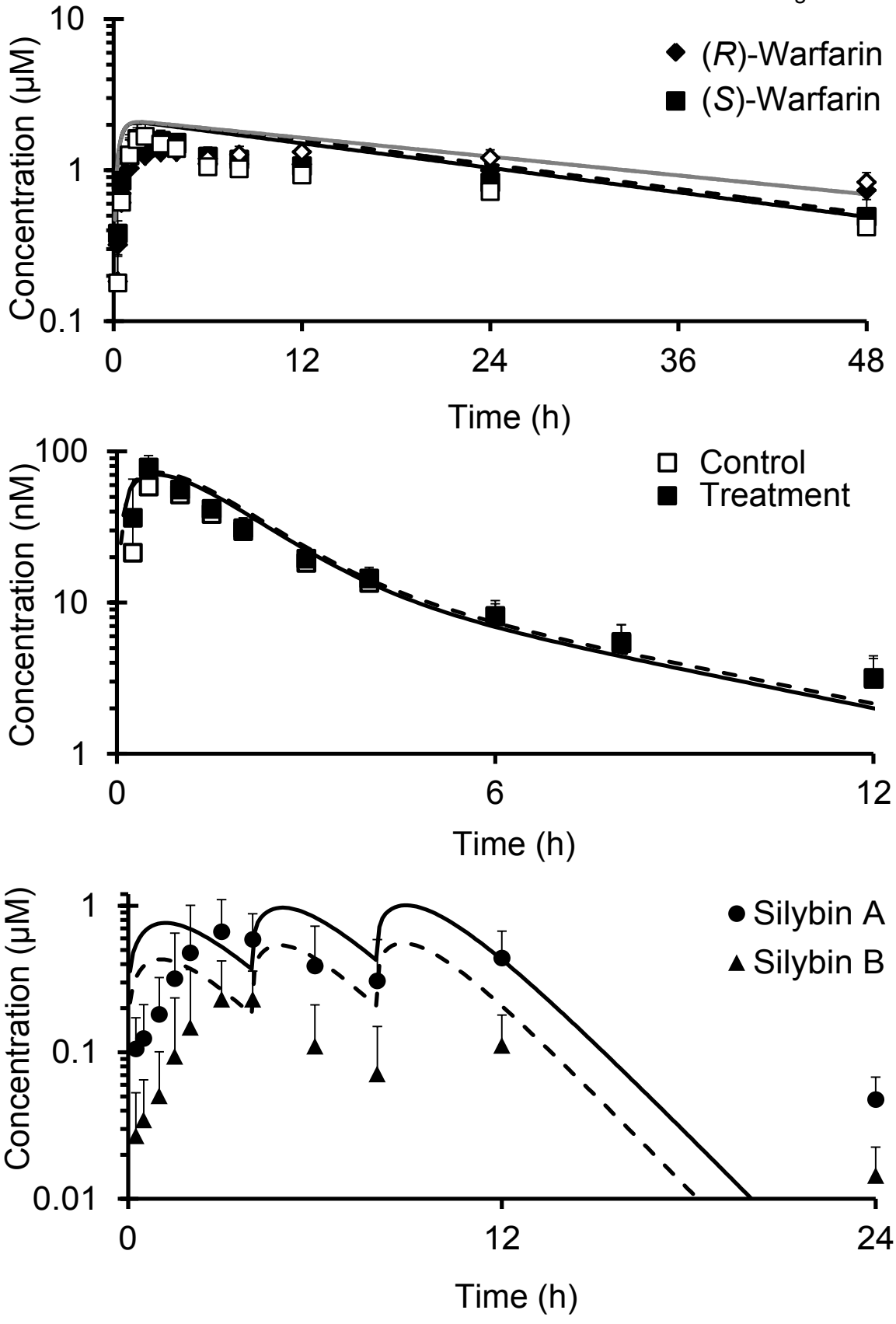
10
1
0.1
Concentration (μM)
(R)-Warfarin
(S)-Warfarin
0
12
24
36
48
Time (h)
100
10
1
Concentration (nM)
Control
Treatment
0
6
12
Time (h)
1
0.1
0.01
Concentration (μM)
Silybin A
Silybin B
0
12
24
Time (h)

Figure 4.4.

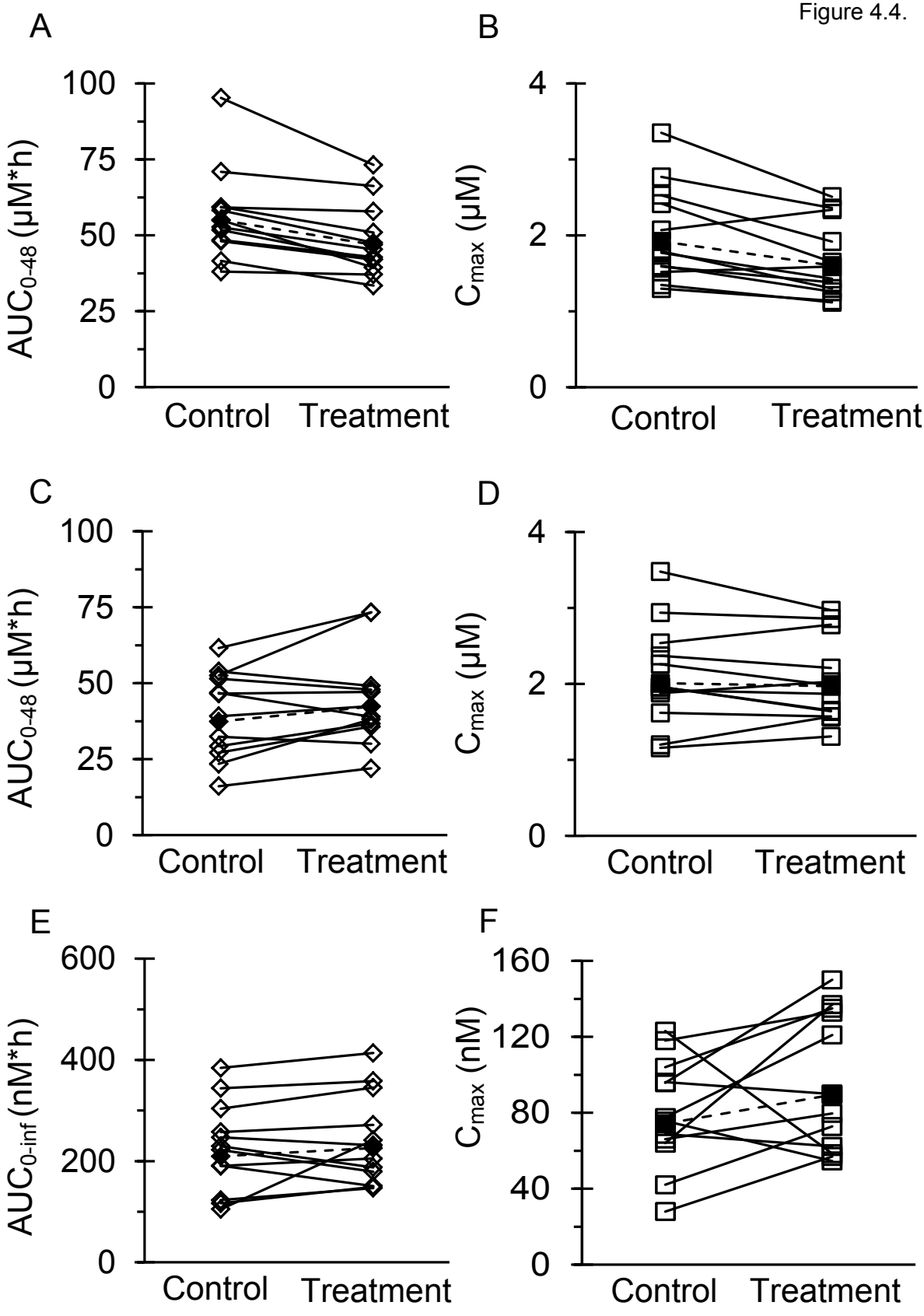
A
100
75
50
25
0
AUC0-48 (µM*h)
Control
Treatment
B
4
2
0
Cmax (µM)
Control
Treatment
C
100
75
50
25
0
AUC0-48 (µM*h)
Control
Treatment
D
4
2
0
Cmax (µM)
Control
Treatment
E
600
400
200
0
AUC0-inf (nM*h)
Control
Treatment
F
160
120
80
40
0
Cmax (nM)
Control
Treatment

Table 4.S.1. Inclusion and exclusion criteria

Inclusion	Exclusion
Men or women between 18 and 65 years of age	History or diagnosis of any significant chronic medical condition such as (but not limited to) diabetes mellitus, hepatitis B, or HIV
Normal screening lab test results	History of any allergy, hypersensitivity, or intolerance to warfarin, midazolam or other benzodiazepine, vitamin K, or milk thistle products
Able to understand the informed consent form	History of intolerance to plants in the aster family (daisies, thistles, ragweed, lettuce, artichoke, sunflower, marigold, chamomile, and echinacea), kiwi fruit, or soy products
Willing to abstain from herbal products for one week prior to and during the study	Baseline INR >1.5 unless approved by study physician
Willing to abstain from alcohol and caffeinated beverages the evening prior to each study day	Women who are pregnant or nursing
	History of significant medical conditions that the study physician believes would increase risk (e.g., bleeding disorders)
	Taking concomitant medications, both prescription and non-prescription (including herbal products), known to alter warfarin, midazolam, and/or vitamin K blood concentrations or to alter CYP2C9 or CYP3A4 activity (women on hormonal methods of birth control were allowed to participate)

Table 4.S.2. Clinical Study Subject Characteristics

	Men (n=6)	Women (n=6)
Age (years), median [range]	50 [23-63]	46 [33-53]
Weight (kg), mean (SD)	95 (19)	74 (20)
Self-Identified Race/Ethnicity, n		
Caucasian	4	5
African American	1	-
Asian	-	1
Hispanic	1	-
Concomitant medications, n		
Oral Contraceptives	-	2
Aspirin	-	1

Supplemental Material 1.

Methods

PBPK model generation. PBPK models were developed to describe the distribution and clearance of warfarin, midazolam, and silibinin (Figure 4.1). Distribution between blood and tissues was assumed to be flow-limited. The following general equations describe the distribution and clearance of victim and perpetrator compounds in non-eliminating organs:

$$V_i * \left(\frac{dC_{i,X}}{dt}\right) = Q_i * \left(C_{art,X} - \frac{C_{i,X}}{P_{i,X}}\right)$$

where Q_i denotes blood flow (l/h) into tissue i, V_i denotes volume (l) of tissue i, $C_{i,X}$ denotes concentration (µmol/l) of compound X into tissue i, $C_{art,X}$ denotes arterial concentration of compound X, and P_i denotes partition of compound X into tissue i.

Organs of metabolic elimination are described by the equations below. In the liver, $V_{max,liver,X}$ and $K_{m,liver,X}$ denote the hepatic Michaelis-Menten kinetic parameters for compound X, and $f_{u,liver,X}$ denotes the unbound hepatic fraction of compound X.

$$V_{liver} * \left(\frac{dC_{liver,X}}{dt}\right) = Q_{liver} * \left(C_{art,X} - \frac{C_{liver,X}}{P_{liver,X}}\right) - Cl_{int,liver}$$

$$Cl_{int,liver} = \frac{V_{max,liver,X} * (f_{u,liver,X} * C_{liver,X})}{K_{m,liver,X} + (f_{u,liver,X} * C_{liver,X})}$$

In the intestinal tract, $f_{u,ent,X}$ denotes the unbound enterocyte fraction of compound X (assumed to be 1 for all compounds), $K_{a,X}$ denotes the absorption rate constant (1/h) of compound X, and X_{dose} denotes the amount (µmol) of compound X remaining in the dosing compartment.

$$V_{ent} * \left(\frac{dC_{ent,X}}{dt}\right) = Q_{ent} * \left(C_{art,X} - \frac{C_{ent,X}}{P_{ent,X}}\right) - Cl_{int,ent} + K_{a,X} * X_{dose}$$

$$Cl_{int,ent} = \frac{V_{max,ent,X} * (f_{u,ent,X} * C_{ent,X})}{K_{m,ent,X} + (f_{u,ent,X} * C_{ent,X})}$$

Hepatic clearance in the presence of reversible inhibition of silybin A and silybin B is modified to include the hepatic concentration of silybin A ($C_{liver,A}$) and silybin B ($C_{liver,B}$), the inhibitory potency of silybin A ($K_{i,A}$) and silybin B ($K_{i,B}$) and the parameter to describe the affinity change of the enzyme-substrate and enzyme-inhibitor complexes for silybin A (α_A) and silybin B (α_B)

$$Cl_{int,liver,reversiblyinhibited} = \frac{V_{max,liver,X} * (f_{u,liver,X} * C_{liver,X})}{K_{m,liver,X} * \left(1 + \frac{C_{liver,A}}{K_{i,A}} + \frac{C_{liver,B}}{K_{i,B}}\right) + (f_u * C_{liver,X}) * \left(1 + \frac{C_{liver,A}}{\alpha_A * K_{i,A}} + \frac{C_{liver,B}}{\alpha_B * K_{i,B}}\right)}$$

Mechanism-based inhibition (MBI) of hepatic clearance is incorporated by multiplying the reversible inhibition equation by the ratio of active hepatic enzyme ($E_{T,Liver}$) to basal hepatic enzyme ($E_{0,liver}$).

$$Cl_{int,liver,MBI} = Cl_{int,liver,reversiblyinhibited} * \left(\frac{E_{T,Liver}}{E_{0,Liver}}\right)$$

The active CYP3A4 enzyme pool is approximated by incorporating enzyme inactivation parameters (k_{inact} and K_I) for silybin A and silybin B into the steady-state enzyme equation, where R_0 denotes the zero-order enzyme synthesis rate and k_{deg} denotes the first-order enzyme degradation rate.

$$\frac{dE_{T,liver}}{dt} = R_0 - k_{deg} * E_{T,liver} - \frac{k_{inact,A} * C_{liver,A}}{K_{I,A} + C_{liver,A}} * E_{T,liver} - \frac{k_{inact,B} * C_{liver,B}}{K_{I,B} + C_{liver,B}} * E_{T,liver}$$

Figure 4.S.1

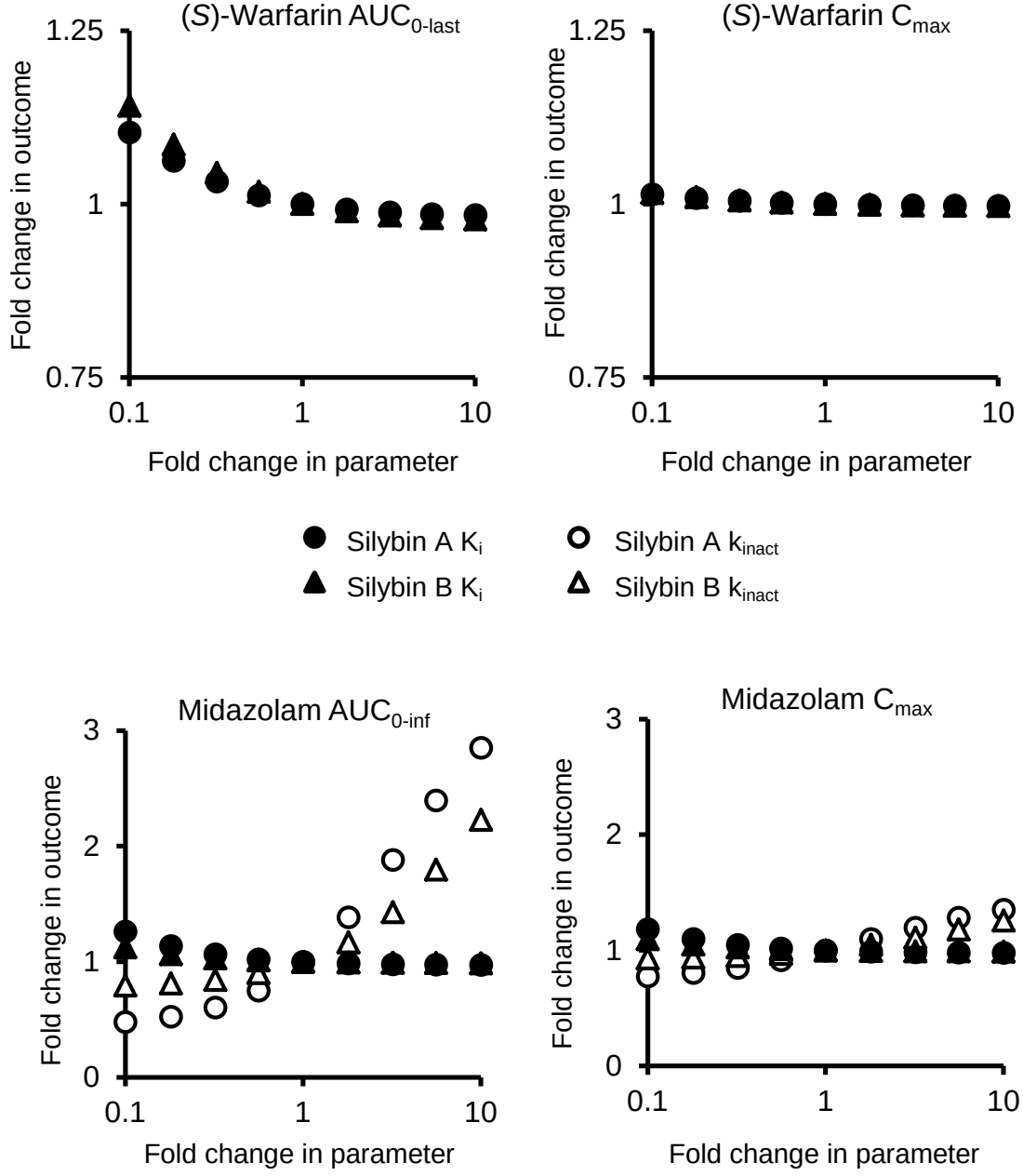
(S)-Warfarin AUC0-last
(S)-Warfarin Cmax
Fold change in outcome
Fold change in parameter
1.25
1
0.75
0.1
1
10
Silybin A Ki
Silybin B Ki
Silybin A kinact
Silybin B kinact
Midazolam AUC0-inf
Midazolam Cmax
3
2
1
0
0.1
1
10

Supplemental Material 2.

Methods

Sensitivity Analysis. Sensitivity analysis of inhibitory parameter estimates on model-predicted peak concentration (C_{max}) and systemic exposure (AUC) was conducted in Berkeley Madonna. Parameters representing reversible or irreversible inhibition of CYP2C9 or CYP3A4/5 were adjusted from ten-fold below to ten-fold above the starting parameter (Table 4.1) in half-log increments.

Figure Legend

Figure 4.S.1. Sensitivity analysis of probe substrate C_{max} and AUC as a function of inhibitory kinetic parameters. Symbols denote pharmacokinetic outcomes recovered by non-compartmental analysis of simulated concentration-time curves resulting from adjusting the inhibitory kinetic parameters. Closed symbols denote reversible inhibition parameters. Open symbols denote irreversible inhibition parameters.

References

Barter ZE, Bayliss MK, Beaune PH, Boobis AR, Carlile DJ, Edwards RJ, Houston JB, Lake BG, Lipscomb JC, Pelkonen OR, Tucker GT and Rostami-Hodjegan A (2007) Scaling factors for the extrapolation of in vivo metabolic drug clearance from in vitro data: reaching a consensus on values of human microsomal protein and hepatocellularity per gram of liver. *Curr Drug Metab* **8:**33-45.

Bent S (2008) Herbal medicine in the United States: review of efficacy, safety, and regulation: grand rounds at University of California, San Francisco Medical Center. *J Gen Intern Med* **23:**854-859.

Bjorkman S, Wada DR, Berling BM and Benoni G (2001) Prediction of the disposition of midazolam in surgical patients by a physiologically based pharmacokinetic model. *Journal of Pharmaceutical Sciences* **90:**1226-1241.

Blumenthal M, Lindstrom A, Lynch M and Rea P (2011) Market Report. Herb Sales Continue Growth -- Up 3.3% in 2010. *HerbalGram* **May-Jul** 4.

Boecker BB (2003) Reference values for basic human anatomical and physiological characteristics for use in radiation protection. *Radiat Prot Dosimetry* **105:**571-574.

Brantley SJ, Kroll DJ, Oberlies NH and Paine MF (2009) Compounds from milk thistle extract differentially modulate human enteric and hepatic CYP3A activity. *Drug Metabolism Reviews* **41:**54.

Brantley SJ, Oberlies NH, Kroll DJ and Paine MF (2010) Two flavonolignans from milk thistle (*Silybum marianum*) inhibit CYP2C9-mediated warfarin metabolism at clinically achievable concentrations. *Journal of Pharmacology & Experimental Therapeutics* **332:**1081-1087.

Chan E, McLachlan AJ, Pegg M, MacKay AD, Cole RB and Rowland M (1994) Disposition of warfarin enantiomers and metabolites in patients during multiple dosing with rac-warfarin. *Br J Clin Pharmacol* **37:**563-569.

Davis-Searles PR, Nakanishi Y, Kim NC, Graf TN, Oberlies NH, Wani MC, Wall ME, Agarwal R and Kroll DJ (2005) Milk thistle and prostate cancer: differential effects of pure flavonolignans from *Silybum marianum* on antiproliferative end points in human prostate carcinoma cells. *Cancer Res* **65:**4448-4457.

de Lima Toccafondo Vieira M and Huang SM (2012) Botanical-drug interactions: a scientific perspective. *Planta Med* **78:**1400-1415.

Deng JW, Shon JH, Shin HJ, Park SJ, Yeo CW, Zhou HH, Song IS and Shin JG (2008) Effect of silymarin supplement on the pharmacokinetics of rosuvastatin. *Pharm Res* **25:**1807-1814.

Doehmer J, Weiss G, McGregor GP and Appel K (2011) Assessment of a dry extract from milk thistle (Silybum marianum) for interference with human liver cytochrome-P450 activities. *Toxicol In Vitro* **25:**21-27.

European Medicines Agency (2012) Guideline on the investigation of drug interactions, London, UK.

Fahmi OA, Hurst S, Plowchalk D, Cook J, Guo F, Youdim K, Dickins M, Phipps A, Darekar A, Hyland R and Obach RS (2009) Comparison of different algorithms for predicting clinical drug-drug interactions, based on the use of CYP3A4 in vitro data: predictions of compounds as precipitants of interaction. *Drug Metab Dispos* **37:**1658-1666.

Gardiner P, Graham RE, Legedza AT, Eisenberg DM and Phillips RS (2006) Factors associated with dietary supplement use among prescription medication users. *Arch Intern Med* **166:**1968-1974.

Graf TN, Wani MC, Agarwal R, Kroll DJ and Oberlies NH (2007) Gram-scale purification of flavonolignan diastereoisomers from *Silybum marianum* (milk thistle) extract in support of preclinical in vivo studies for prostate cancer chemoprevention. *Planta Med* **73:**1495-1501.

Gurley B, Hubbard MA, Williams DK, Thaden J, Tong Y, Gentry WB, Breen P, Carrier DJ and Cheboyina S (2006) Assessing the clinical significance of botanical supplementation on human cytochrome P450 3A activity: comparison of a milk thistle and black cohosh product to rifampin and clarithromycin. *J Clin Pharmacol* **46:**201-213.

Gurley BJ (2012) Pharmacokinetic herb-drug interactions (part 1): origins, mechanisms, and the impact of botanical dietary supplements. *Planta Med* **78:**1478-1489.

Gurley BJ, Fifer EK and Gardner Z (2012) Pharmacokinetic herb-drug interactions (part 2): drug interactions involving popular botanical dietary supplements and their clinical relevance. *Planta Med* **78:**1490-1514.

Gurley BJ, Gardner SF, Hubbard MA, Williams DK, Gentry WB, Carrier J, Khan IA, Edwards DJ and Shah A (2004) In vivo assessment of botanical supplementation on human cytochrome P450 phenotypes: Citrus aurantium, Echinacea purpurea, milk thistle, and saw palmetto. *Clinical Pharmacology & Therapeutics* **76:**428-440.

Han Y, Guo D, Chen Y, Tan ZR and Zhou HH (2009) Effect of silymarin on the pharmacokinetics of losartan and its active metabolite E-3174 in healthy Chinese volunteers. *Eur J Clin Pharmacol* **65:**585-591.

Hanley MJ, Masse G, Harmatz JS, Court MH and Greenblatt DJ (2012) Pomegranate juice and pomegranate extract do not impair oral clearance of flurbiprofen in human volunteers: divergence from in vitro results. *Clinical Pharmacology & Therapeutics* **92:**651-657.

Hawke RL, Schrieber SJ, Soule TA, Wen Z, Smith PC, Reddy KR, Wahed AS, Belle SH, Afdhal NH, Navarro VJ, Berman J, Liu QY, Doo E and Fried MW (2010) Silymarin ascending multiple oral dosing phase I study in noncirrhotic patients with chronic hepatitis C. *J Clin Pharmacol* **50:**434-449.

Hermann R and von Richter O (2012) Clinical evidence of herbal drugs as perpetrators of pharmacokinetic drug interactions. *Planta Med* **78:**1458-1477.

Huang SM and Rowland M (2012) The role of physiologically based pharmacokinetic modeling in regulatory review. *Clin Pharmacol Ther* **91:**542-549.

Kashuba AD, Bertino JS, Jr., Rocci ML, Jr., Kulawy RW, Beck DJ and Nafziger AN (1998) Quantification of 3-month intraindividual variability and the influence of sex and menstrual cycle phase on CYP3A activity as measured by phenotyping with intravenous midazolam. *Clin Pharmacol Ther* **64:**269-277.

Kennedy J, Wang CC and Wu CH (2008) Patient Disclosure about Herb and Supplement Use among Adults in the US. *Evid Based Complement Alternat Med* **5:**451-456.

Kharasch ED, Jubert C, Senn T, Bowdle TA and Thummel KE (1999) Intraindividual variability in male hepatic CYP3A4 activity assessed by alfentanil and midazolam clearance. *J Clin Pharmacol* **39:**664-669.

Kim NC, Graf TN, Sparacino CM, Wani MC and Wall ME (2003) Complete isolation and characterization of silybins and isosilybins from milk thistle (Silybum marianum). *Org Biomol Chem* **1:**1684-1689.

Kroll DJ, Shaw HS and Oberlies NH (2007) Milk thistle nomenclature: why it matters in cancer research and pharmacokinetic studies. *Integr Cancer Ther* **6:**110-119.

Kunze KL, Eddy AC, Gibaldi M and Trager WF (1991) Metabolic enantiomeric interactions: the inhibition of human (S)-warfarin-7-hydroxylase by (R)-warfarin. *Chirality* **3:**24-29.

Ladas EJ, Kroll DJ, Oberlies NH, Cheng B, Ndao DH, Rheingold SR and Kelly KM (2010) A randomized, controlled, double-blind, pilot study of milk thistle for the treatment of hepatotoxicity in childhood acute lymphoblastic leukemia (ALL). *Cancer* **116:**506-513.

Langlois S, Kreeft JH, Chouinard G, Ross-Chouinard A, East S and Ogilvie RI (1987) Midazolam: kinetics and effects on memory, sensorium, and haemodynamics. *Br J Clin Pharmacol* **23:**273-278.

Lo MW, Goldberg MR, McCrea JB, Lu H, Furtek CI and Bjornsson TD (1995) Pharmacokinetics of losartan, an angiotensin II receptor antagonist, and its active metabolite EXP3174 in humans. *Clin Pharmacol Ther* **58:**641-649.

Loizou G and Hogg A (2011) MEGen: A Physiologically Based Pharmacokinetic Model Generator. *Front Pharmacol* **2:**56.

Luecke RH, Wosilait WD, Pearce BA and Young JF (1994) A physiologically based pharmacokinetic computer model for human pregnancy. *Teratology* **49:**90-103.

Ma JD, Nafziger AN, Kashuba AD, Kim MJ, Gaedigk A, Rowland E, Kim JS and Bertino JS, Jr. (2004) Limited sampling strategy of S-warfarin concentrations, but not

warfarin S/R ratios, accurately predicts S-warfarin AUC during baseline and inhibition in CYP2C9 extensive metabolizers. *J Clin Pharmacol* **44:**570-576.

Monti D, Gazak R, Marhol P, Biedermann D, Purchartova K, Fedrigo M, Riva S and Kren V (2010) Enzymatic kinetic resolution of silybin diastereoisomers. *J Nat Prod* **73:**613-619.

Ngo N, Brantley SJ, Carrizosa DR, Kashuba ADM, Dees EC, Kroll DJ, Oberlies NH and Paine MF (2010) The warfarin-cranberry juice interaction revisited: a systematic *in vitro-in vivo* evaluation. *J Exp Pharmacol* **in press**.

Ngo N, Yan Z, Graf TN, Carrizosa DR, Kashuba AD, Dees EC, Oberlies NH and Paine MF (2009) Identification of a cranberry juice product that inhibits enteric CYP3A-mediated first-pass metabolism in humans. *Drug Metab Dispos* **37:**514-522.

Obach RS (2011) Predicting clearance in humans from in vitro data. *Curr Top Med Chem* **11:**334-339.

Paine MF and Oberlies NH (2007) Clinical relevance of the small intestine as an organ of drug elimination: drug-fruit juice interactions. *Expert Opin Drug Metab Toxicol* **3:**67-80.

Poulin P, Schoenlein K and Theil FP (2001) Prediction of adipose tissue: plasma partition coefficients for structurally unrelated drugs. *Journal of Pharmaceutical Sciences* **90:**436-447.

Sridar C, Goosen TC, Kent UM, Williams JA and Hollenberg PF (2004) Silybin inactivates cytochromes P450 3A4 and 2C9 and inhibits major hepatic glucuronosyltransferases. *Drug Metabolism & Disposition* **32:**587-594.

Wen Z, Dumas TE, Schrieber SJ, Hawke RL, Fried MW and Smith PC (2008) Pharmacokinetics and metabolic profile of free, conjugated, and total silymarin flavonolignans in human plasma after oral administration of milk thistle extract. *Drug Metabolism & Disposition* **36:**65-72.

US Food and Drug Administration (2001) Guidance for industry: Bioanalytical method validation, Rockville, MD.

US Food and Drug Administration (2012) Draft Guidance: Drug interaction studies-study desig, data analysis, implications for dosing, and labeling recommendations, Rockville, MD.

Yacobi A, Masson E, Moros D, Ganes D, Lapointe C, Abolfathi Z, LeBel M, Golander Y, Doepner D, Blumberg T, Cohen Y and Levitt B (2000) Who needs individual bioequivalence studies for narrow therapeutic index drugs? A case for warfarin. *J Clin Pharmacol* **40:**826-835.

Zuber R, Modriansky M, Dvorak Z, Rohovsky P, Ulrichova J, Simanek V and Anzenbacher P (2002) Effect of silybin and its congeners on human liver microsomal cytochrome P450 activities. *Phytother Res* **16:**632-638.

Chapter 5

Conclusions

Summary and Discussion

Herbal product usage in the United States has increased exponentially in recent years as consumers turn increasingly to these products as a means to decrease health care costs *via* self-diagnosis and treatment. The misperception that herbal products are safe has perpetuated multibillion dollar sales of these products, exposing the public to potentially harmful herb-drug interactions when constituents in the herbal product inhibit drug metabolizing enzymes. Since herbal products are not regulated as drug products, several regulatory agencies, including the US FDA, do not request information about herb-drug interaction (HDI) potential prior to marketing. In addition to limited regulatory focus, evaluations of HDI liability are subject to inherent limitations. First, as herbal products are derived from natural sources, both between- and within-brand variability greatly exceeds that of drug products. Second, herbal products are complex mixtures of bioactive constituents, and the inhibitory constituent(s) responsible for the interaction often are not identified. Third, because herbal products are self-administered, standard dosing regimens are nonexistent. These inherent challenges can be addressed by determining requisite kinetic parameters from individual herbal product constituents and incorporating into physiologically-based pharmacokinetic (PBPK) interaction models.

The overall goal of this dissertation research was to evaluate the HDI potential of the exemplar herbal product milk thistle using PBPK modeling techniques. The global hypothesis was that integration of *in vitro* inhibitory kinetic parameters of individual milk

thistle constituents into a PBPK interaction model would permit more accurate predictions of herb-drug interactions than traditional static models. The short term goal of this project was to improve the understanding of the *in vitro*-*in vivo* disconnect regarding milk thistle-drug interactions. The long term goal was to improve the design of *in vitro* and clinical herb-drug interaction studies. Subsequent discussion will focus on major observations, limitations, and opportunities for future research resulting from this dissertation.

Evaluate milk thistle-drug interaction potential using established *in vitro* systems.

The inhibitory potential of individual milk thistle constituents toward CYP2C9 (Chapter 2, Appendix A) and CYP3A4/5 (Chapter 3) were evaluated using standard *in vitro* assays of CYP activity. Individual flavonolignans differentially inhibited both CYP2C9 and CYP3A4/5, with no apparent correlation in inhibitory potency between the two enzymes. Initial evaluation identified silybin A and silybin B as potent inhibitors of CYP2C9 activity (K_i = 10 and 4.8 μM, respectively) (Chapter 2), with subsequent evaluation highlighting the potency of silychristin and silydianin (Appendix A). In contrast to low inhibitory potency (<25% inhibition at 100 μM) towards CYP2C9, the relatively less abundant constituents isosilybin A and isosilybin B were two of the more potent inhibitors of CYP3A4/5 activity. The crude extract silymarin, rather than single constituents, was consistently one of the most potent inhibitors of CYP2C9 (Appendix A) and CYP3A4/5 (Chapter 3) activity in microsomal preparations. In an attempt to elucidate the mechanism underlying the increased potency of silymarin, an “artificial” silymarin preparation was generated (Appendix B), which contained all flavonolignans and the sole flavonoid, but lacked fatty acids and other polyphenolic compounds. Comparison of the IC_{50} of the commercial and artificial silymarin preparations demonstrated a roughly three-fold increase in potency when fatty acids/other polyphenolic compounds were included (Appendix B). Taken together, the net effect of

the fatty acids and other polyphenolic compounds in the commercial preparation is to increase the inhibitory potency of silymarin. This apparent increase could be due to direct inhibition of CYP3A4/5 by fatty acids and/or other polyphenolic compounds. Alternatively, the fatty acids/other polyphenolic compounds could inhibit CYP3A4/5 activity indirectly by synergistic inhibition with flavonolignans or by increasing the solubility of inhibitory flavonolignans. Identification and quantification of the fatty acids and/or polyphenolic compounds would facilitate evaluation of direct modulation of CYP activity. Without this information, incubations with human serum albumin may allow indirect assessment of the interaction potential of adulterant compounds. In theory, albumin will sequester the fatty acid fraction of silymarin and abrogate the increased potency towards CYP activity (Rowland et al., 2008; Wattanachai et al., 2012). Milk thistle flavonolignans have poor water solubility but are believed to be soluble at concentrations approaching 200 μM when solvents such as DMSO (0.1% v/v final concentration) are used. Solubility measurements with and without fatty acids can be used to assess the likelihood of solubility enhancement when the fatty acids are present.

Administration of 420 mg/day silymarin for 14 days was associated with an increase in the systemic exposure of the CYP2C9/3A substrate losartan (Han et al., 2009), whereas administration of 1.4 g/day silibinin for 7 days had no effect on (*S*)-warfarin exposure (Chapter 4). In addition to the theories posited in Chapter 4, another explanation for this discrepancy is that one of the constituents in silymarin (but not silibinin) yet to be identified and fully characterized is a potent inhibitor of CYP2C9. Based on preliminary results (Appendix A), the constituents silychristin and silydianin should be evaluated as additional inhibitors of CYP2C9 using methods described in Chapters 2 and 3. Potent reversible or mechanism-based inhibition of CYP2C9 by these constituents would help to explain these inconsistent clinical drug interactions with milk thistle preparations and compel clinical evaluation.

Although the current work focused on cytochromes P450 2C9 and 3A4/5, milk thistle constituents may also modulate the activity of other drug metabolizing enzymes. Usage of milk thistle products has increased over the last decade among cancer patients, in part as a means to decrease chemotherapeutic agent-induced liver damage. The clearance of several chemotherapeutic agents, including paclitaxel (CYP2C8), tamoxifen (CYP2D6), and irinotecan (UGT1A1), are sensitive to modulations in activity of a single enzyme. Subsequent analysis of milk thistle interaction potential should prioritize enzymes such as CYP2C8, CYP2D6, and UGT1A1, for which serious adverse events could be expected with co-administration of milk thistle products and chemotherapeutic agents. While cancer patients, due to high milk thistle usage rates, are likely candidates for adverse events with milk thistle products, myriad additional drugs are sensitive to inhibition of a single enzyme. For this reason, the milk thistle interaction potential with other important drug metabolizing enzymes should be evaluated. Interaction potential assessment of milk thistle constituents towards the aforementioned enzymes can be conducted according to the framework described in Chapters 2 and 3.

Methylated analogs of silybin B were developed as a means to decrease metabolic lability *in vivo* and to determine the chemical moieties key for biologic activity *in vitro* (Sy-Cordero et al., 2013). Evaluation of these compounds as inhibitors of CYP2C9 activity demonstrated either increased or decreased inhibitory potency depending on the site and extent of methylation (Appendix A). Continued selective modification of milk thistle constituents can help determine the key regions for inhibition of CYP activity, as well as sites of metabolism. Although indirect evidence suggests that the 1-4 dioxane moiety of silybin A and silybin B is responsible for the mechanism-based inhibition (MBI) of CYP3A4, MBI from this moiety has not been demonstrated directly. Selective halogenation of this moiety theoretically could prevent oxidation and abrogate CYP3A4 inactivation. In addition to mechanistic information regarding the site of oxidation

resulting in CYP3A4 inactivation, selective modification of milk thistle flavonolignans may prevent oxidative or conjugative metabolism. The resultant decreased clearance could increase bioavailability and potentially lead to increased pharmacologic action.

Following oral administration of a milk thistle preparation, individual constituents are metabolized rapidly, with the resultant conjugated metabolites achieving systemic concentrations much higher than parent compounds. Despite this increase in systemic exposure, knowledge regarding the pharmacologic activity or interaction potential of these metabolites is limited. Comprehensive evaluation of the interaction potential of milk thistle preparations requires testing of the metabolites in addition to the parent compounds. To date, difficulties in the isolation and purification of the conjugated metabolites have hampered evaluation of these compounds. Future emphasis on these processes should produce sufficient quantities of the metabolites to support evaluation of drug interaction liability according to the framework discussed in Chapters 2 and 3.

Despite demonstrating MBI with recombinant CYP3A4 and a positive signal in an IC_{50} shift assay with both recombinant CYP3A4 and human microsomes (Chapter 3), silybin A and silibinin demonstrated no discernible MBI with microsomal preparations (Appendix C). Recombinant CYP3A4 was markedly more sensitive to MBI in the IC_{50} shift assays (Chapter 3), indicating that differences in the enzyme preparation may influence the positive predictive value of the test system. To elucidate fully the interaction potential of milk thistle constituents, the discrepant extent of MBI should be investigated. Initial evaluation should focus on absolute identification of MBI with recombinant enzymes. Identification of a compound as a mechanism-based inhibitor requires meeting several experimental criteria: time-dependent inactivation, saturation of inactivation, substrate protection, irreversibility, inactivator stoichiometry, involvement of a catalytic step, and inactivation prior to release of active species (Silverman and Daniel, 1995). The current experiments have demonstrated time-dependent and saturable

inactivation with recombinant CYP3A4 and inactivation prior to the release of active species (Chapter 3). However, true irreversibility and substrate protection have not been assessed. Following incubation of milk thistle constituents and recombinant enzymes, addition of potassium ferricyanide or dialysis of 'inactivated' enzyme will differentiate time-dependent from mechanism-based inhibition. Addition of other CYP3A4/5 substrates such as testosterone, alprazolam, or nifedipine may mitigate CYP3A4/5 inactivation through a process termed 'substrate protection'. As the inhibitor and substrate should bind to the active site of the enzyme, the additional substrate will inhibit competitively the inhibitor binding and result in decreased enzyme inactivation. Following identification of a constituent as an MBI of recombinant CYP3A4, subsequent experiments with microsomal preparations should focus on higher concentrations of the MBI. As the observed K_I with recombinant enzymes is roughly 100 μM, concentrations approaching 200 μM should be evaluated.

Milk thistle constituents have been established to undergo rapid conjugation following oral administration; however, the rates and extents of these metabolic processes have not been determined. Likewise, the rate and extent of protein-mediated flux of these compounds has not been reported. Whereas conventional pharmaceutical agents undergo rigorous reaction phenotyping to identify the enzymes and transporters important for distribution or clearance, natural products generally are not subjected to such testing. Elucidation of distributional and metabolic parameters would facilitate estimations of drug interaction liability by accurately reflecting concentrations in the relevant tissues (typically liver and intestine), as well as reflecting the duration of exposure. Since the compounds are cleared mainly by UGTs, the first priority should be to determine the enzyme kinetic parameters of conjugation in microsomal preparations and recombinant UGTs. Scarcity of authentic standards may necessitate measuring

substrate loss initially, but advances in analytical methods (Kren et al., 2000) should facilitate generation of glucuronide standards and measurement of metabolite formation.

In addition to metabolic clearance, transport-mediated distribution of milk thistle constituents should be evaluated. Milk thistle preparations and individual constituents have been tested as inhibitors of transport-mediated flux (reviewed in Chapter 1); however, no study to date has focused on these constituents as substrates of transporters. Uptake kinetics for milk thistle constituents can be determined by measuring accumulation in suspended hepatocytes or mammalian cell lines such as human embryonic kidney (HEK) or Madin-Darby canine kidney (MDCK) cells that have been transfected with human transporters (Cvetkovic et al., 1999; Cui et al., 2001; Kindla et al., 2011; Kimoto et al., 2013; Köck et al., 2013). The methods for such experiments can be adopted from previously published studies determining the extent of uptake transporter inhibition by silymarin or milk thistle constituents as reviewed in Chapter 1. Efflux kinetics may be determined *via* experiments with sandwich-cultured hepatocytes, inside-out membrane vesicles, or Caco-2 cells (Liu et al., 1999; Wheeler et al., 2000; Annaert et al., 2001; Troutman and Thakker, 2003; Hemauer et al., 2010). Milk thistle constituents are rapidly conjugated in systems with functioning drug metabolizing enzymes, making the membrane vesicles the 'cleaner' system for initial evaluation. Inhibition of UGTs in the other cell systems with the prototypic inhibitors diclofenac or quercetin may remove the potential confounding metabolism.

Predict the clinical impact of silymarin co-administration with prototypic cytochrome P450 probe substrates.

A PBPK modeling and simulation approach was utilized to predict the clinical impact of milk thistle co-administration with the CYP probe substrates warfarin (CYP2C9) and midazolam (CYP3A4/5). As discussed in Chapter 4, the PBPK model accurately described the distribution and clearance of the probe substrates. Further

refinement of the warfarin model should incorporate *in vitro* metabolic clearance parameters to eliminate the need to fit the model to existing clinical concentration-time data. Further evaluation of the midazolam model should incorporate intravenous dosing to ensure that the hepatic clearance and volume of distribution are reflected accurately in the model. The current midazolam model assumes complete metabolic clearance of midazolam by CYP3A4/5. Incorporation of alternate pathways such as 4-hydroxylation, *N*-glucuronidation, and renal elimination will minimize potential overpredictions of interaction potential (Klieber et al., 2008; Yang et al., 2012).

PBPK modeling and simulation are limited, in part, due to the vast number of parameters necessary for accurate depictions of the complex biologic systems involved in the distribution and elimination of compounds. Compound-independent parameters such as physiologic blood flows and organ volumes are well-established in the literature (Brown et al., 1997; Boecker, 2003). Methods to predict partition coefficients are accurate for drug-like molecules but may begin to demonstrate bias and imprecision for compounds that deviate from the conventional pharmaceutical chemical space (Poulin and Theil, 2000; Rodgers and Rowland, 2007). Although the partition coefficients computed for milk thistle constituents likely are reasonable approximations, further model refinement should incorporate partition coefficients derived from rodent or human tissue to ensure accuracy. Incorporation of clearance and transport kinetic parameters derived from *in vitro* systems also can improve model predictions for silybin A and silybin B. The systemic exposure of a selected milk thistle preparation, silibinin, was reflected accurately by the current PBPK model. Incorporation of additional milk thistle constituents will allow modeling and simulation of other preparations, such as silymarin. The majority of existing research has focused on silymarin or milk thistle extract, underscoring the necessity to expand the current model to incorporate additional milk thistle constituents.

In addition to addressing challenges inherent to investigations of herbal product drug interaction liability, PBPK modeling and simulation can address other complex clinical scenarios. Milk thistle-drug interactions caused by reversible inhibition of drug metabolizing enzymes and transporters potentially can be minimized by offsetting the administration of milk thistle products and sensitive substrates. The dynamic nature of PBPK models can be used to determine a dosing regimen that would minimize this interaction liability. Simulations of trials in special populations can be facilitated through incorporation of relevant physiologic parameters obtained from the literature. Prospective simulation of herb-drug interactions in patient populations can determine the interaction liability without placing such patients into potentially harmful situations. Genetic polymorphisms in relevant drug metabolizing enzymes and transporters also can be incorporated into PBPK models to determine the mechanistic consequences of such polymorphisms. Incorporation of multiple interaction mechanisms may more accurately reflect the complex biological systems involved in the distribution and clearance of both victim and perpetrator compounds and may allow more accurate predictions of drug interactions involving substrates that have more than one clearance pathway.

Evaluate PBPK model predictions using a proof-of-concept clinical study.

As predicted from the PBPK modeling and simulation, the geometric mean effects of high-'dose' silibinin on the pharmacokinetics of (*S*)-warfarin and midazolam were minimal. Although geometric mean (*S*)-warfarin exposure did not increase markedly, three of the twelve subjects experienced more than a 33% increase in systemic exposure. Increases of this magnitude for substrates with a narrow therapeutic index such as warfarin could lead to adverse events. Accordingly, the CYP2C9 interaction potential of silibinin cannot be disregarded completely. The systemic exposure of midazolam was increased markedly (>33%) in only one subject.

Subsequent analysis indicated that the increase in systemic exposure in that subject likely was due to markedly lower-than-average exposure at baseline, consistent with taking an inducing agent, rather than to an increase in exposure mediated by silibinin. Taken together, the interaction liability of silibinin and midazolam likely is minimal. However, interactions between silibinin and other sensitive substrates, such as simvastatin and nifedipine, or narrow therapeutic index drugs, such as the immunosuppressants cyclosporine, tacrolimus, and sirolimus, cannot be excluded.

Future clinical evaluation of herb-drug interactions should be predicated upon compelling results from the aforementioned future directions. For example, the inhibitory potency of silibinin toward UGT1A1 (Chapter 1) indicated potential for interactions with sensitive substrates such as ezetimibe and raloxifene. Other drug metabolizing enzymes, transporters, and alternate trial design strategies can be employed to evaluate the utility of the newly developed PBPK models. Ultimately, pharmacodynamic endpoints (*e.g.*, pupil diameter as a measure of opiate-like central nervous system effects) can be approximated to allow pharmacodynamic-based clinical studies.

Significance

This dissertation project developed novel translational methods to predict, quantitatively, metabolic herb-drug interactions using milk thistle as an exemplar herbal product. Integration of *in vitro*-derived inhibitory kinetic parameters and estimates of systemic exposure to individual constituents into a PBPK interaction model facilitated accurate predictions of the lack of interaction between silibinin and the probe substrates warfarin and midazolam. Application of these methods could facilitate regulatory guidelines by providing a framework for systematic evaluation of herb-drug interaction liability that can be used prospectively. Clinically relevant herb-drug interactions, as identified by these methods, can impact label changes of sensitive victim drugs. Translation of bench-top scientific information to clinical practice will facilitate the

identification and management of herb-drug interactions, ultimately promoting safe co-administration of herbal products and conventional pharmacotherapies.

References

Annaert PP, Turncliff RZ, Booth CL, Thakker DR and Brouwer KL (2001) P-glycoprotein-mediated in vitro biliary excretion in sandwich-cultured rat hepatocytes. *Drug Metab Dispos* **29:**1277-1283.

Boecker BB (2003) Reference values for basic human anatomical and physiological characteristics for use in radiation protection. *Radiat Prot Dosimetry* **105:**571-574.

Brown RP, Delp MD, Lindstedt SL, Rhomberg LR and Beliles RP (1997) Physiological parameter values for physiologically based pharmacokinetic models. *Toxicol Ind Health* **13:**407-484.

Cui Y, Konig J and Keppler D (2001) Vectorial transport by double-transfected cells expressing the human uptake transporter SLC21A8 and the apical export pump ABCC2. *Mol Pharmacol* **60:**934-943.

Cvetkovic M, Leake B, Fromm MF, Wilkinson GR and Kim RB (1999) OATP and P-glycoprotein transporters mediate the cellular uptake and excretion of fexofenadine. *Drug Metab Dispos* **27:**866-871.

Han Y, Guo D, Chen Y, Tan ZR and Zhou HH (2009) Effect of silymarin on the pharmacokinetics of losartan and its active metabolite E-3174 in healthy Chinese volunteers. *Eur J Clin Pharmacol* **65:**585-591.

Hemauer SJ, Patrikeeva SL, Nanovskaya TN, Hankins GD and Ahmed MS (2010) Role of human placental apical membrane transporters in the efflux of glyburide, rosiglitazone, and metformin. *Am J Obstet Gynecol* **202:**383 e381-387.

Kimoto E, Yoshida K, Balogh LM, Bi YA, Maeda K, El-Kattan A, Sugiyama Y and Lai Y (2013) Characterization of Organic Anion Transporting Polypeptide (OATP) Expression and Its Functional Contribution to the Uptake of Substrates in Human Hepatocytes. *Mol Pharm*.

Kindla J, Muller F, Mieth M, Fromm MF and Konig J (2011) Influence of non-steroidal anti-inflammatory drugs on organic anion transporting polypeptide (OATP) 1B1- and OATP1B3-mediated drug transport. *Drug Metab Dispos* **39:**1047-1053.

Klieber S, Hugla S, Ngo R, Arabeyre-Fabre C, Meunier V, Sadoun F, Fedeli O, Rival M, Bourrie M, Guillou F, Maurel P and Fabre G (2008) Contribution of the N-glucuronidation pathway to the overall in vitro metabolic clearance of midazolam in humans. *Drug Metab Dispos* **36:**851-862.

Kock K, Xie Y, Oberlies NH, Hawke RL and Brouwer KL (2013) Interaction of Silymarin Flavonolignans with Organic Anion Transporting Polypeptides (OATPs). *Drug Metab Dispos*.

Kren V, Ulrichova J, Kosina P, Stevenson D, Sedmera P, Prikrylova V, Halada P and Simanek V (2000) Chemoenzymatic preparation of silybin beta-glucuronides and their biological evaluation. *Drug Metab Dispos* **28:**1513-1517.

Liu X, LeCluyse EL, Brouwer KR, Gan LS, Lemasters JJ, Stieger B, Meier PJ and Brouwer KL (1999) Biliary excretion in primary rat hepatocytes cultured in a collagen-sandwich configuration. *Am J Physiol* **277:**G12-21.

Poulin P and Theil FP (2000) A priori prediction of tissue:plasma partition coefficients of drugs to facilitate the use of physiologically-based pharmacokinetic models in drug discovery. *J Pharm Sci* **89:**16-35.

Rodgers T and Rowland M (2007) Mechanistic approaches to volume of distribution predictions: understanding the processes. *Pharm Res* **24:**918-933.

Rowland A, Elliot DJ, Knights KM, Mackenzie PI and Miners JO (2008) The "albumin effect" and in vitro-in vivo extrapolation: sequestration of long-chain unsaturated fatty acids enhances phenytoin hydroxylation by human liver microsomal and recombinant cytochrome P450 2C9. *Drug Metab Dispos* **36:**870-877.

Silverman RB and Daniel LP (1995) [10] Mechanism-based enzyme inactivators, in: *Methods in Enzymology*, pp 240-283, Academic Press.

Sy-Cordero AA, Graf TN, Runyon SP, Wani MC, Kroll DJ, Agarwal R, Brantley SJ, Paine MF, Polyak SJ and Oberlies NH (2013) Enhanced bioactivity of silybin B methylation products. *Bioorg Med Chem* **21:**742-747.

Troutman MD and Thakker DR (2003) Efflux ratio cannot assess P-glycoprotein-mediated attenuation of absorptive transport: asymmetric effect of P-glycoprotein on absorptive and secretory transport across Caco-2 cell monolayers. *Pharm Res* **20:**1200-1209.

Wattanachai N, Tassaneeyakul W, Rowland A, Elliot DJ, Bowalgaha K, Knights KM and Miners JO (2012) Effect of albumin on human liver microsomal and recombinant CYP1A2 activities: impact on in vitro-in vivo extrapolation of drug clearance. *Drug Metab Dispos* **40:**982-989.

Wheeler R, Neo SY, Chew J, Hladky SB and Barrand MA (2000) Use of membrane vesicles to investigate drug interactions with transporter proteins, P-glycoprotein and multidrug resistance-associated protein. *Int J Clin Pharmacol Ther* **38:**122-129.

Yang J, Atkins WM, Isoherranen N, Paine MF and Thummel KE (2012) Evidence of CYP3A allosterism in vivo: analysis of interaction between fluconazole and midazolam. *Clin Pharmacol Ther* **91:**442-449.

Appendix A: Inhibition of CYP2C9 by milk thistle constituents and silybin B methylation products[1,2]

Materials and Methods

Chemicals and reagents. Common reagents were procured as described in Chapter 2. Milk thistle constituents were isolated as described previously (Graf et al., 2007). Methylated analogues of silybin B (Compound 1) were prepared according to published methods (Dzubak et al., 2006). Briefly, dimethyl sulfate was added to a solution of silybin B and potassium carbonate in anhydrous acetone. The mixture was heated at reflux for 30 min, cooled to room temperature, acidified with dilute hydrochloric acid, and extracted with ethyl acetate. The organic extracts were combined and concentrated to dryness under reduced pressure. The resulting oil was purified using RP-HPLC to yield five major products (Figure A.1) in greater than 95% purity as measured by analytical RP-HPLC.

Evaluation of milk thistle constituents and methylated analogues as inhibitors of CYP2C9. The inhibitory effects of milk thistle constituents and silybin B methylated analogues were evaluated as described in Chapter 2.

Results

Milk thistle constituents differentially inhibit CYP2C9 activity. The potency of the milk thistle constituents and crude extract not tested previously (Chapter 2) was evaluated against CYP2C9 activity ((*S*)-warfarin 7-hydroxylation). Silychristin and silymarin inhibited CYP2C9 activity in a concentration-dependent manner (1 vs. 10 μM) (Figure A.2). When tested at 100 μM, both preparations inhibited activity to levels below the lower limit of quantitation. Isosilychristin and silydianin inhibited activity in a

[1] A. A. Sy-Cordero et al. *Bioorg. Med. Chem.* 21 (2013) 742–747

[2] Reprinted with permission from Elsevier.

concentration-dependent manner from 10 to 100 μM but not from 1 to 10 μM. Activity was reduced by at least 50% when incubated with all constituents at 100 μM.

Methylation of silybin B impacts inhibitory potency toward CYP2C9 activity. The CYP2C9 inhibitory potencies of the methylated analogues (2–5) were compared (Fig. A.3); compound 6 was not evaluated due to paucity of sample. With the exception of 5, all compounds inhibited CYP2C9 activity in a concentration-dependent manner (1 vs 10 μM). Compound 2 was less potent than 1 at 100 μM, whereas compounds 3 and 4, representing monomethylation at the 7-OH and dimethylation at the 7- and 400-OH moieties, respectively, were more potent than 1, with activities below the limit of quantification when tested at 100 μM.

Figure A.1.

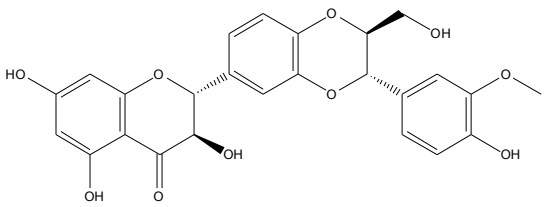

Silybin B

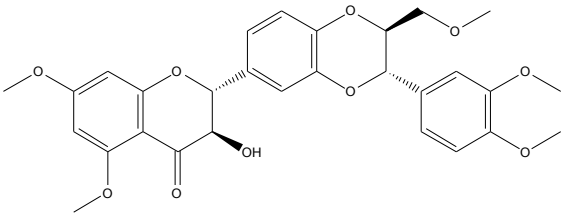

Compound 2

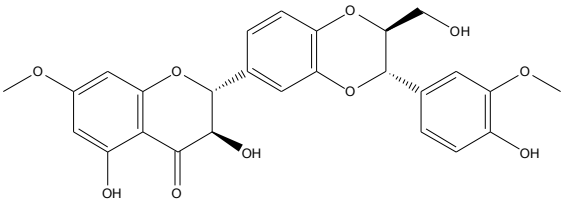

Compound 3

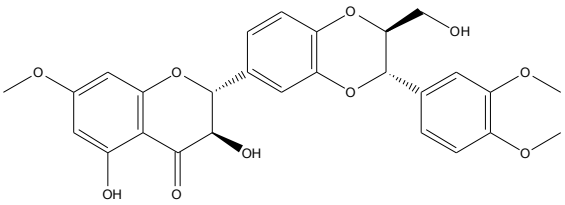

Compound 4

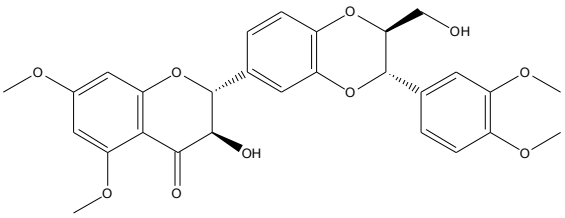

Compound 5

Figure A.2.

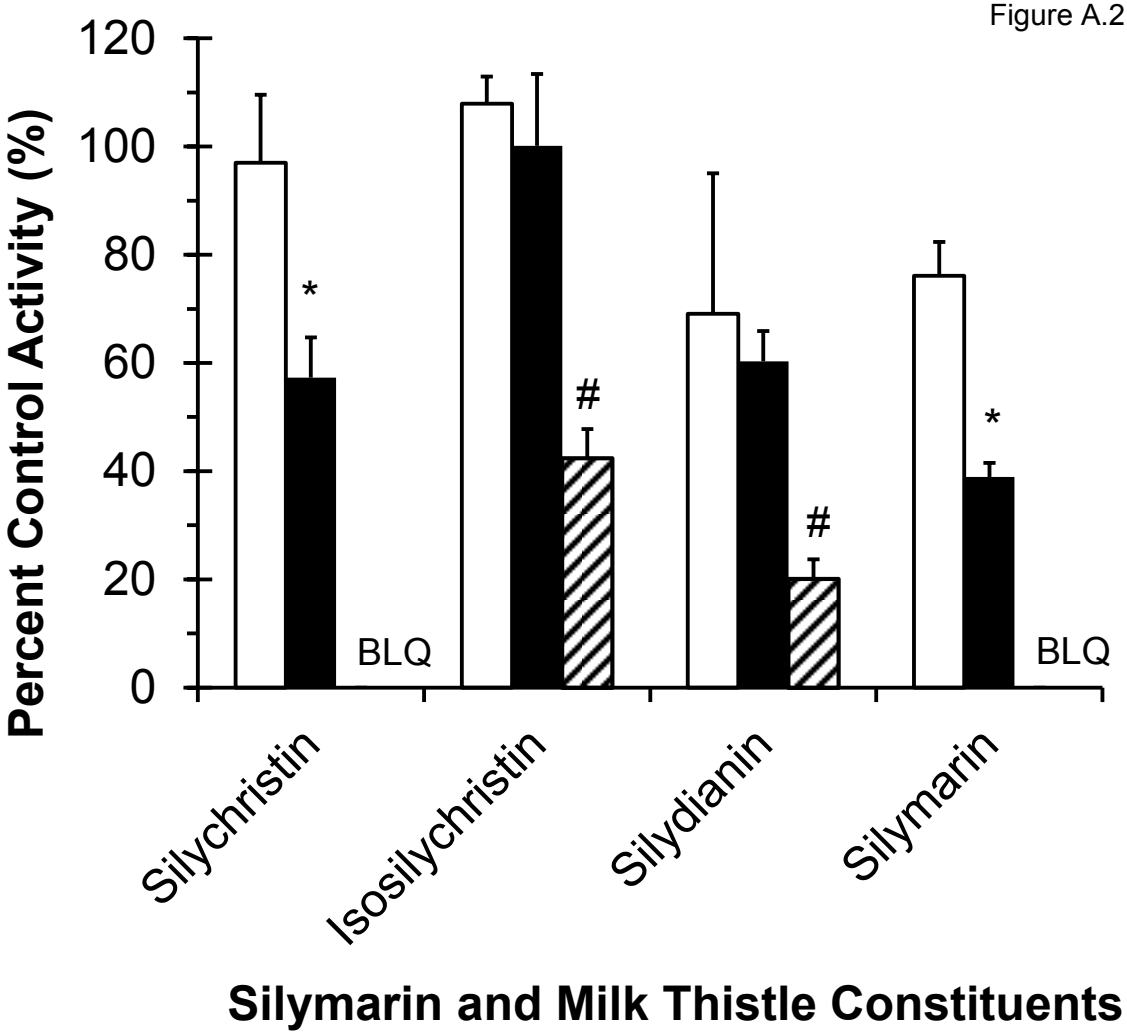
120
100
80
60
40
20
0
Percent Control Activity (%)
*
BLQ
#
#
*
BLQ
Silychristin
Isosilychristin
Silydianin
Silymarin
Silymarin and Milk Thistle Constituents

Figure A.3.

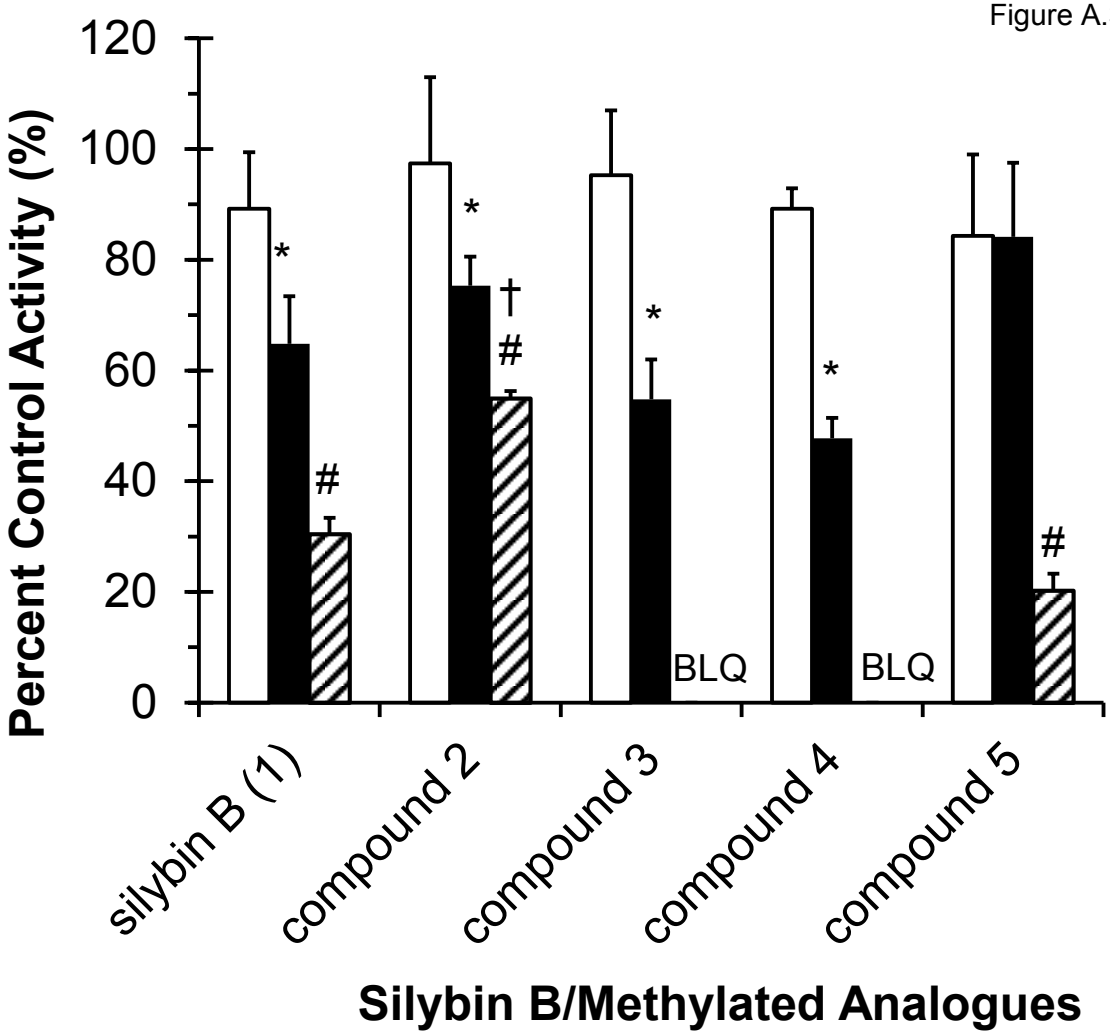
Percent Control Activity (%)
120
100
80
60
40
20
0
*
*
†
#
*
*
BLQ
BLQ
#
silybin B (1)
compound 2
compound 3
compound 4
compound 5
Silybin B/Methylated Analogues

Legends to Figures

Figure A.1. Chemical structures of silybin B and methylated analogues.

Figure A.2. Effects of silymarin and milk thistle constituents on CYP2C9-mediated (*S*)-warfarin 7-hydroxylation in human liver microsomes (HLM). Incubation mixtures consisted of HLM (0.1 mg/mL), (S)-warfarin (4 μM), silybin B or methylated analogue (1, 10, or 100 μM; open, solid, and hatched bars, respectively) and potassium phosphate buffer (100 mM, pH 7.4). Reactions were initiated by the addition of NADPH (1 mM) and were terminated after 30 min with ice-cold MeOH (2 volumes). Activity in the presence of vehicle control (0.75% MeOH, v/v) was 4.3 ± 0.26 pmol/min/mg microsomal protein. Bars and error bars denote means and SDs, respectively, of triplicate incubations. BLQ, below limit of quantification. *$p<0.05$, 1 versus 10 μM; $^{\#}p<0.05$, 10 versus 100 μM (two-way ANOVA followed by Tukey's test).

Figure A.3. Effects of silybin B (1) and methylated analogues (2–5) on CYP2C9-mediated (*S*)-warfarin 7-hydroxylation in human liver microsomes (HLM). Incubation mixtures consisted of HLM (0.1 mg/mL), (S)-warfarin (4 μM), silybin B or methylated analogue (1, 10, or 100 μM; open, solid, and hatched bars, respectively) and potassium phosphate buffer (100 mM, pH 7.4). Reactions were initiated by the addition of NADPH (1 mM) and were terminated after 30 min with ice-cold MeOH (2 volumes). Activity in the presence of vehicle control (0.75% MeOH, v/v) was 4.3 ± 0.26 pmol/min/mg microsomal protein. Bars and error bars denote means and SDs, respectively, of triplicate incubations. BLQ, below limit of quantification. *$p<0.05$, 1 versus 10 μM; $^{\#}p<0.05$, 10 versus 100 μM; $^{\dagger}p<0.05$ versus silybin B at 100 μM (two-way ANOVA followed by Tukey's test).

References

Dzubak P, Hajduch M, Gazak R, Svobodova A, Psotova J, Walterova D, Sedmera P and Kren V (2006) New derivatives of silybin and 2,3-dehydrosilybin and their cytotoxic and P-glycoprotein modulatory activity. *Bioorg Med Chem* **14:**3793-3810.

Graf TN, Wani MC, Agarwal R, Kroll DJ and Oberlies NH (2007) Gram-scale purification of flavonolignan diastereoisomers from *Silybum marianum* (milk thistle) extract in support of preclinical in vivo studies for prostate cancer chemoprevention. *Planta Med* **73:**1495-1501.

Sy-Cordero AA, Graf TN, Runyon SP, Wani MC, Kroll DJ, Agarwal R, Brantley SJ, Paine MF, Polyak SJ and Oberlies NH (2013) Enhanced bioactivity of silybin B methylation products. *Bioorg Med Chem* **21:**742-747.

Appendix B. Evaluation of the inhibitory potency of a commercial silymarin preparation and an artificial preparation towards CYP3A activity.

Materials and Methods

Chemicals and reagents. Common reagents were procured as described in Chapter 3. Commercial preparation of silymarin was obtained from the Rottapharm Madaus subsidiary Euromed S.A. (Barcelona, Spain). Artificial silymarin was produced by combining individual milk thistle constituents (Graf et al., 2007) in the respective abundance of the commercial silymarin preparation (Davis-Searles et al., 2005) (Figure B.1). The composition of artificial silymarin should mirror that of commercial silymarin with respect to the flavonolignans and flavonoid but lack the fatty acids.

Evaluation of milk thistle constituents and methylated analogues as inhibitors of CYP3A4/5. The inhibitory effects of artificial and commercial silymarin were evaluated as described in Chapter 3, with the addition of a single donor human intestinal microsomal preparation (HI-5 J7).

Results

Silymarin preparations differentially inhibit CYP3A4/5 activity. Artificial silymarin was a more potent inhibitor of CYP3A4/5 mediated midazolam 1'-hydroxylation in all enzyme preparations (Figure B.2). This increased potency was reflected in a roughly 3-fold increase in IC_{50} following the "removal" of the fatty acid fraction of silymarin (Table B.1). The inhibitory potencies of commercial and artificial silymarin were similar between enzyme preparations.

Figure B.1

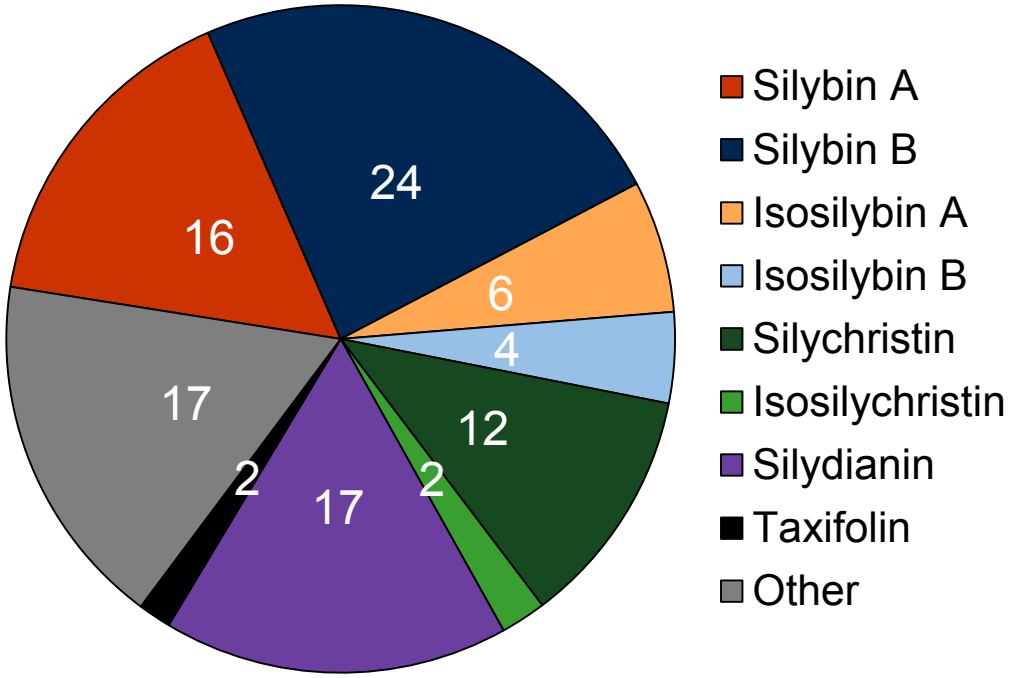
24
16
6
4
17
12
2
2
17
Silybin A
Silybin B
Isosilybin A
Isosilybin B
Silychristin
Isosilychristin
Silydianin
Taxifolin
Other

Figure B.2

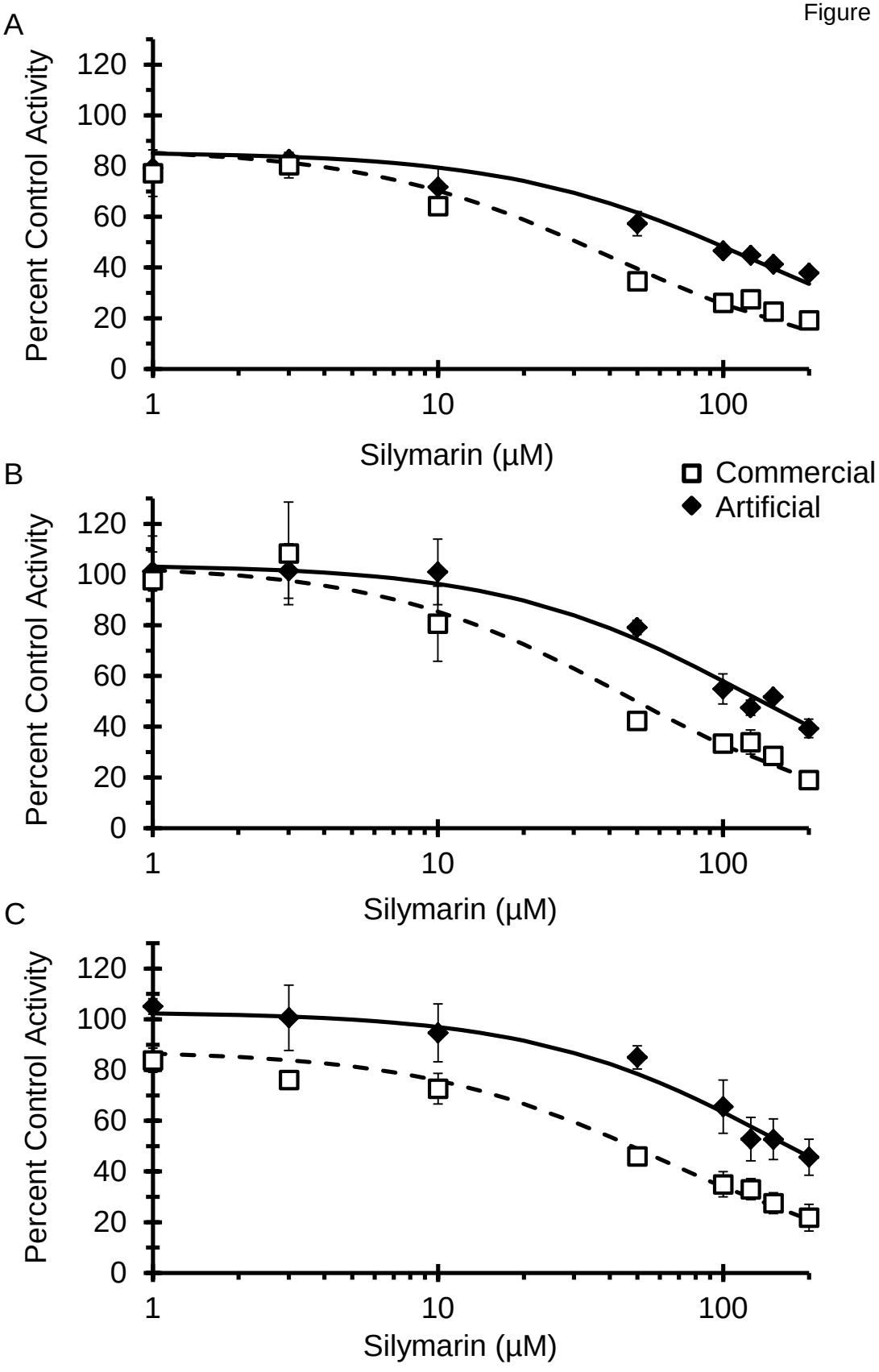
A
Percent Control Activity
120
100
80
60
40
20
0
1
10
100
Silymarin (µM)
B
Commercial
Artificial
Percent Control Activity
120
100
80
60
40
20
0
1
10
100
Silymarin (µM)
C
Percent Control Activity
120
100
80
60
40
20
0
1
10
100
Silymarin (µM)

Legends to Figures

Figure B.1. Relative composition of the commercial silymarin product.

Figure B.2. Inhibitory effects of commercial and artificial silymarin preparations on midazolam 1'-hydroxylation activity in pooled human liver microsomes (A), pooled human intestinal microsomes (B), and single donor human intestinal microsomes (D). Microsomes (0.05 mg/mL) were incubated with midazolam (4 μM) and silymarin preparation (0-200 μM) for 2 (liver microsomes) or 4 (intestinal microsmes) min. Reactions were initiated with NADPH (1 mM). Midazolam 1'-hydroxylation activity in the presence of vehicle control [0.1% (v/v) DMSO] was 1900 ± 170, 440 ± 34, or 1460 ± 65 pmol/min/mg microsomal protein for human liver microsomes, pooled human intestinal microsomes, and single donor human intestinal microsomes, respectively. Symbols and error bars denote means and SDs, respectively, of triplicate incubations. Solid and dashed curves denote nonlinear least-squares regression of observed data using WinNonlin (version 5.3)

Table B.1. Comparison of IC_{50}s[a] (μM) for Commercial (CS) and Artificial (AS) silymarin in human liver microsomes (HLM), pooled human intestinal microsomes (pHIM), and single-donor human intestinal microsomes (iHIM).

Microsomes	CS	AS	*p*-value[b]
HLM	41 ± 5.0	130 ± 15	0.005
pHIM	46 ± 6.8	130 ± 12	0.004
iHIM	63 ± 6.6	160 ± 17	0.006

[a]Estimates ± SEs; [b]CS vs. AS, Student's *t*-test

References

Davis-Searles PR, Nakanishi Y, Kim NC, Graf TN, Oberlies NH, Wani MC, Wall ME, Agarwal R and Kroll DJ (2005) Milk thistle and prostate cancer: differential effects of pure flavonolignans from *Silybum marianum* on antiproliferative end points in human prostate carcinoma cells. *Cancer Res* **65:**4448-4457.

Graf TN, Wani MC, Agarwal R, Kroll DJ and Oberlies NH (2007) Gram-scale purification of flavonolignan diastereoisomers from *Silybum marianum* (milk thistle) extract in support of preclinical in vivo studies for prostate cancer chemoprevention. *Planta Med* **73:**1495-1501.

Appendix C: Mechanism-based inhibition of CYP3A4/5 activity in microsomal preparations

Methods

Chemicals and reagents. All chemicals and reagents were procured as described in Chapter 3.

Determination of mechanism-based inhibition kinetics. Time- and concentration-dependent inhibition of CYP3A4 was assessed as described previously (Paine et al., 2004) and detailed in Chapter 3. Briefly, primary incubation mixtures consisting of HLM or HIM, milk thistle constituent/extract (0-100 μM), and potassium phosphate buffer were equilibrated at 37°C for 5 min before initiating the primary reactions with NADPH. As a positive control for mechanism-based inhibition, reaction mixtures contained 5 μM DHB in place of milk thistle constituent/extract. At designated time points (0-15 min), an aliquot (4 μL) was removed and diluted 50-fold into a secondary reaction mixture containing midazolam (8 μM) and NADPH (1 mM). The secondary reactions were terminated and processed as described for the reversible inhibition experiments.

Results

Silybin A and Silibinin Do Not Demonstrate Mechanism-Based Inhibition of CYP3A Activity. The time- and concentration-dependent inhibition of CYP3A4/5 activity by silybin A and silibinin was determined to derive mechanism-based inhibition inhibitory kinetics. Unlike with rCYP3A4 (Chapter 3), neither silybin A (Fig. C.1A,C and Fig. C.2A) nor silibinin (Fig. C.1B,D and Fig. C.2B) demonstrated time-dependent inhibition of CYP3A4/5 activity.

Figure C.1

A

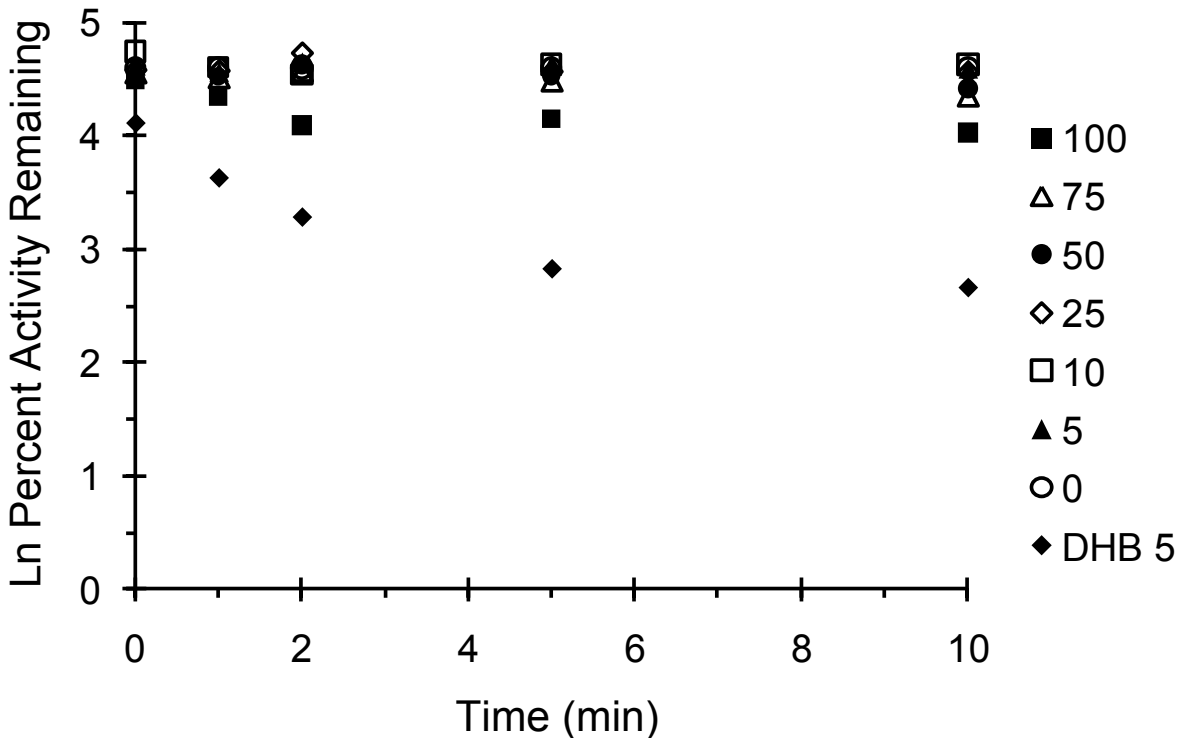
Ln Percent Activity Remaining
0
1
2
3
4
5
0
2
4
6
8
10
Time (min)
100
75
50
25
10
5
0
DHB 5

B

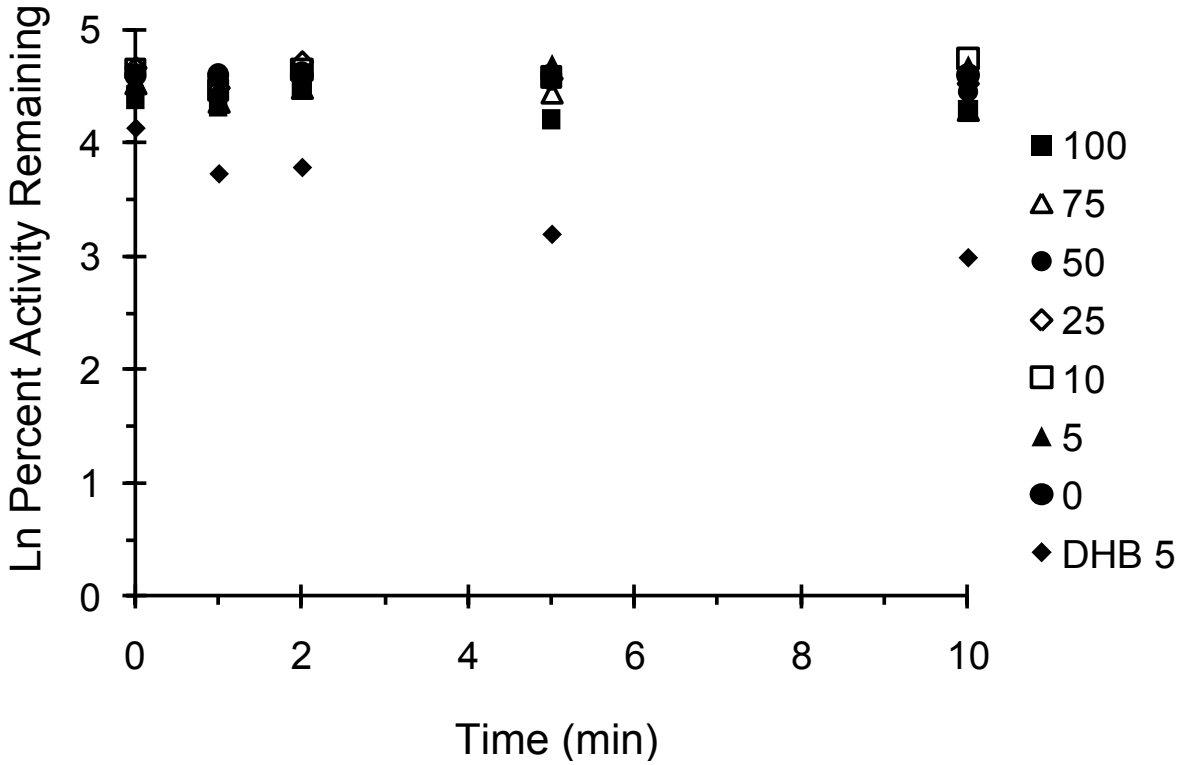
Ln Percent Activity Remaining
0
1
2
3
4
5
0
2
4
6
8
10
Time (min)
100
75
50
25
10
5
0
DHB 5

C

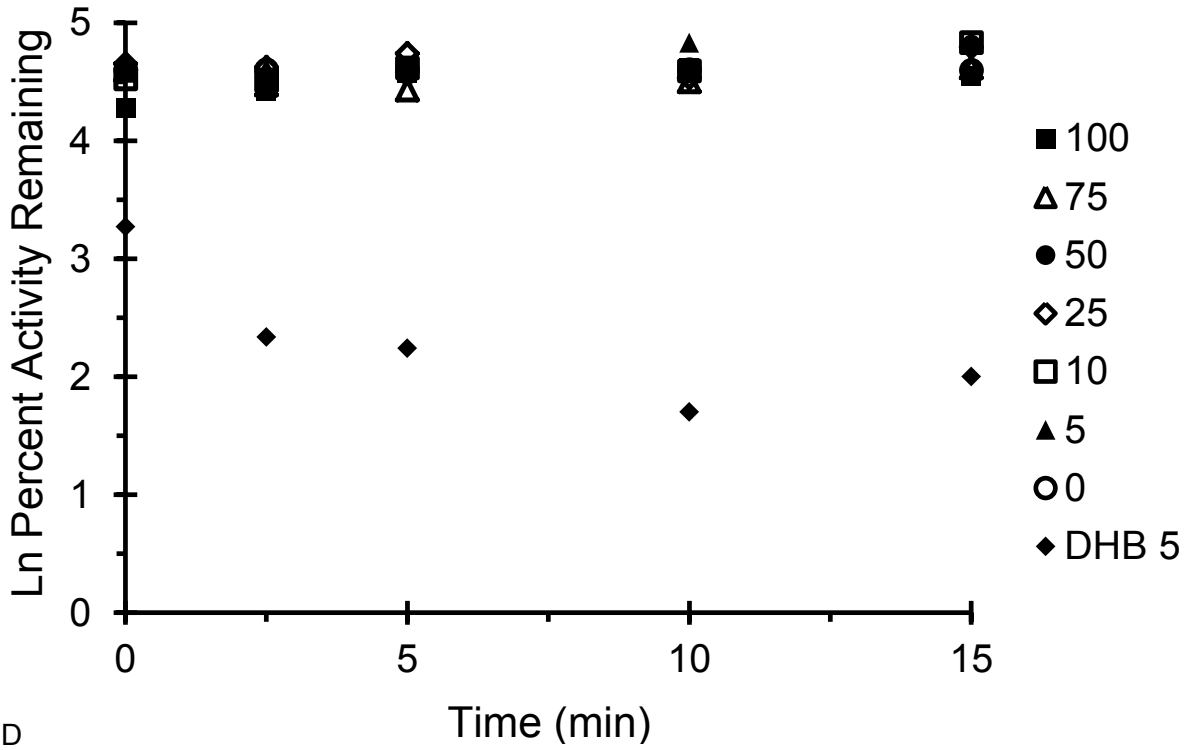
Ln Percent Activity Remaining
0
1
2
3
4
5
0
5
10
15
Time (min)
100
75
50
25
10
5
0
DHB 5

D

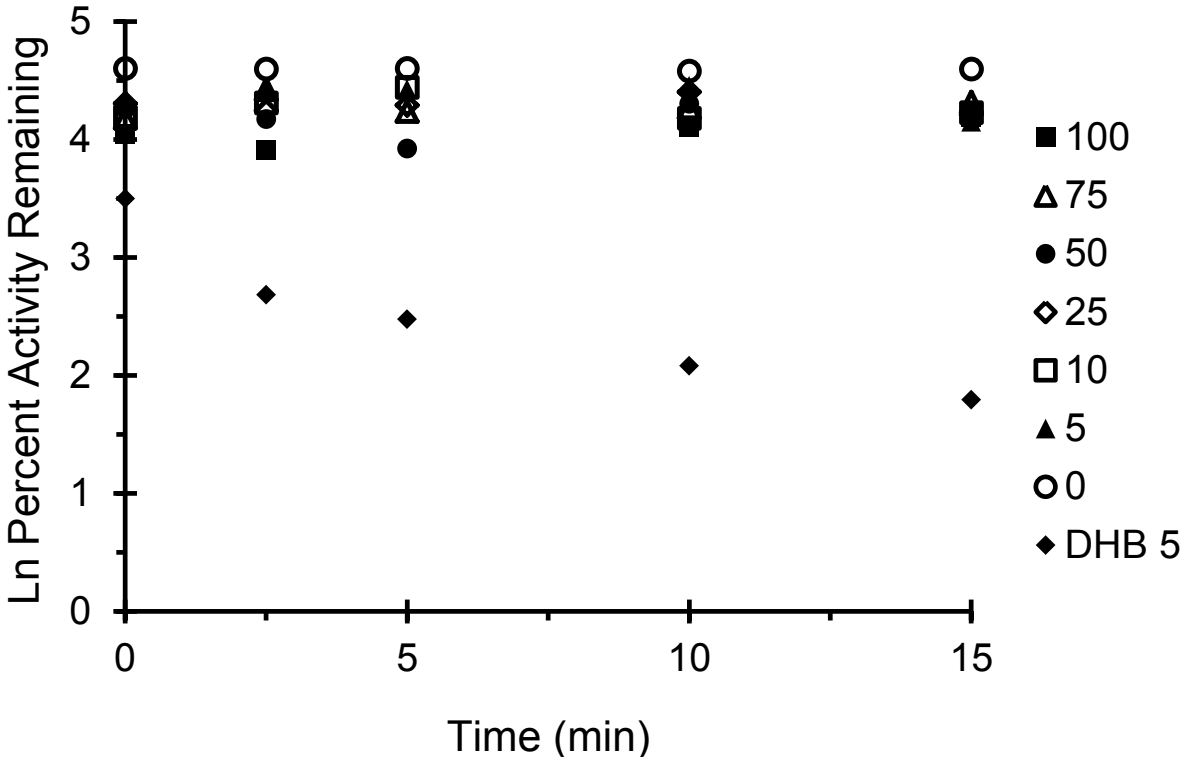
Ln Percent Activity Remaining
0
1
2
3
4
5
0
5
10
15
Time (min)
100
75
50
25
10
5
0
DHB 5

Figure C.2

A

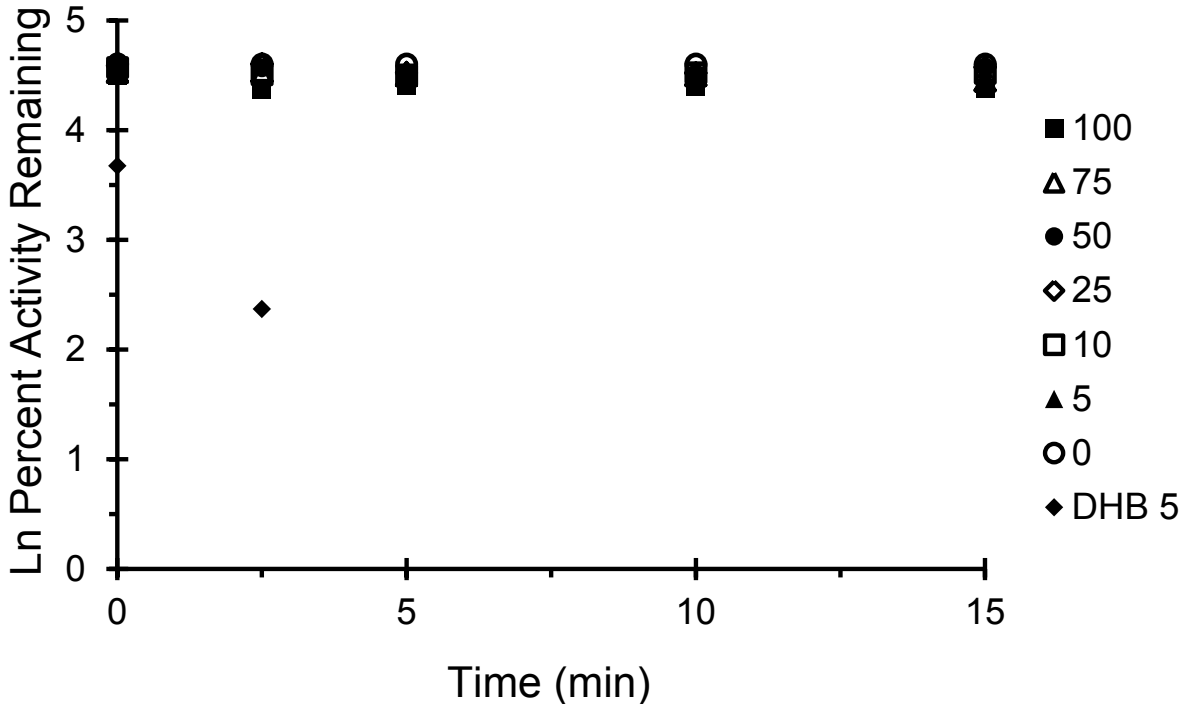
Ln Percent Activity Remaining
0
1
2
3
4
5
0
5
10
15
Time (min)
100
75
50
25
10
5
0
DHB 5

B

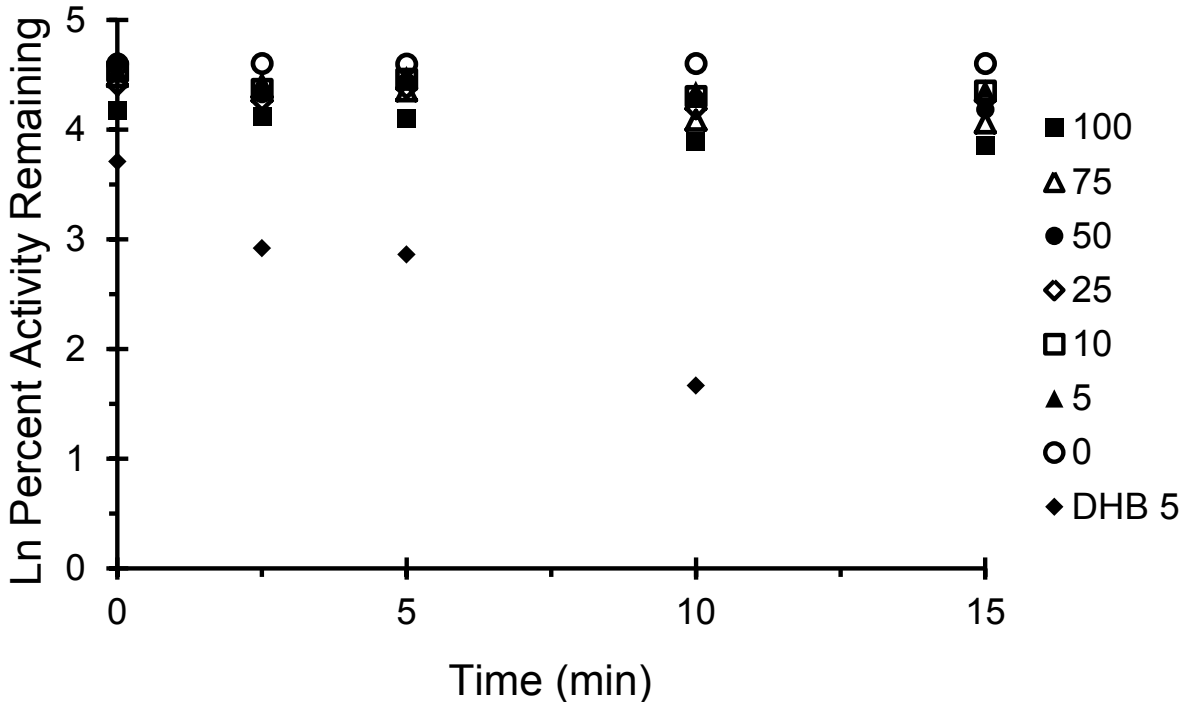
Ln Percent Activity Remaining
0
1
2
3
4
5
0
5
10
15
Time (min)
100
75
50
25
10
5
0
DHB 5

Legends to Figures

Figure C.1. Time- and concentration-dependent inhibition plot of CYP3A4/5 activity. Human liver (A, B) or intestinal microsomes (C, D) were incubated with silybin A (A,C) and silibinin (B,D) (0-100 μM). The primary reaction mixture was diluted 50-fold to initiate the secondary reaction, which contained NADPH (1 mM) and midazolam (8 μM), at designated times. Symbols denote means of duplicate incubations. As a positive control for mechanism-based inhibition, reaction mixtures contained 5 μM DHB in place of silybin A/silibinin.

Figure C.2. Time- and concentration-dependent inhibition plot of CYP3A4/5 activity. Human liver microsomes were incubated with silybin A (A) and silibinin (B) (0-100 μM). The primary reaction mixture was diluted 5-fold to initiate the secondary reaction, which contained NADPH (1 mM) and midazolam (8 μM), at designated times. Symbols denote means of duplicate incubations. As a positive control for mechanism-based inhibition, reaction mixtures contained 5 μM DHB in place of silybin A/silibinin.

References

Paine MF, Criss AB and Watkins PB (2004) Two major grapefruit juice components differ in intestinal CYP3A4 inhibition kinetic and binding properties. *Drug Metab Dispos* **32**:1146-1153.